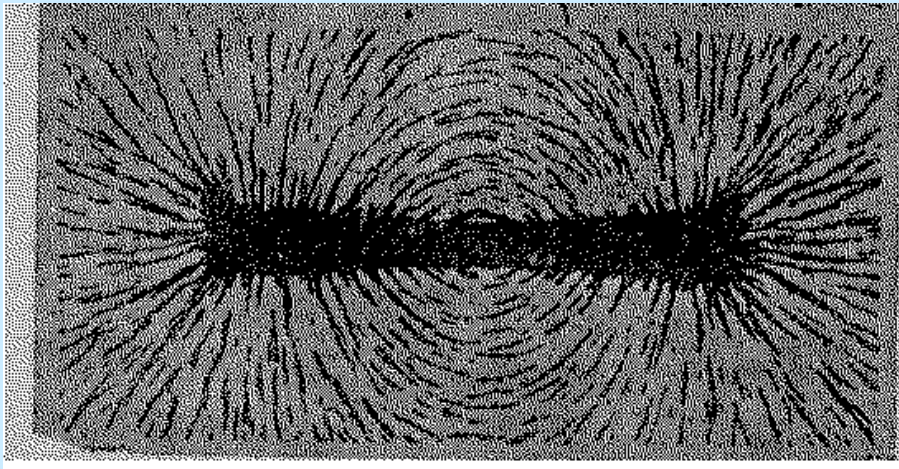


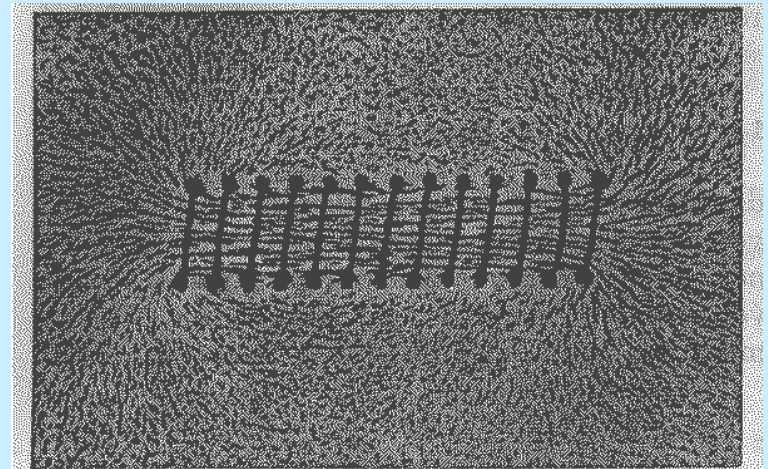
MAGNETIC PROPERTIES OF ROCKS

Magnetic Field – magnet and/or coil fed by electrical current exerts force effect on magnetic particles in its vicinity

Bar Magnet

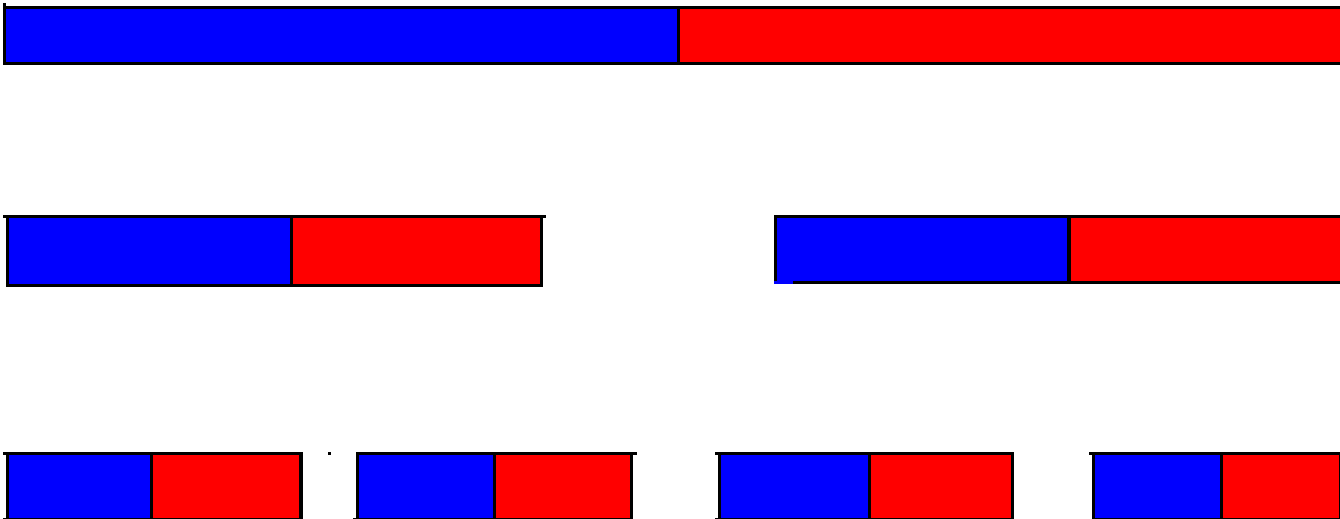


Solenoid



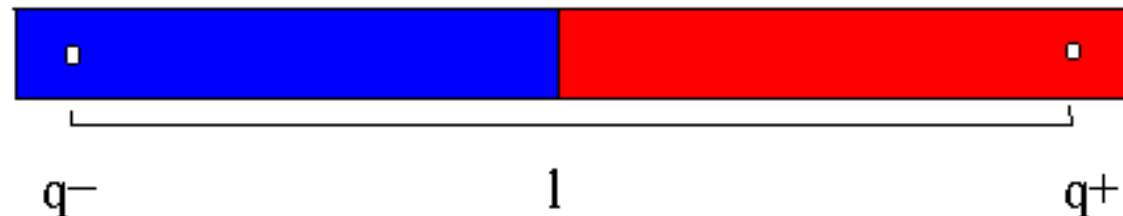
lines of magnetic flux can be visualized by saw dust

DIPOLE CHARACTER OF MAGNETISM



magnets remain dipoles even after cutting them into pieces

Magnetic Moment, Magnetization, Magnetic Susceptibility



$$m = ql$$

m – magnetic moment

q - magnetic charge

l - distance

Magnetization

$$M = \Sigma m/v$$

[A/m]

Magnetic susceptibility k [10⁻⁶ SI]

Magnetization induced by field $M = k H$

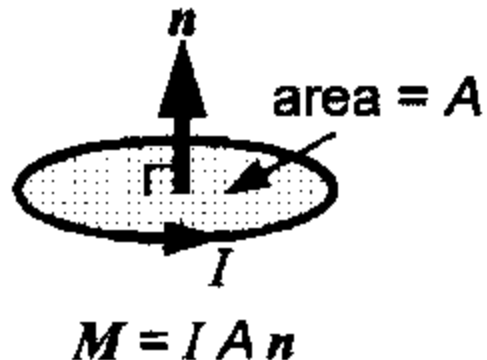
Magnetization of rocks $M = kH + NRM$

M – magnetization, v - specimen volume

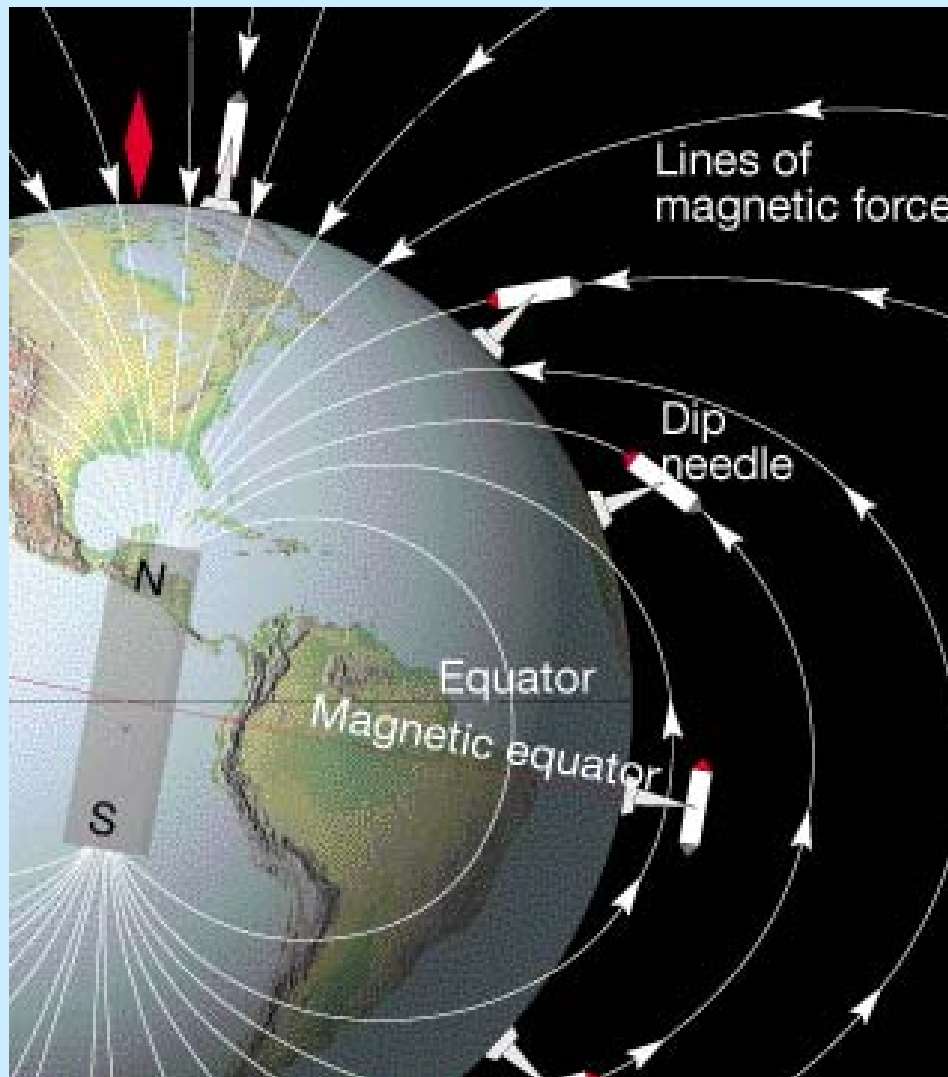
k – magnetic susceptibility, H – intensity of magnetic field

NRM – natural remanent magnetization [A/m]

MAGNETIC DIPOLE OF A COIL



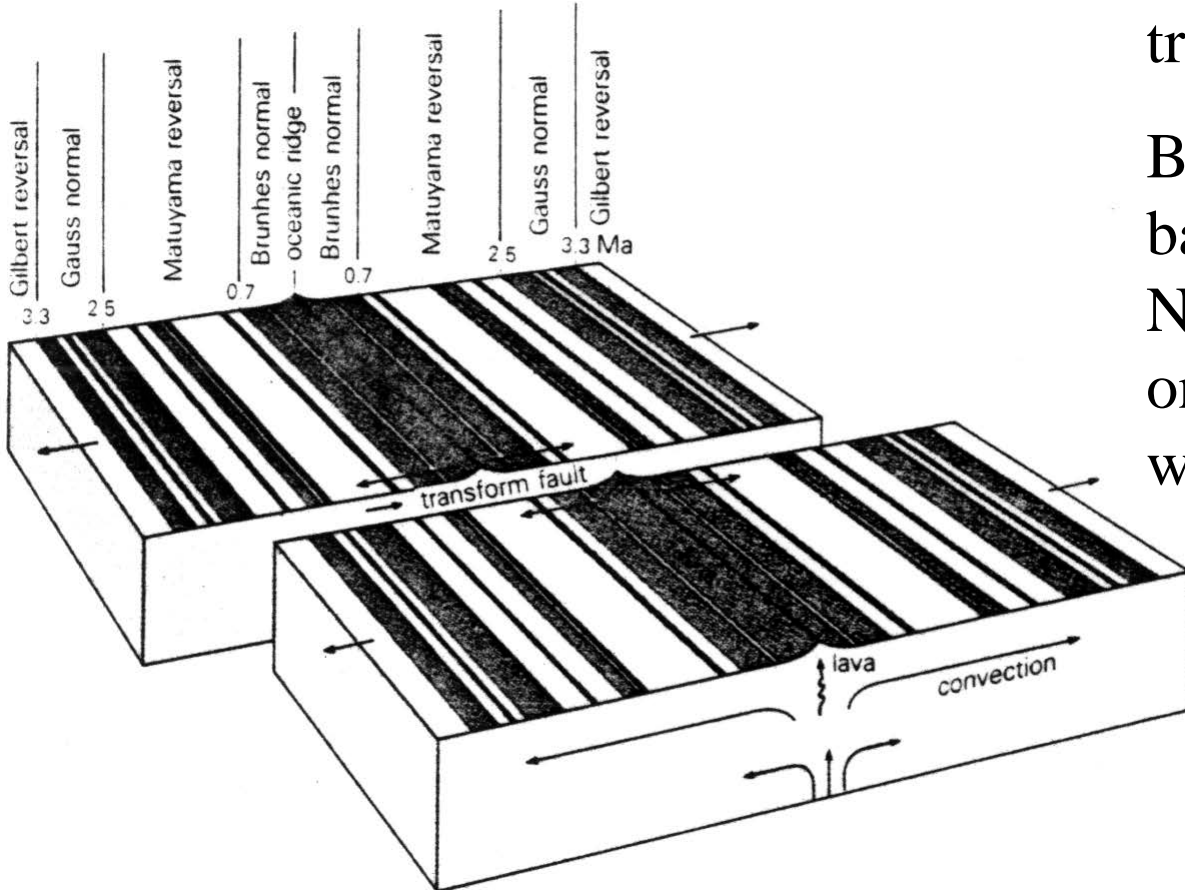
Dipole Field of the Earth



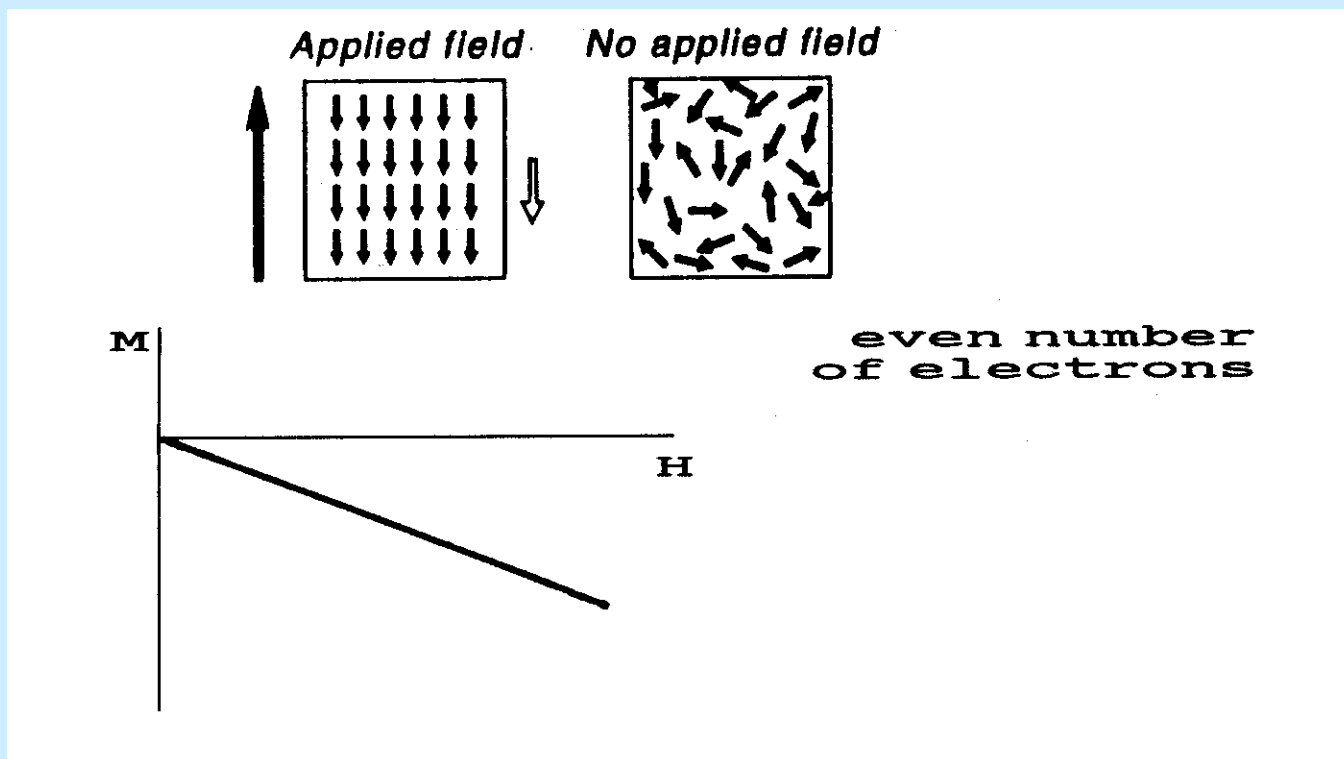
Magnetic anomalies on ocean rift

Shift of anomalies on transform fault.

Black belts indicate basalts with normal NRM polarity, white ones indicate basalts with reverse polarity.



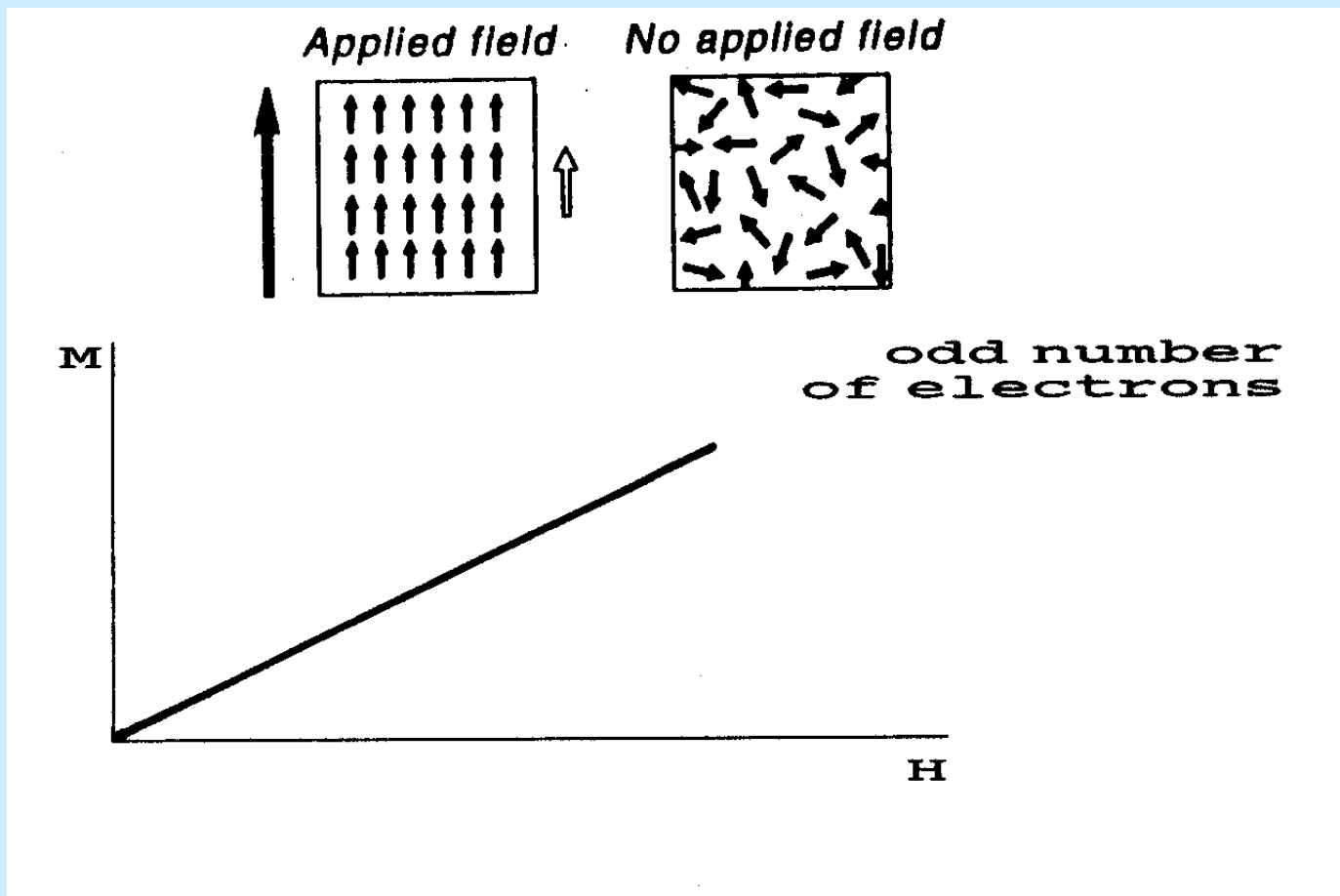
DIAMAGNETISM



quartz, $k = -15.4 \times 10^{-6}$
orthoclase, $k = -13.7 \times 10^{-6}$
calcite, $k = -13.1 \times 10^{-6}$

opal, $k = -12.9 \times 10^{-6}$
halite, $k = -10.3 \times 10^{-6}$
aragonite, $k = -15.0 \times 10^{-6}$

PARAMAGNETISM



olivine, $k = 124$ to 4270×10^{-6}

pyroxene, $k = 121$ to 3700×10^{-6}

hornblende, $k = 750$ to 1368×10^{-6}

dolomite, $k = 11.3 \times 10^{-6}$

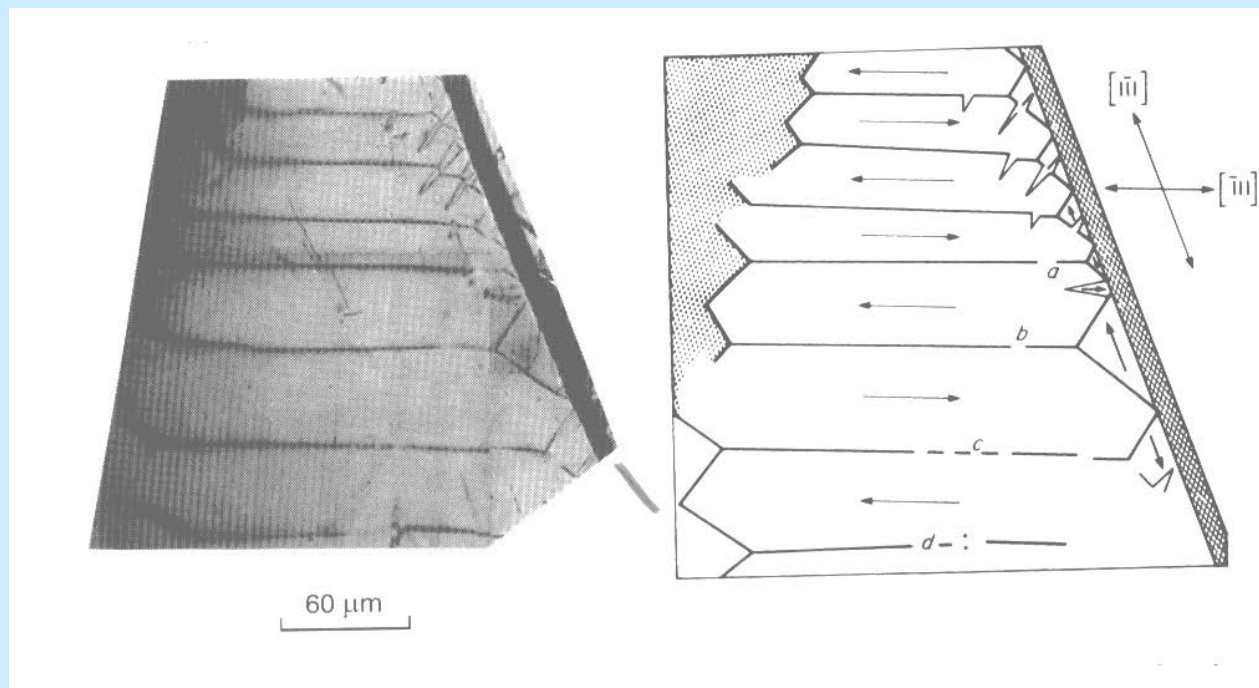
micas, $k = 36$ to 3040×10^{-6}

garnets, $k = 502$ to 6780×10^{-6}

FERROMAGNETISM *sensu lato*

Ferrimagnetism, Antiferromagnetism, Ferromagnetism *sensu stricto*

Magnetic Domains – regions with spontaneously oriented magnetic moments

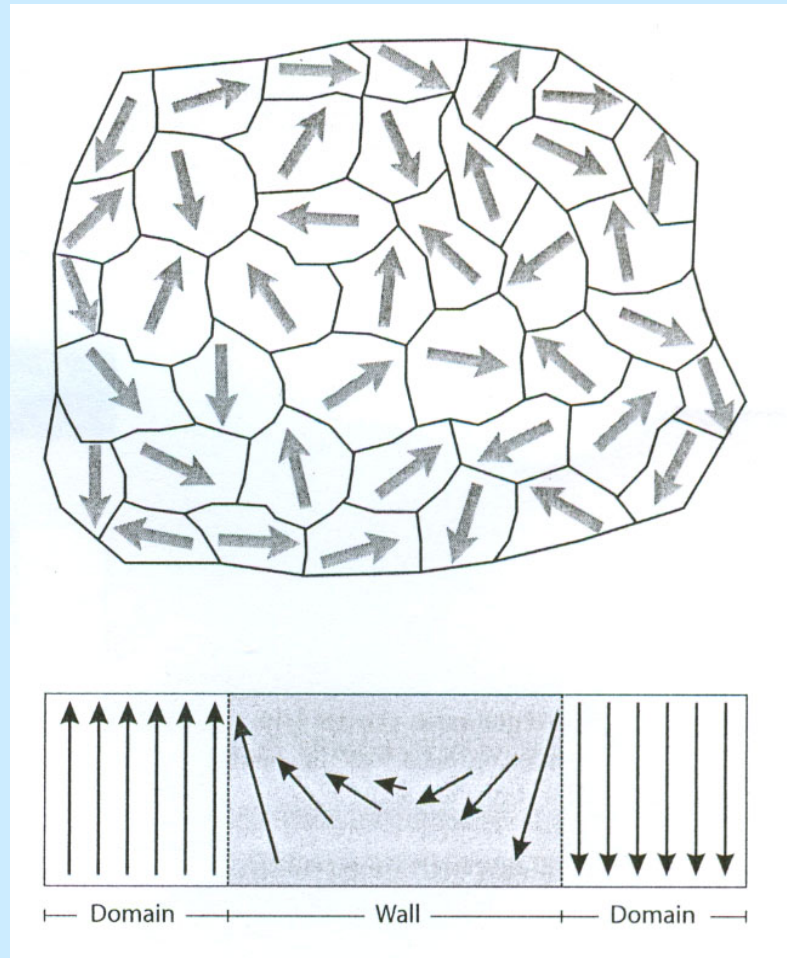


Doménová stavba feromagnetika

Doménová stavba bez vlivu
vnějšího magnetického pole



Nulový magnetický moment



Změna magnetizace na
hranici domén



Magnetizace feromagnetika

Hysterézní smyčka :

H – magnetické pole (přesněji intenzita magnetického pole)

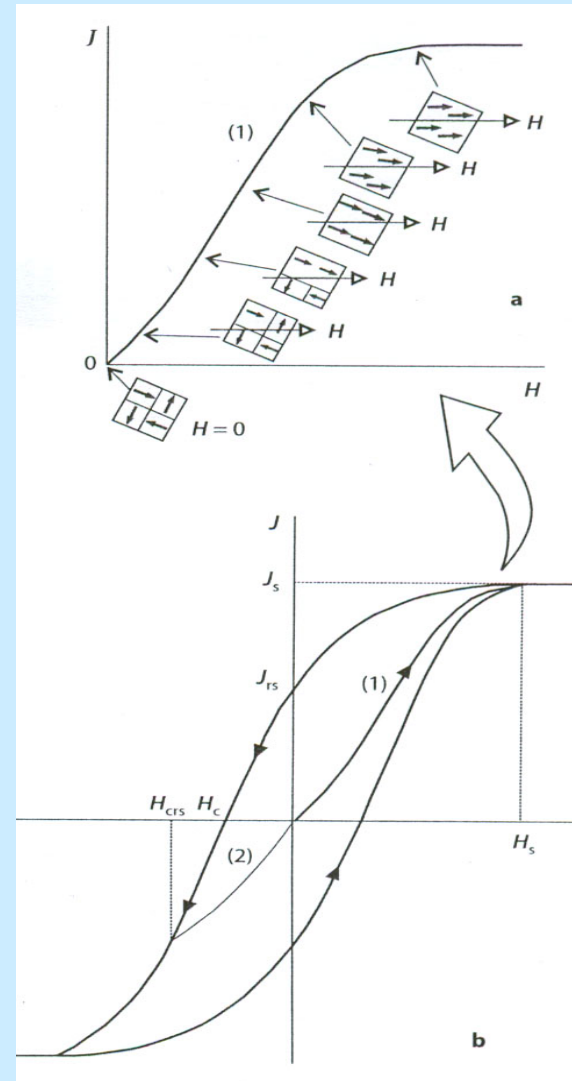
J – magnetizace

J_s – sytná magnetizace

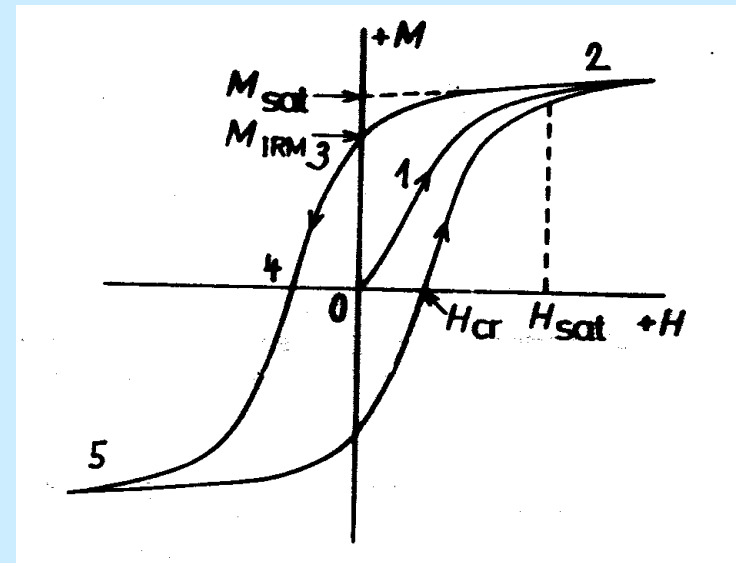
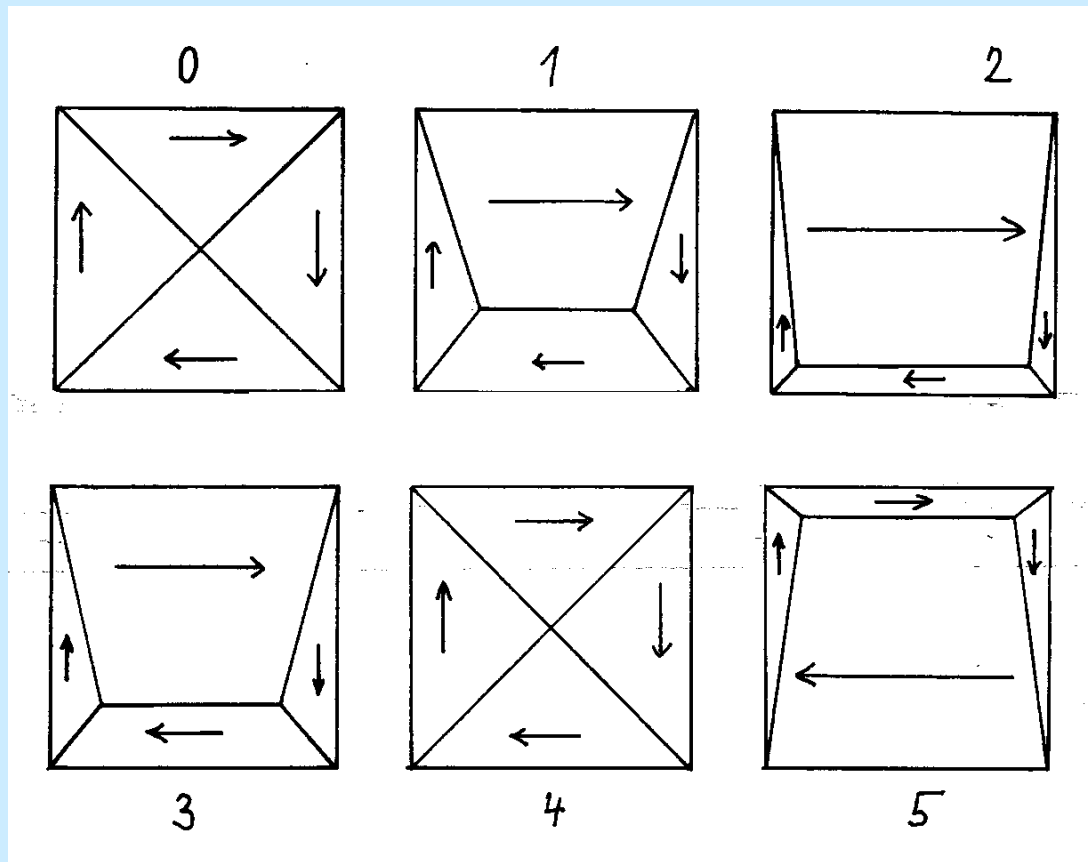
J_r – remanentní magnetizace

H_c – koercitivní síla

H_{cr} – koercitivita remanentní magnetizace



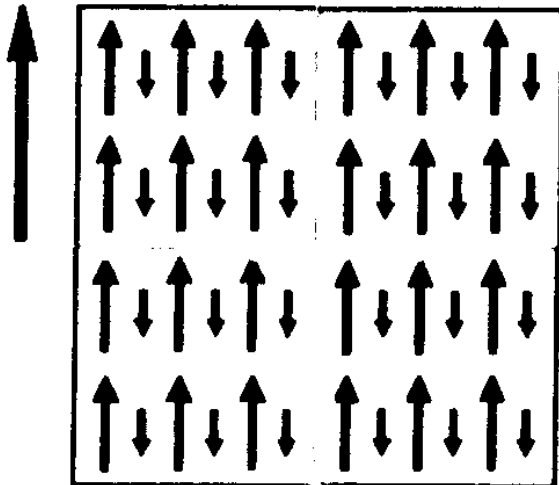
HYSTERESIS LOOP in Ferromagnetic *sensu lato* Materials



M_{sat} – saturation magnetization, H_{sat} – saturating field

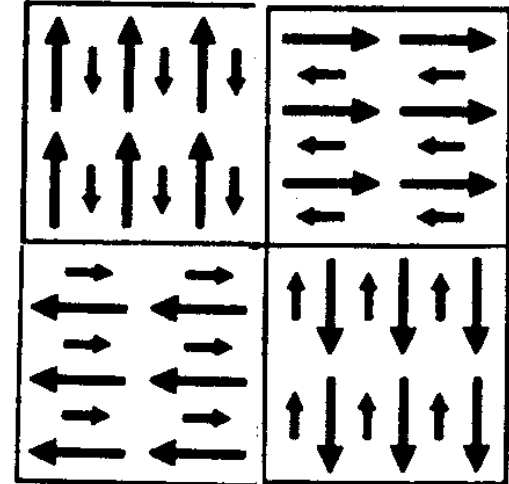
M_{rm} – remanent magnetization, H_{cr} – coercive force

FERRIMAGNETISM



Applied field

Ferrimagnetic

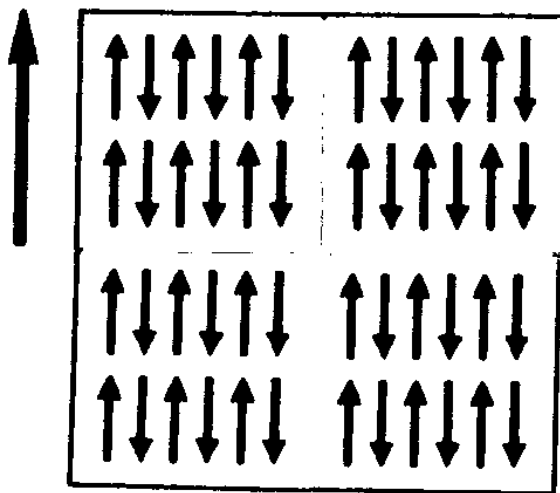


No applied field

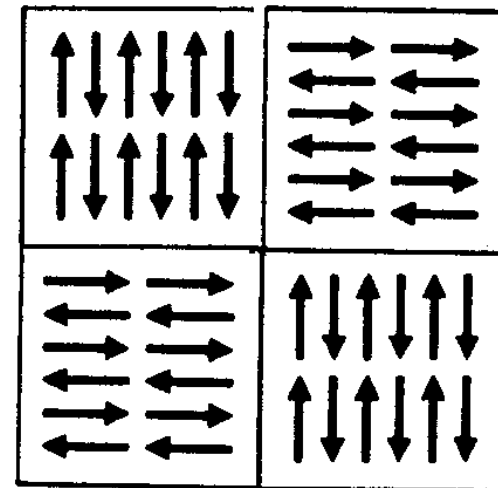
Magnetite,
Titanomagnetite,
monoclinic Pyrrhotite,

$k = 3$ to 6
 $k = 0.5$ to 3.5
 $k = 0.2$ to 0.7

ANTIFERROMAGNETISM



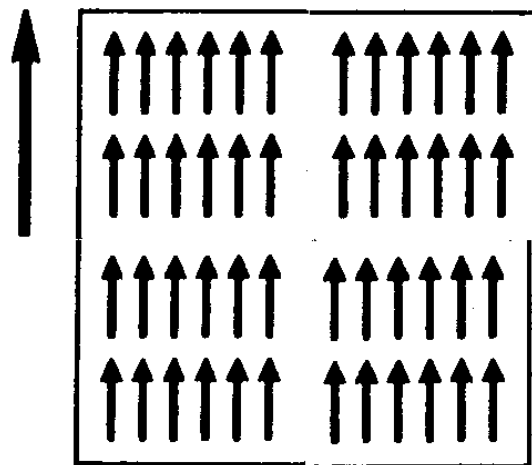
Antiferromagnetic



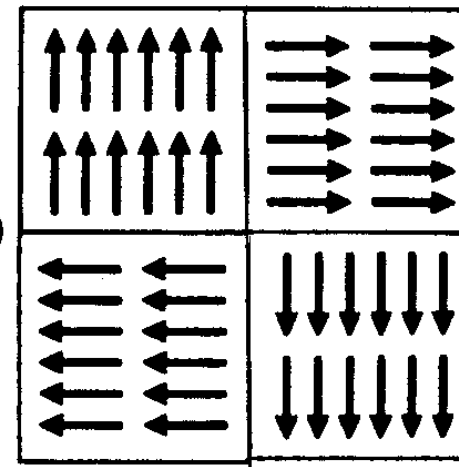
Hematite,
hexagonal Pyrrhotite

$k = 0.001 \text{ to } 0.2$

FERROMAGNETISM *sensu stricto*



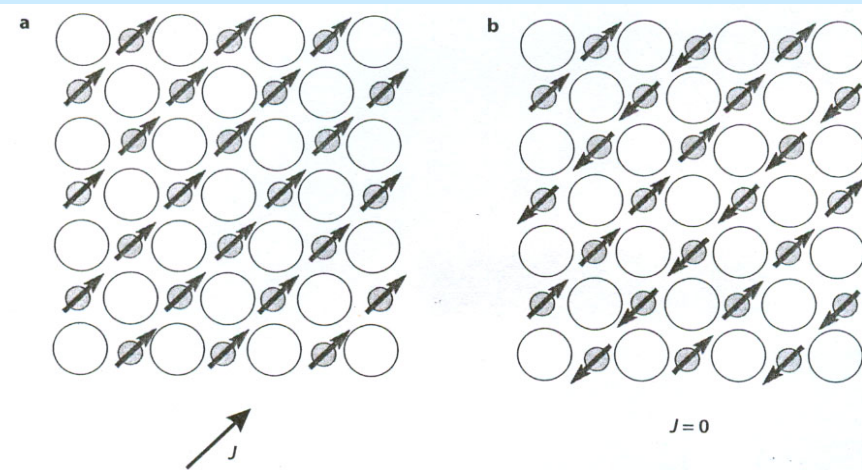
Ferromagnetic (s.s.)



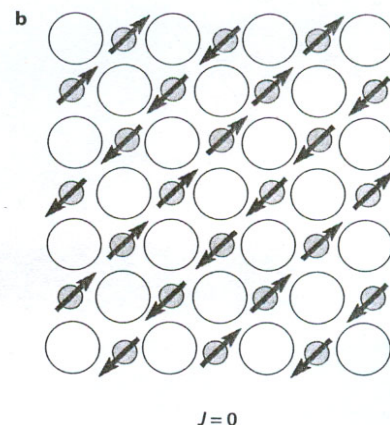
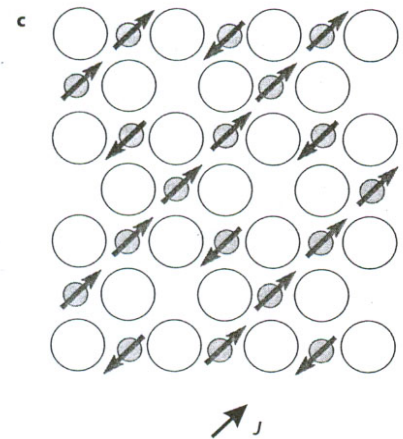
Metallic Iron

Parazitický feromagnetismus antiferomagnetika

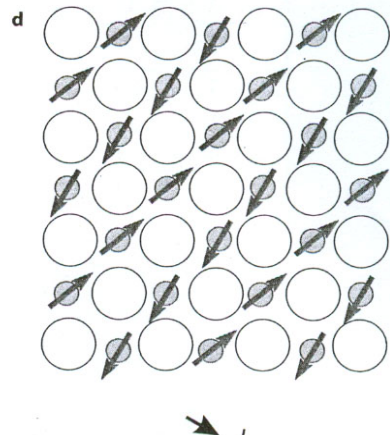
feromagnetismus



ferimagnetismus



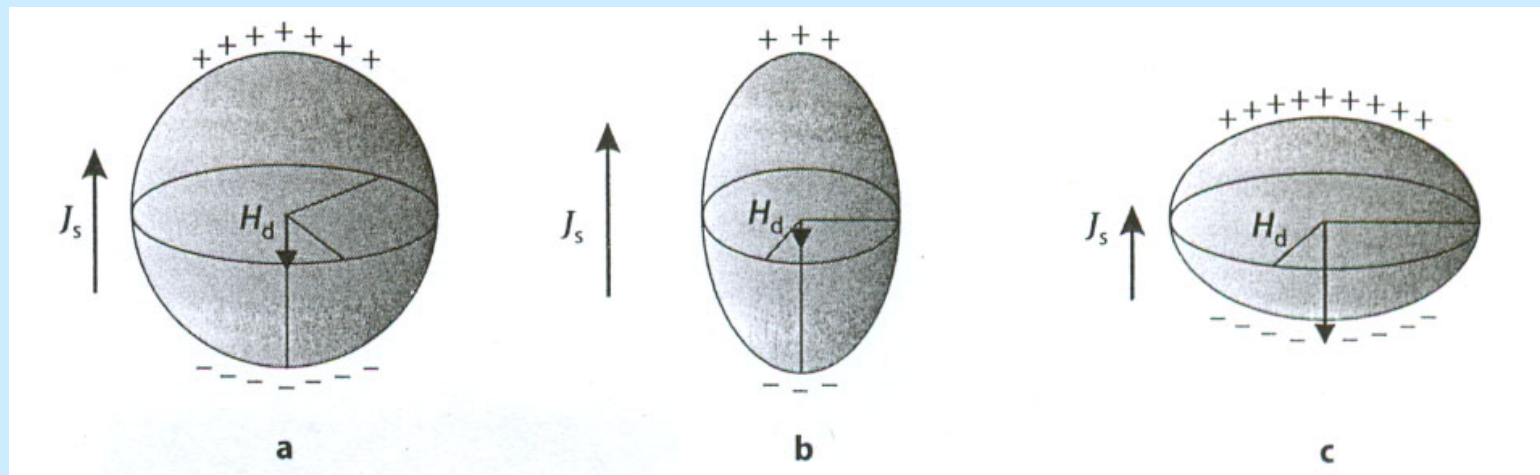
antiferomagneti-
smus
čistý



Antiferomagneti-
smus s
parazitickým
feromagnetismem

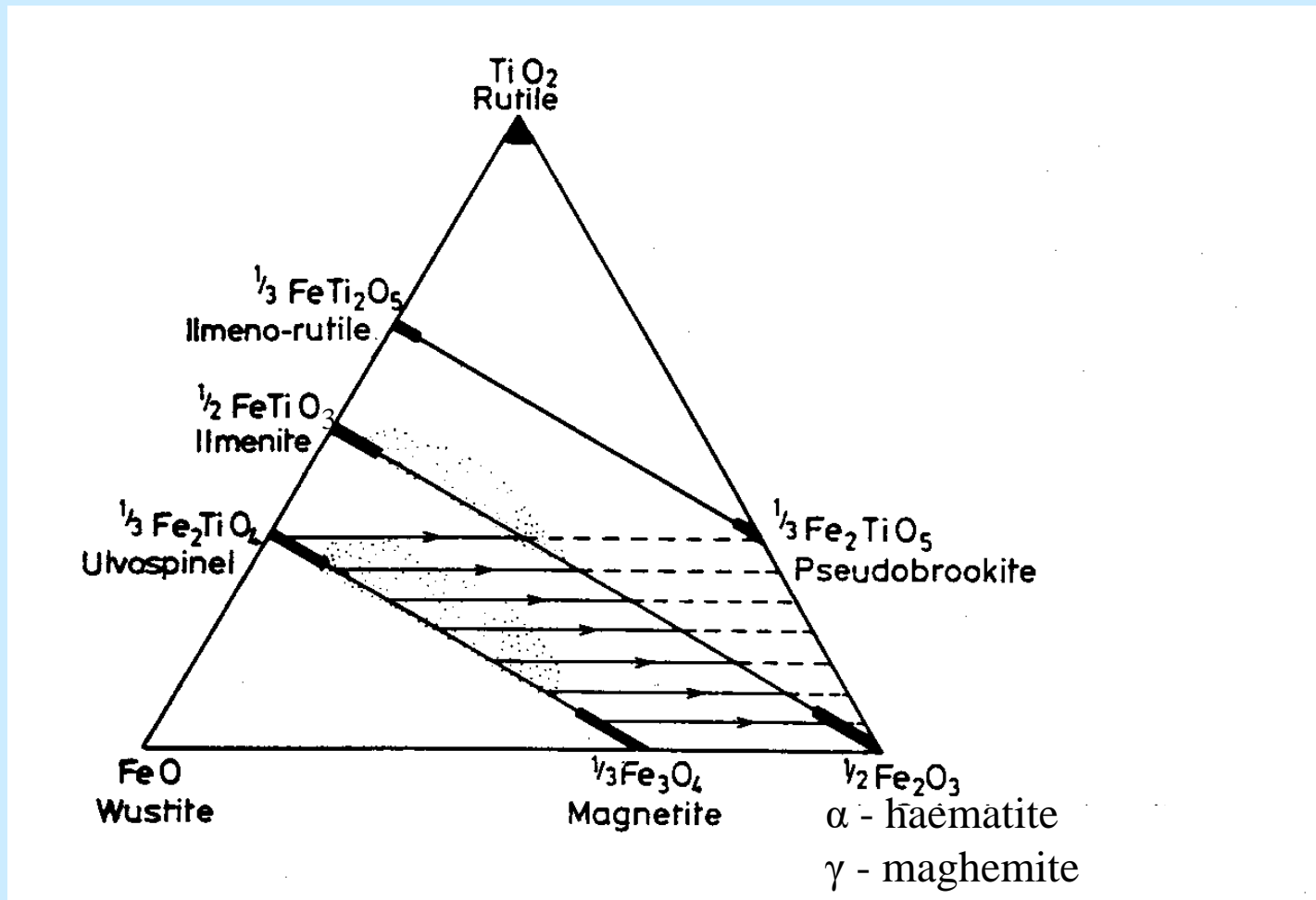
Demagnetizační faktor N

Je definován rovnicí : $k_{\text{ext}} = k_{\text{int}}/[1 + Nk_{\text{int}}]$

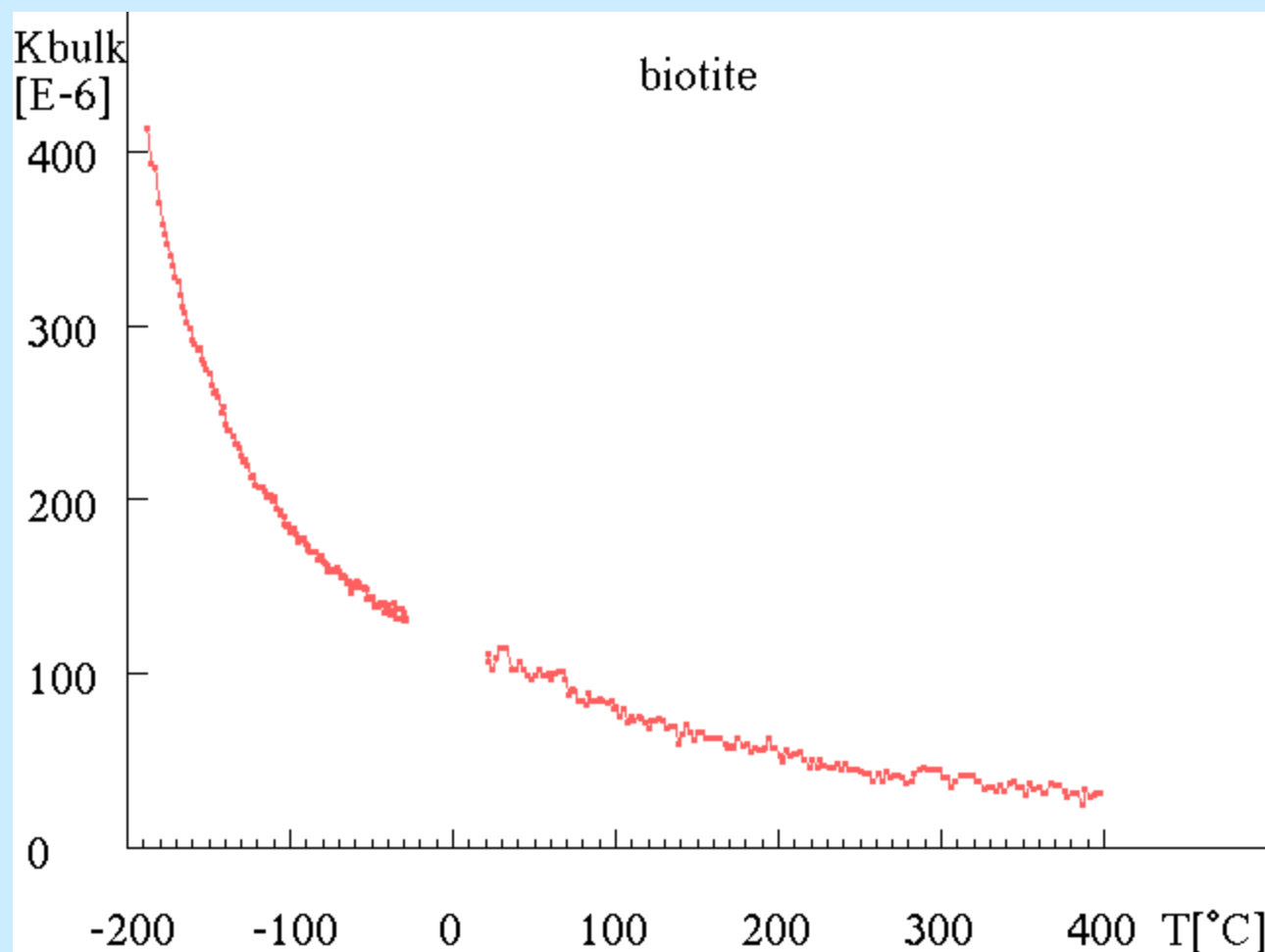


K_{ext} se liší od k_{int} u silně magnetických látek, z minerálů např. u magnetitu a maghemitu. Výsledná magnetizace závisí na tvaru zrna (b,c) a jeho orientaci v magnetickém poli. Demagnetizační faktor je příčinou tzv. tvarové magnetické anizotropie.

TERNARY DIAGRAM FOR IRON-TITANIUM OXIDES

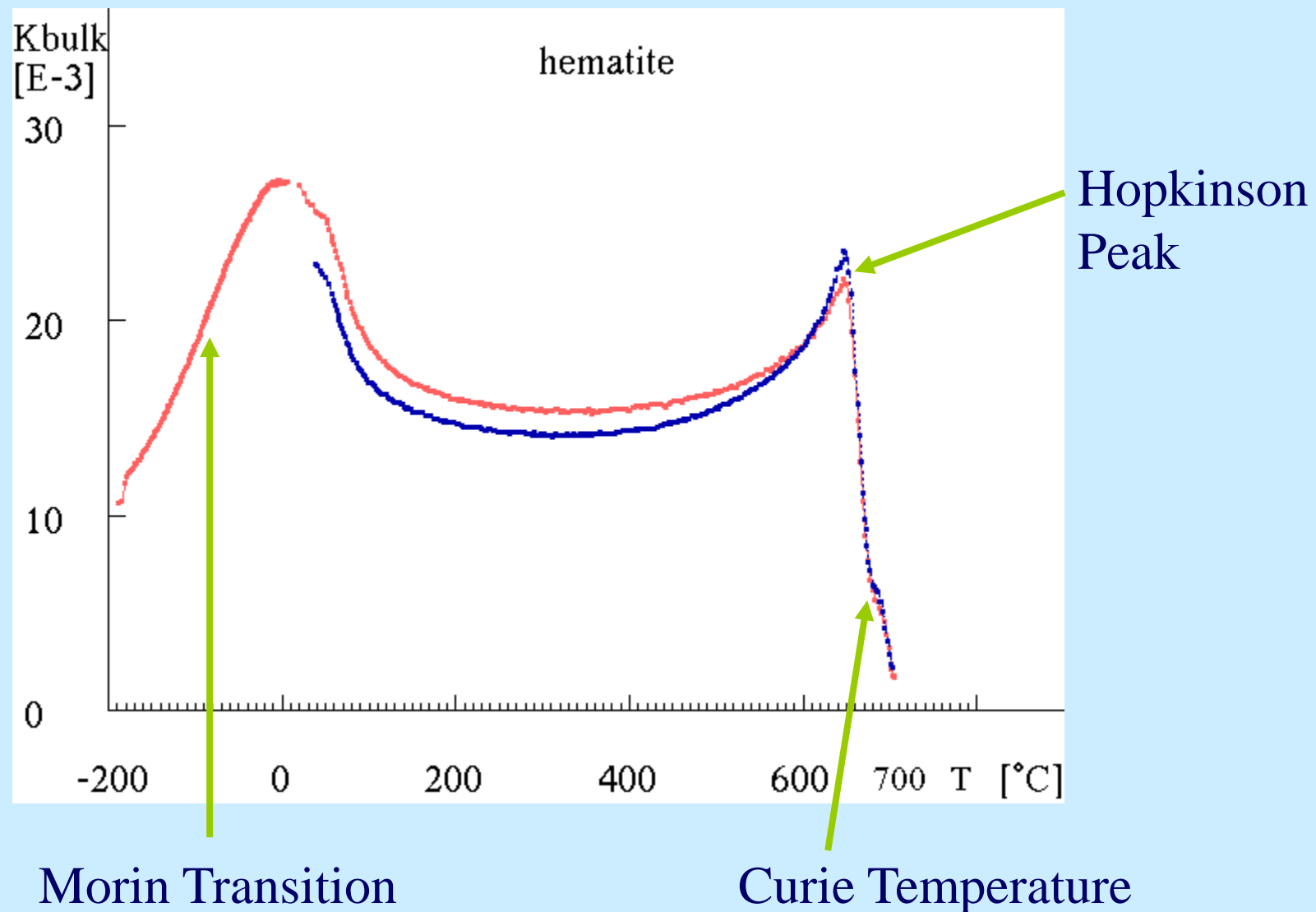


Temperature Variation of Susceptibility in Paramagnetics

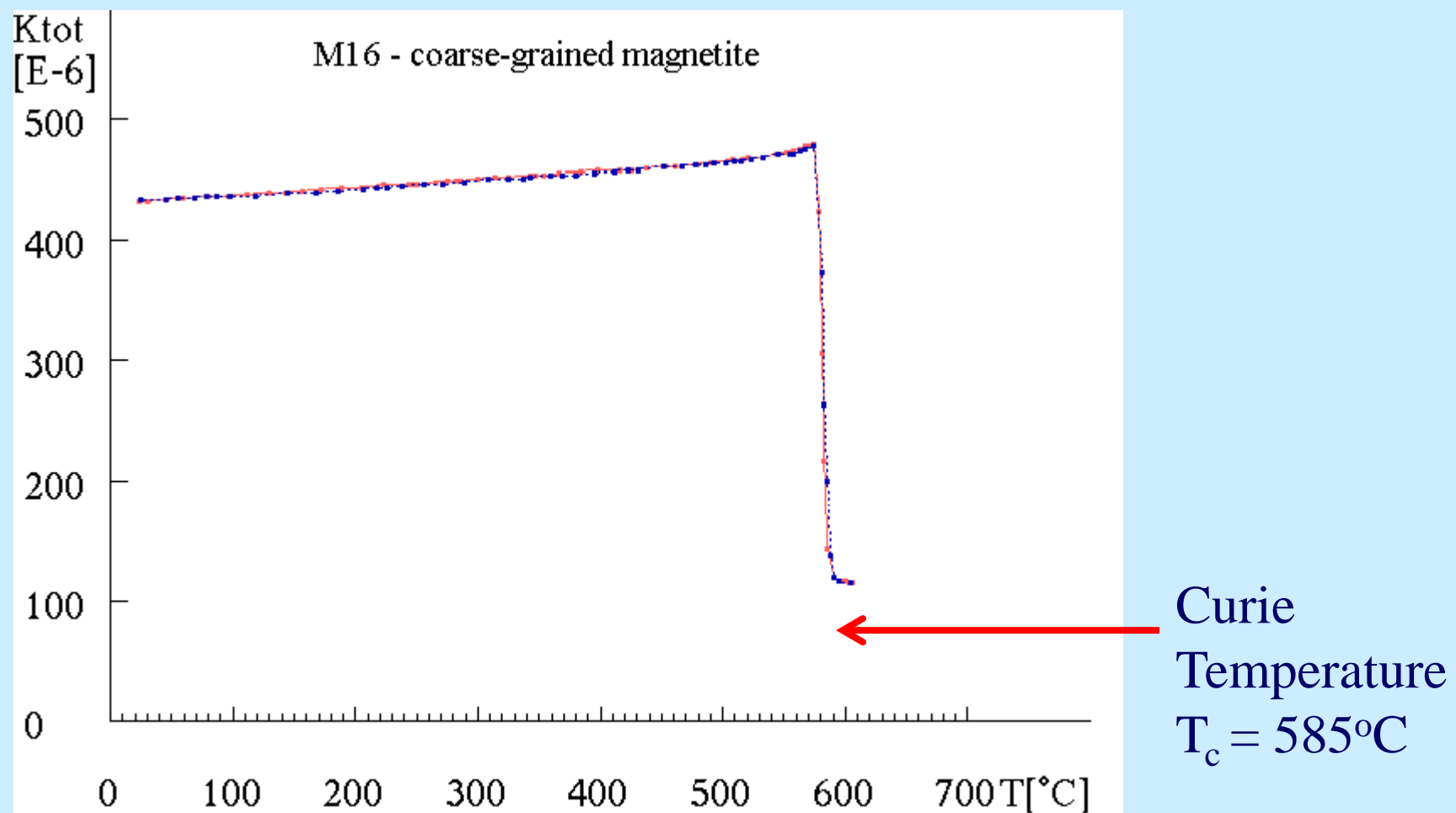


Hyperbolic course according to the Curie Law, $k = C/T$
C – proportionality constant, T – absolute temperature

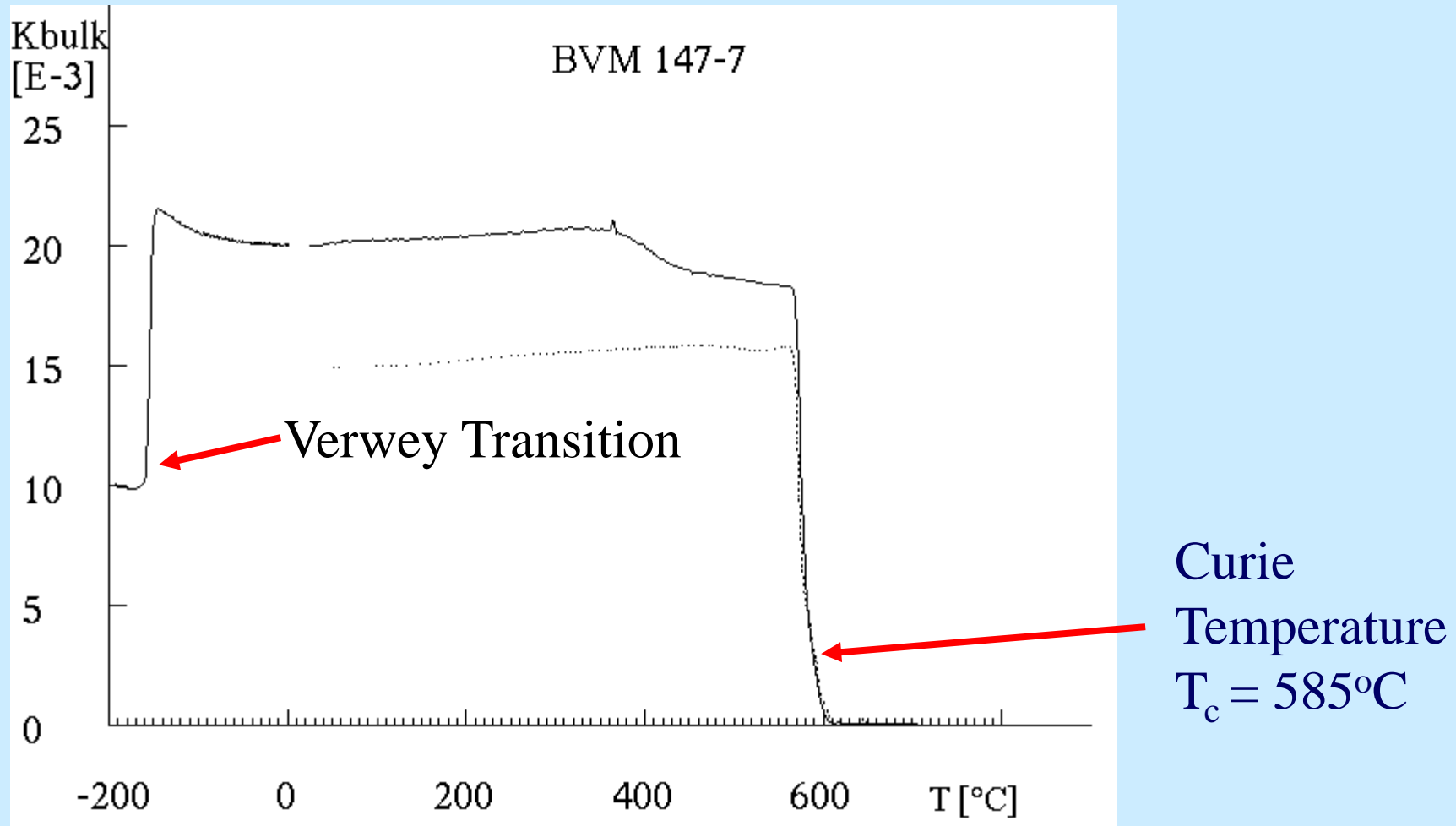
Temperature Variation of Susceptibility in Hematite



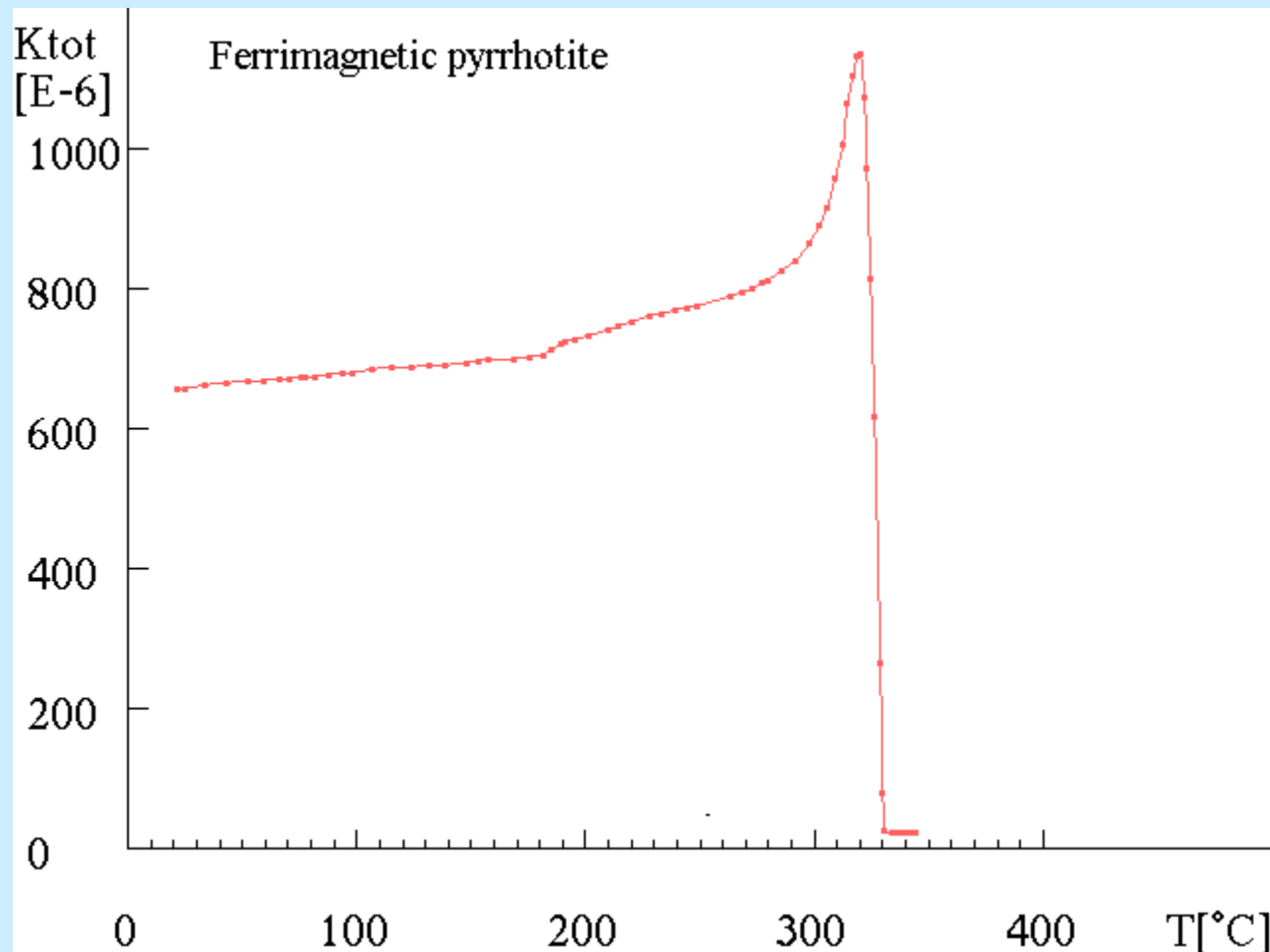
Temperature Variation of Susceptibility in Magnetite



Temperature Variation of Susceptibility in Magnetite

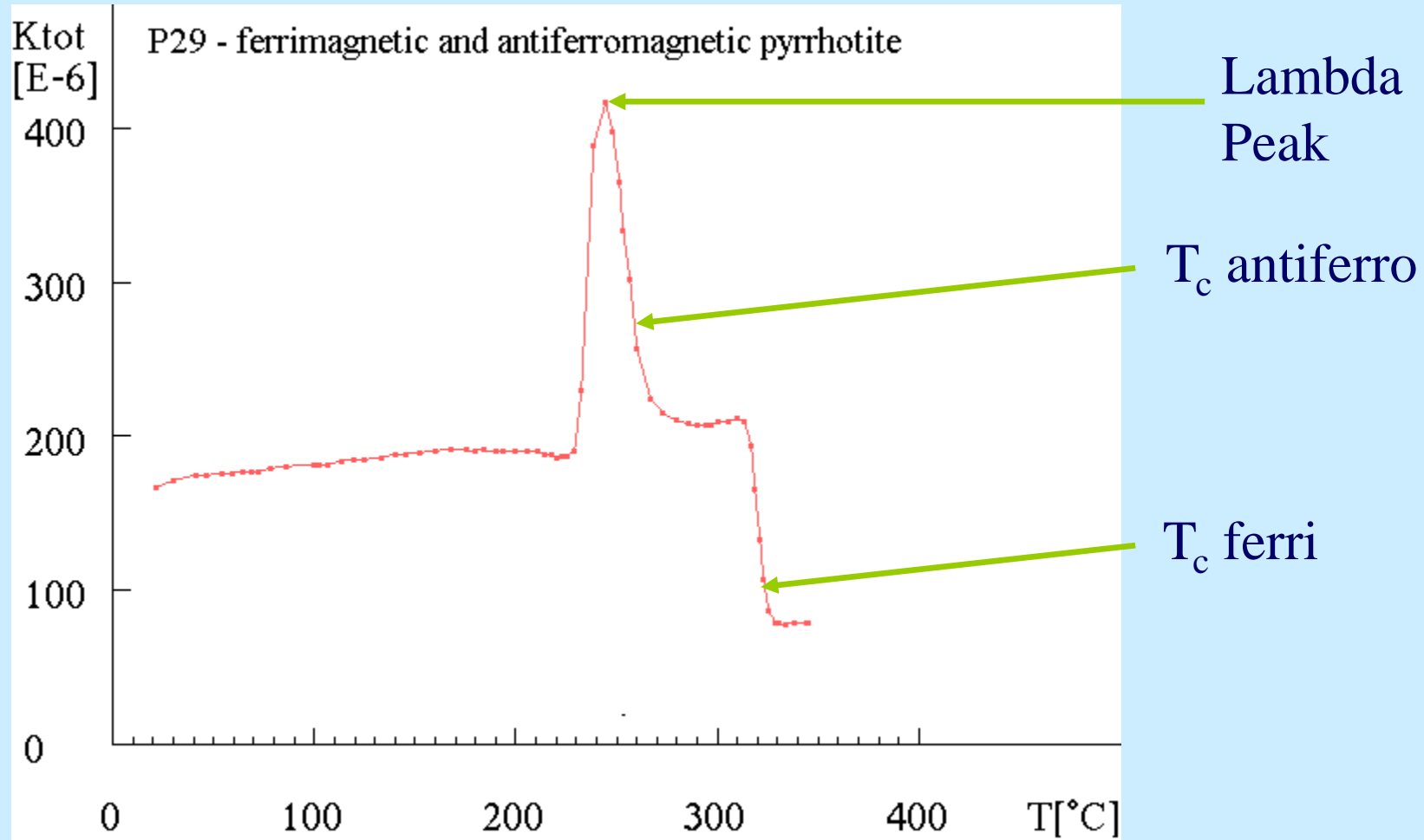


Temperature Variation of Susceptibility in Monoclinic Pyrrhotite

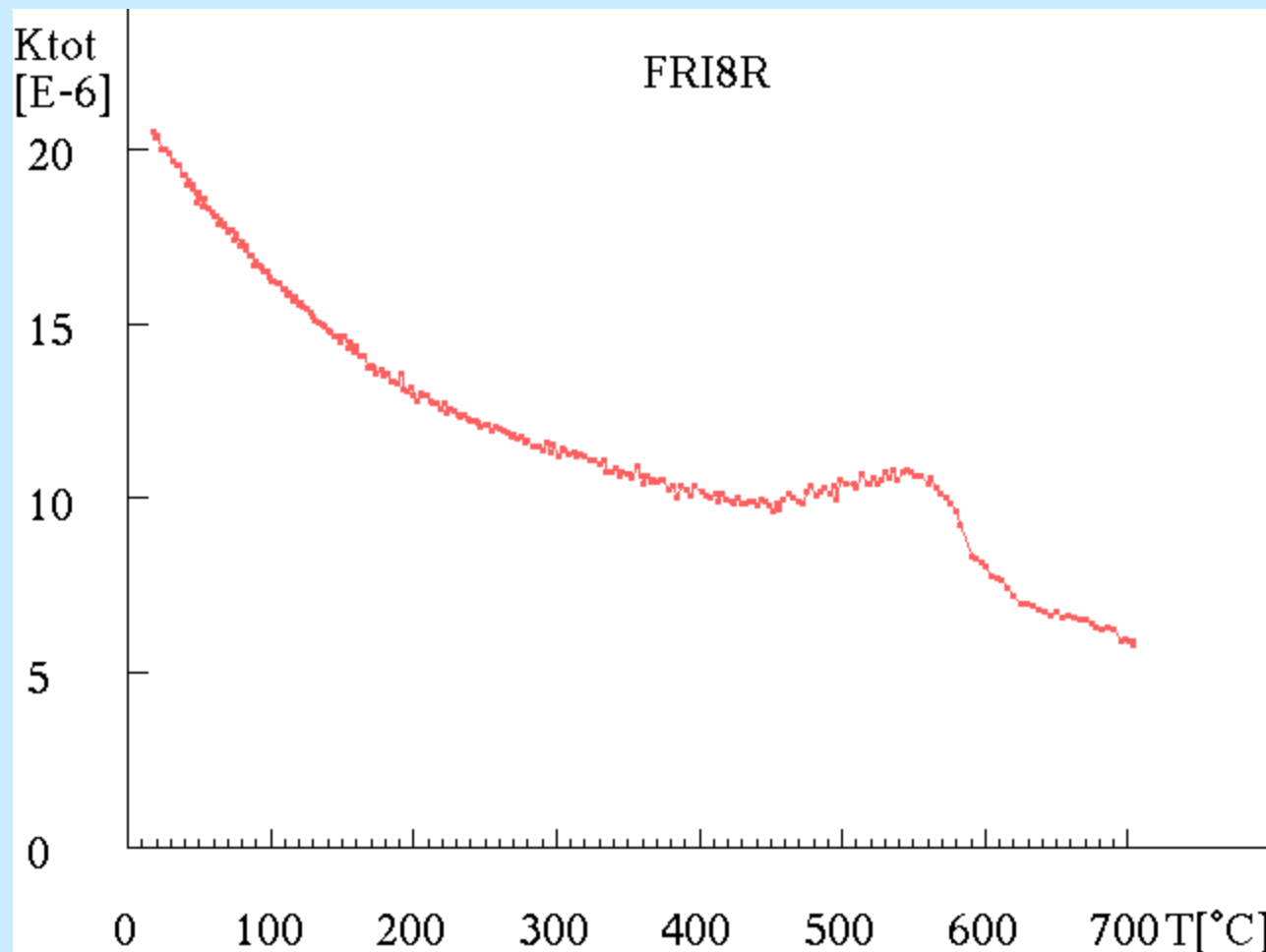


$$T_c = 325^\circ\text{C}$$

Temperature Variation of Susceptibility in mixture of monoclinic and hexagonal pyrrhotite

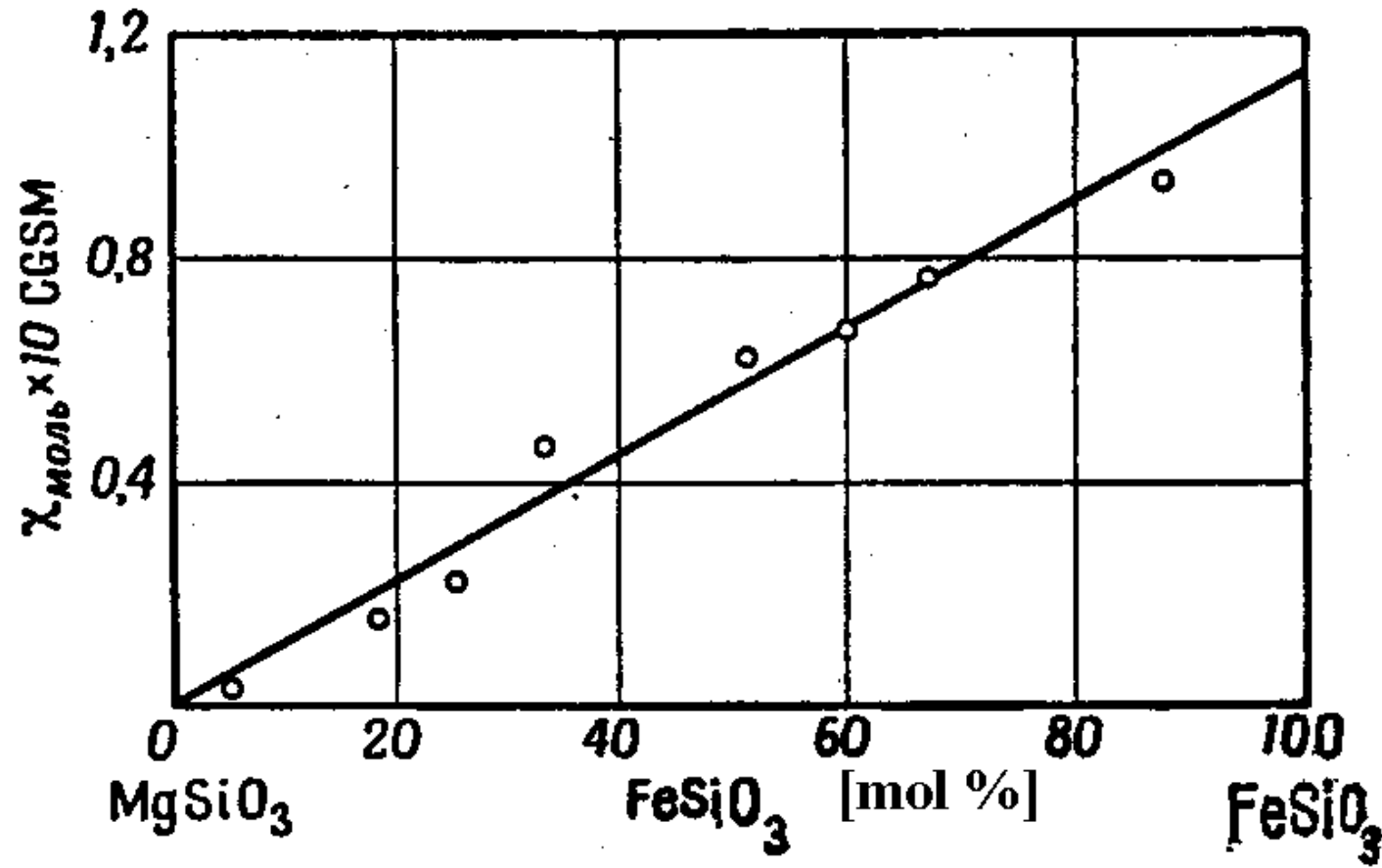


AMPHIBOLITE (Hornblende + Magnetite)



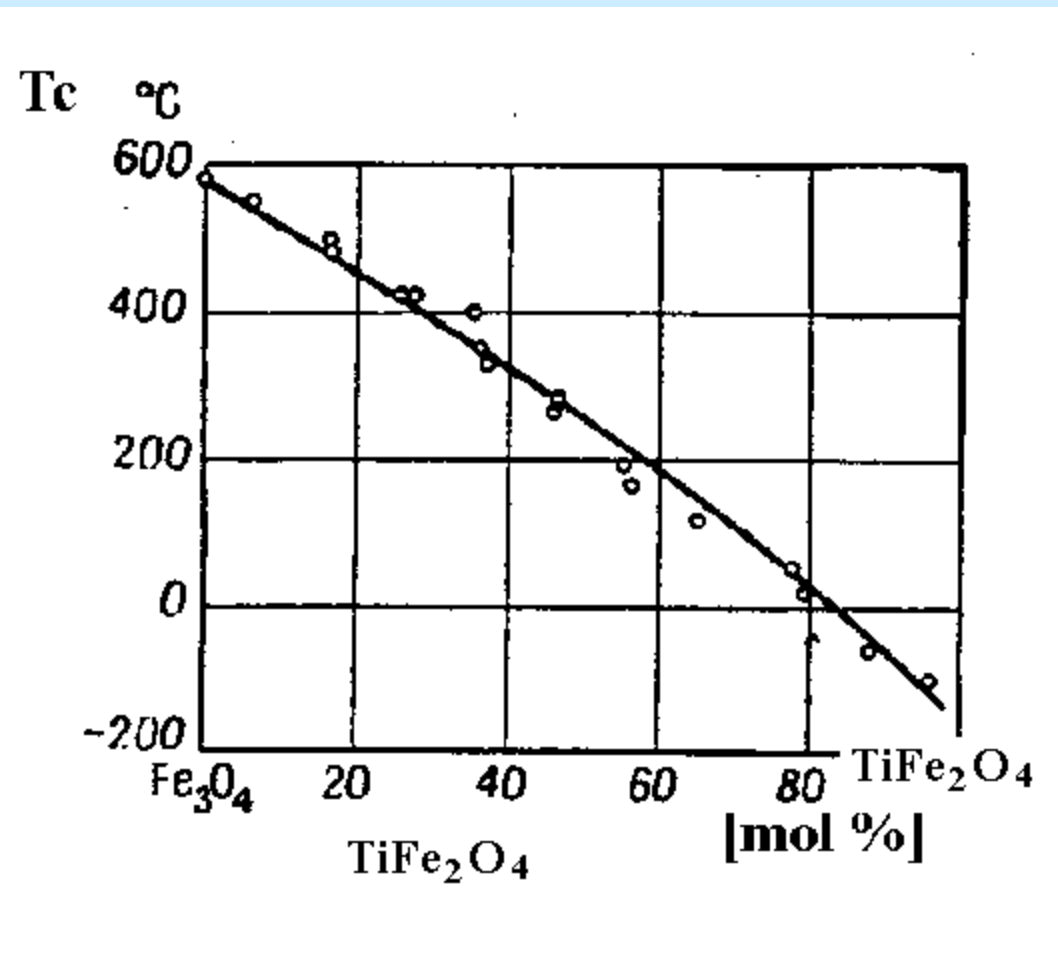
Susceptibility Variation with Mineral Composition

orthopyroxene

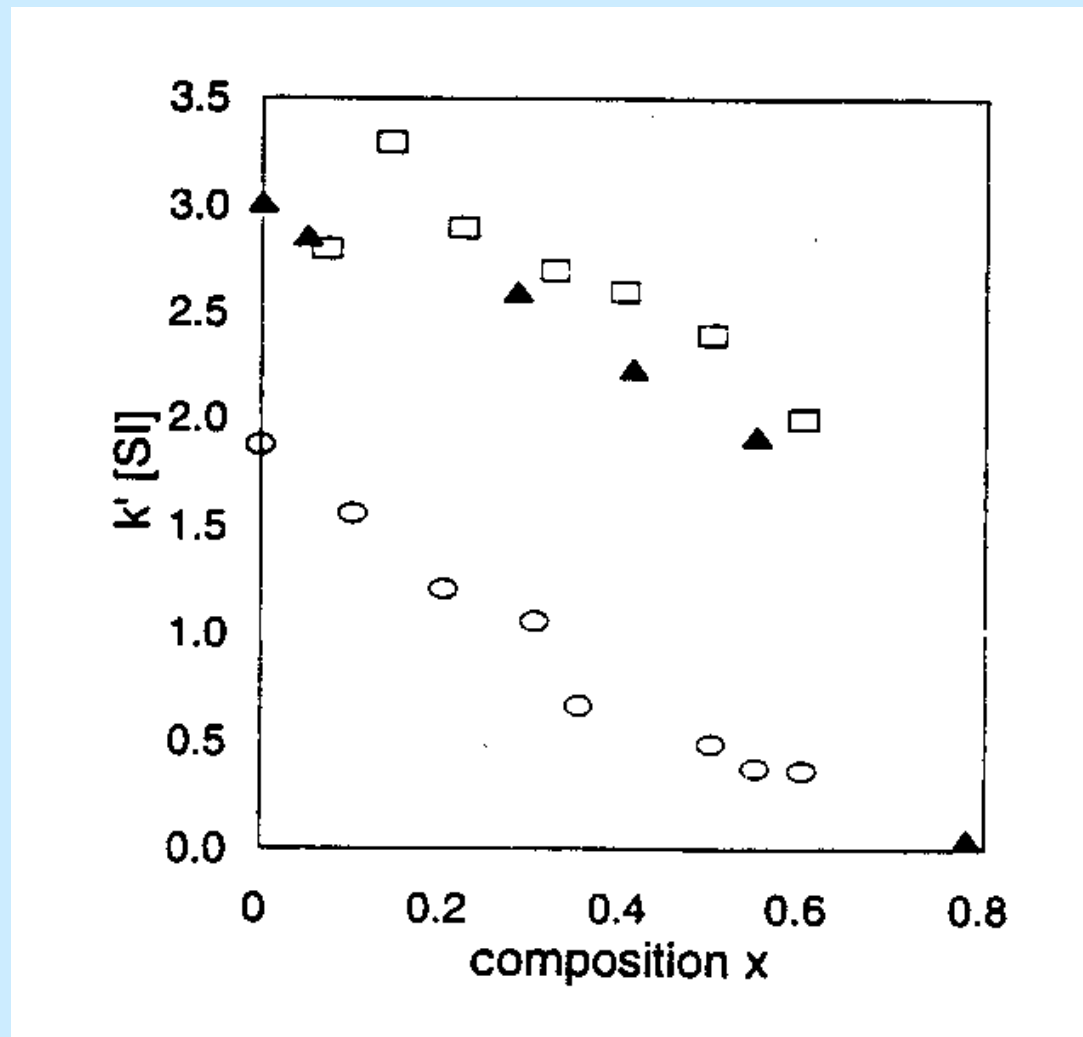


Variation of Curie Temperature with Mineral Composition

magnetite – ulvöspinel series

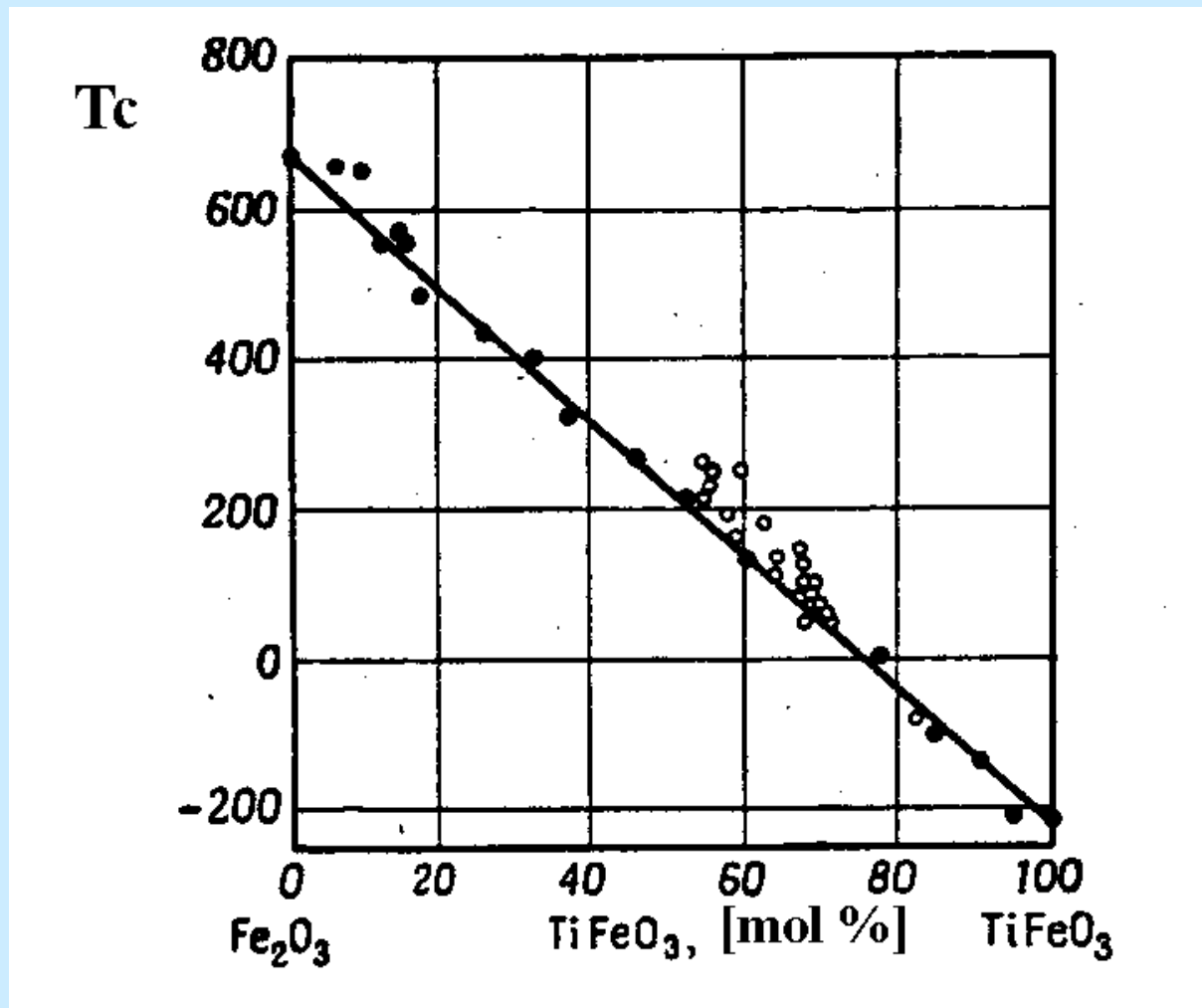


Susceptibility Variation with Composition in Titanomagnetites

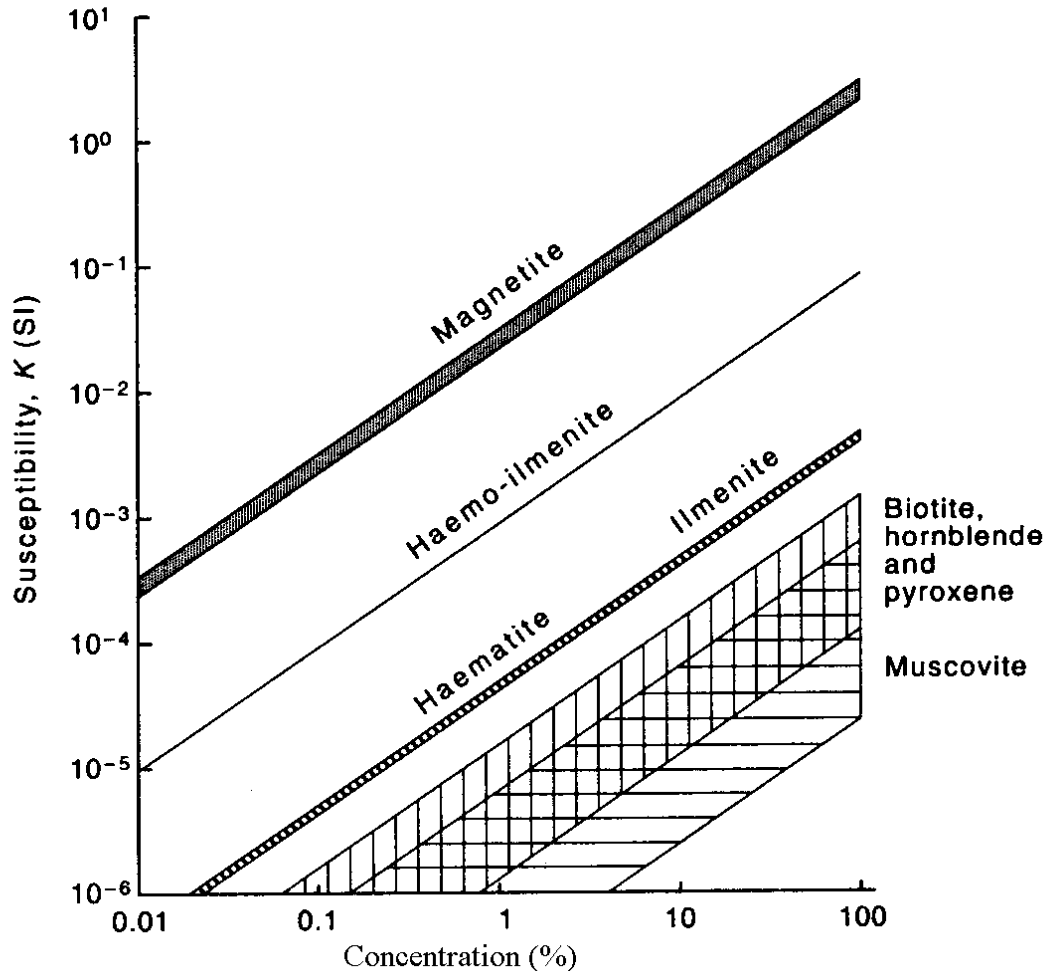


Variation of Curie Temperature with Mineral Composition

ilmenite – hematite series



Magnetic Susceptibility of Minerals

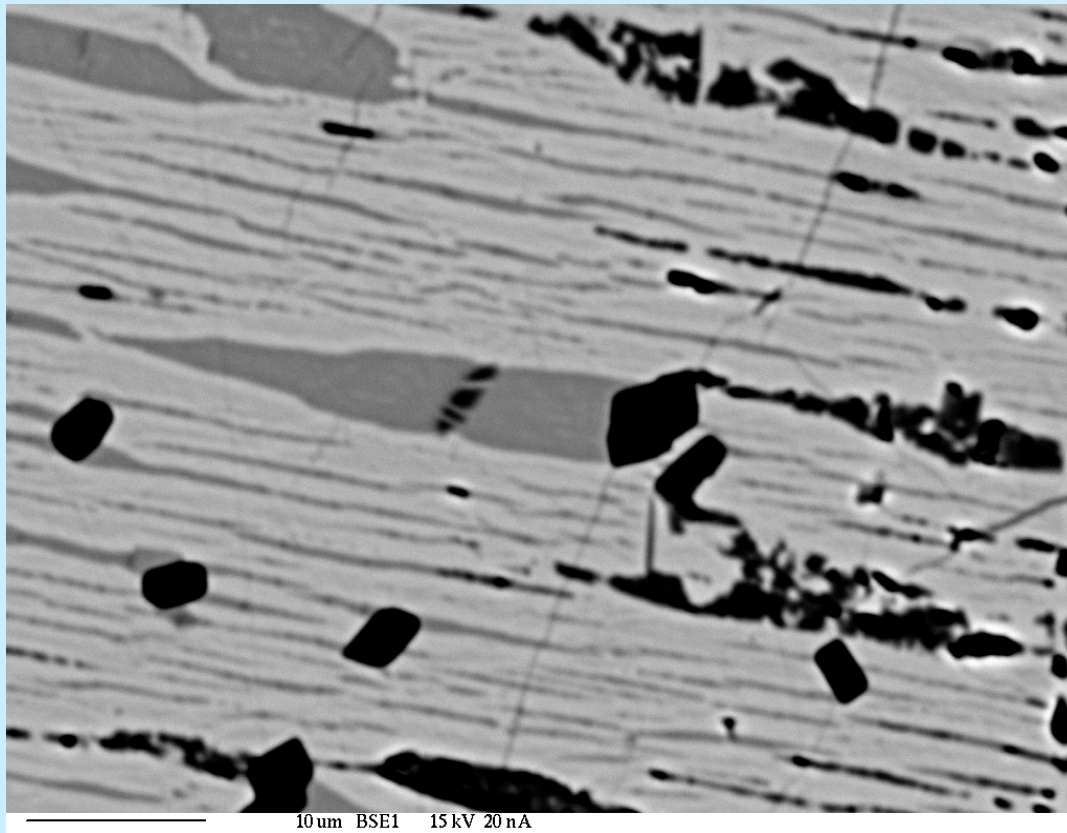


Oxidace Fe-Ti minerálů

V průběhu geologického vývoje dochází ke změnám PT podmínek vzhledem k těm, ve kterých se původně horniny vytvářely. U vulkanitů, intruzív a výše metamorfovaných hornin dochází při jejich ochlazování a výstupu k povrchu k tzv. oxidaci Fe-Ti minerálů, a to jak titanomagnetitů, tak ilmenohematitů a hemoilmenitů.

Oxidace se projevuje lamelováním původních zrn, tj. vznikem lamel bohatších na Ti a lamel naopak chudých na Ti. Proces končí lamelami ilmenit-magnetitovými nebo ilmenit-hematitovými.

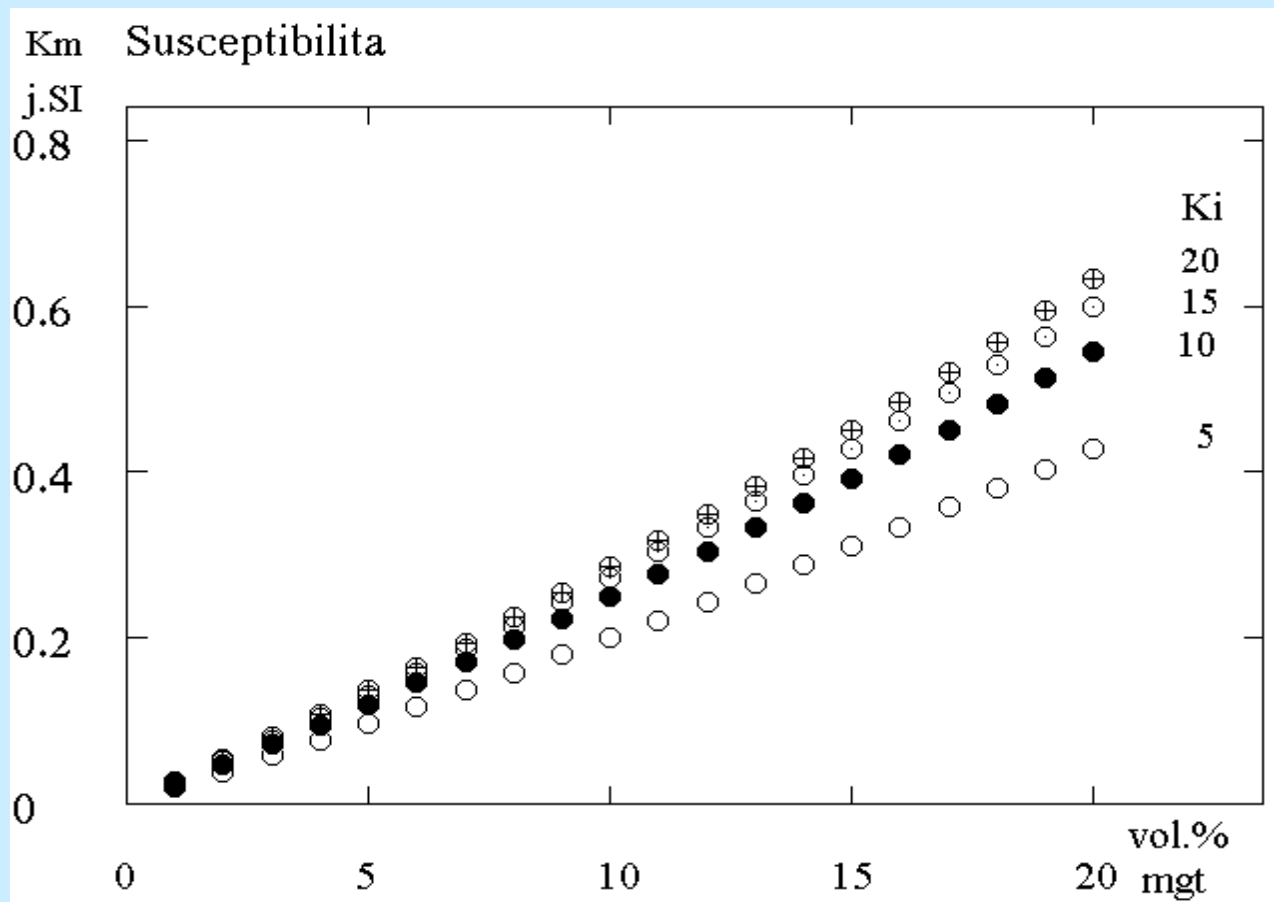
Oxidace ferimagnetických minerálů v horninách



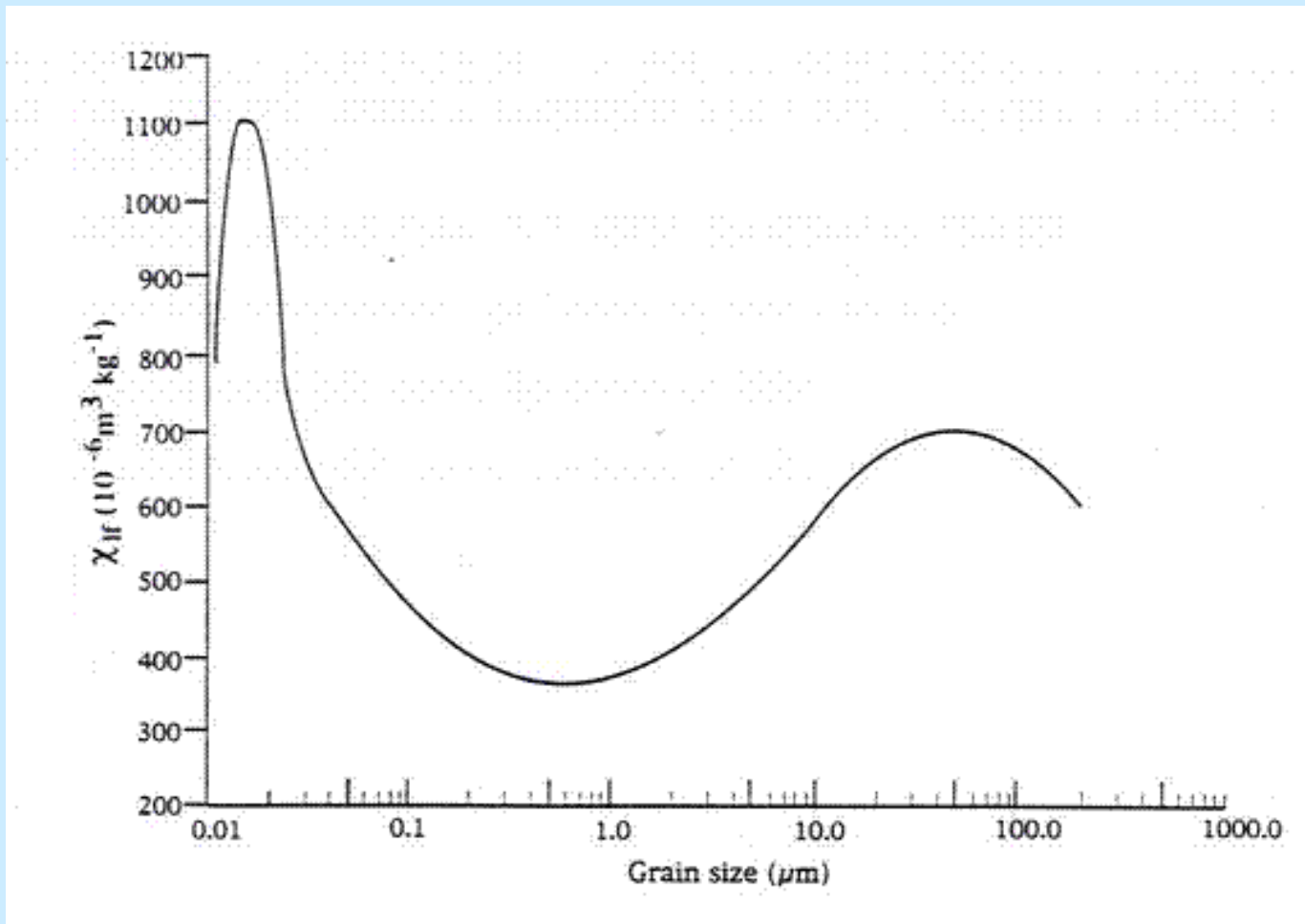
Hemoilmenit s magnetitem z lokality Orlík u Humpolce (foto V. Procházka)

Tenké lamely hemoilmenitu (šedé) v hematitu (světlý), magnetit je černý.

Bulk susceptibility and magnetite content

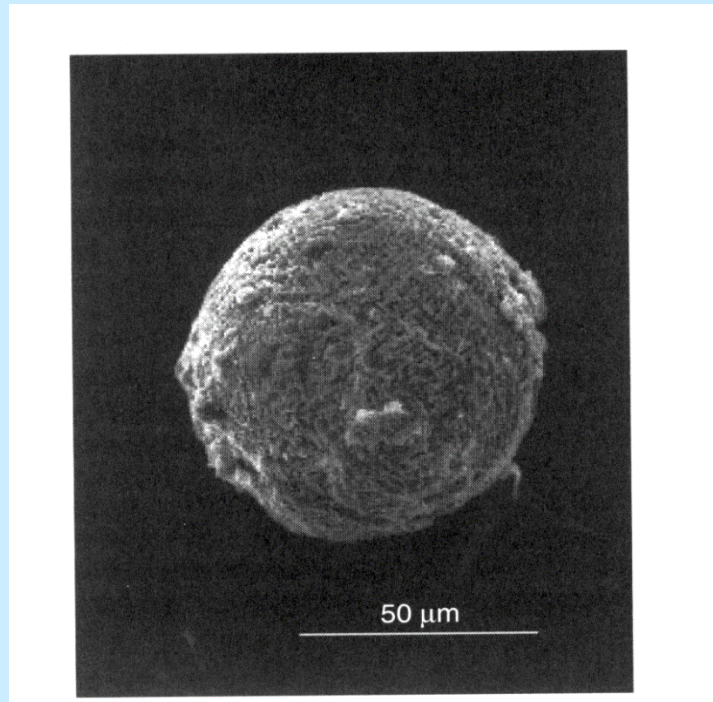


Závislost susceptibility na velikosti zrna



Iron-rich spherule

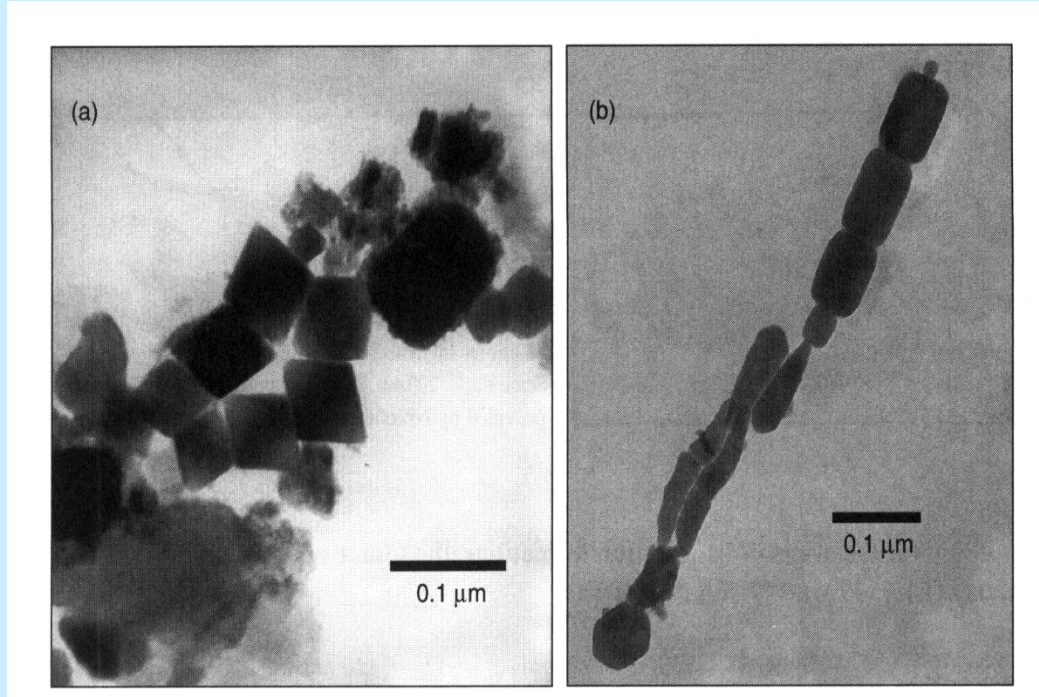
Magnetic spherule from
the topsoil from Jaworzno power
Station (Poland)



Bacterial magnetites

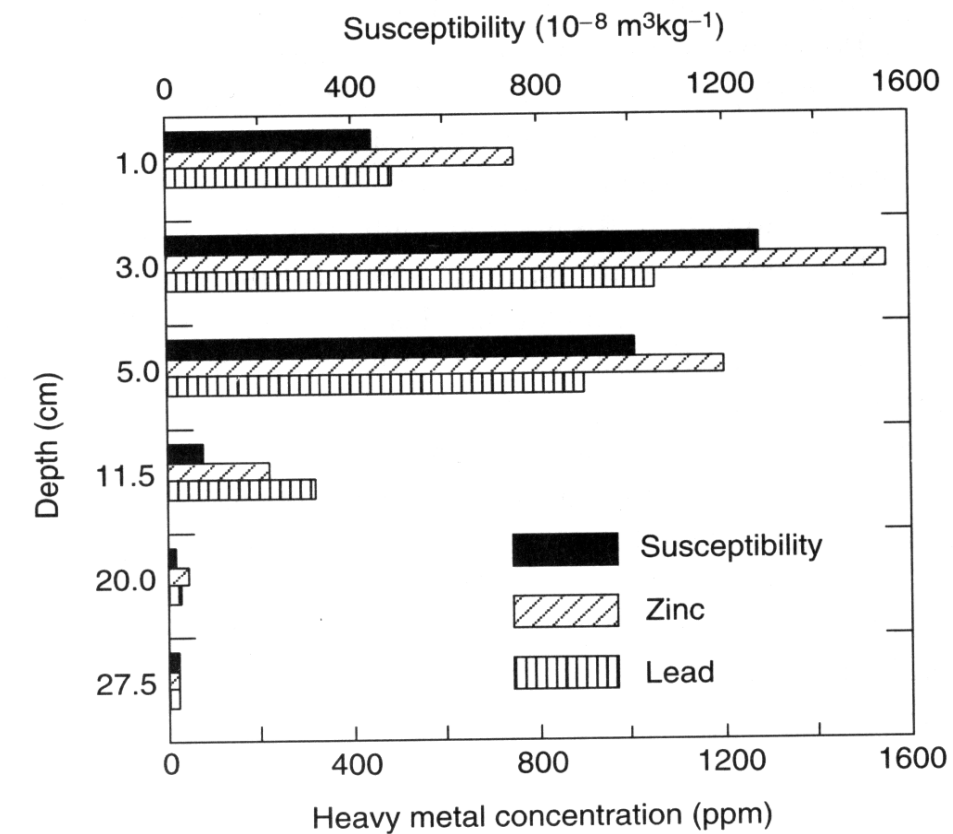
TEM images of different shapes of bacterial magnetites in a core from the Tasman Sea, 4520 m water depth

Different species produce different shapes of magnetosome particles



Susceptibility and HM pollution

Correlation of magnetic susceptibility with lead and zinc contents in a soil pit near Jaworzno power station (Poland)

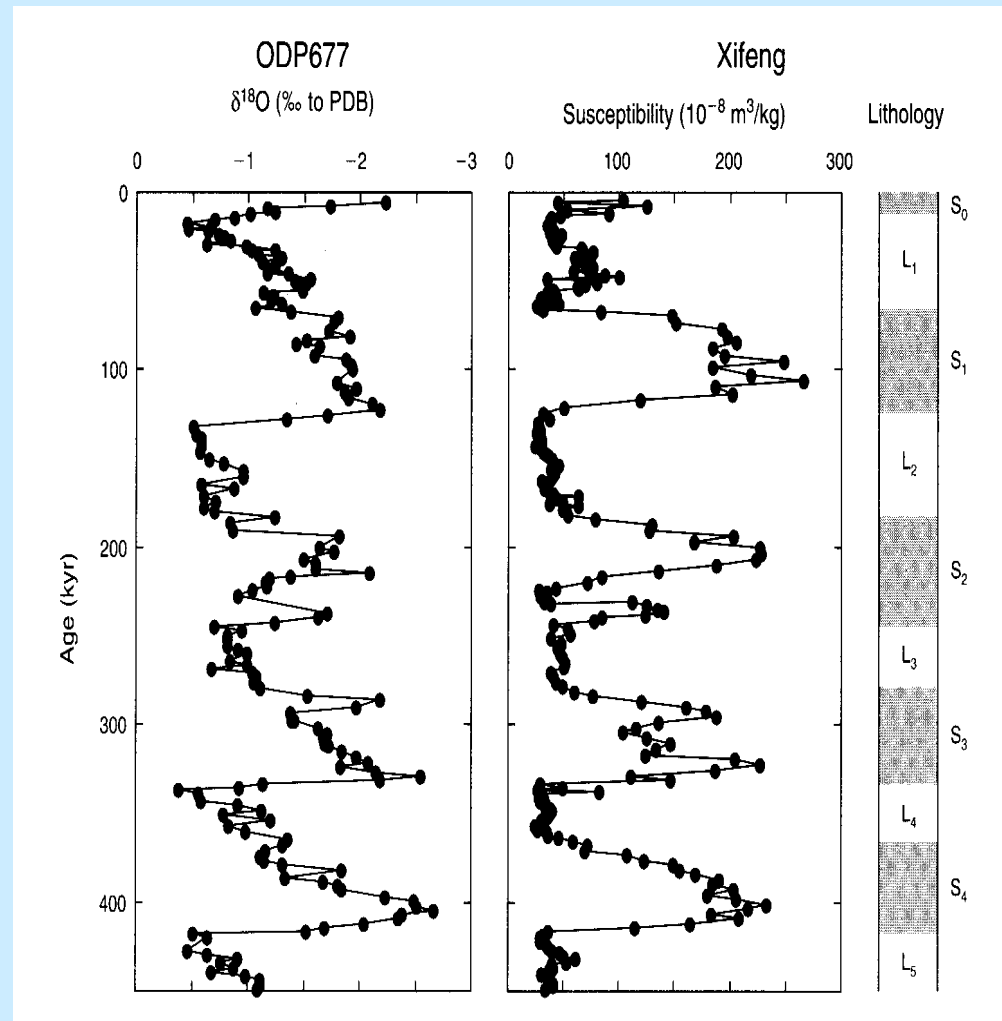


Susceptibility profile, China

Susceptibility profile at Xifeng, China, compared with oxygen isotope profile

The sequence of soils (S) and Loess (L)

Age in kYr, mass susceptibility in $10^{-8} \text{ m}^3/\text{kg}$



GEOLOGICAL APPLICATIONS OF MAGNETIC SUSCEPTIBILITY

Geological Mapping of Magnetically Different Rocks

Delineation of Metamorphic Zones

Discrimination of I-type and S-type Granites

Indication of Alteration Processes

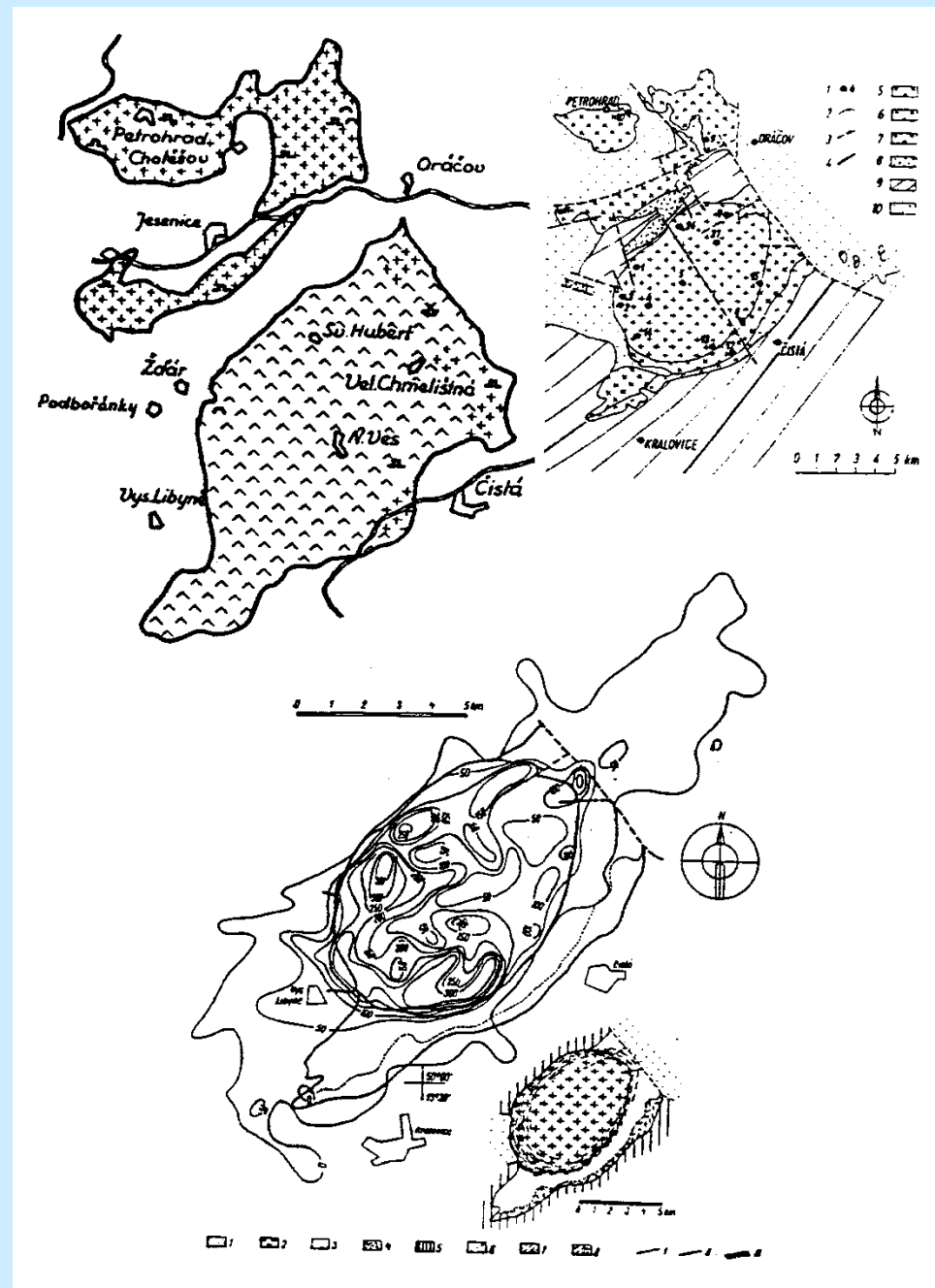
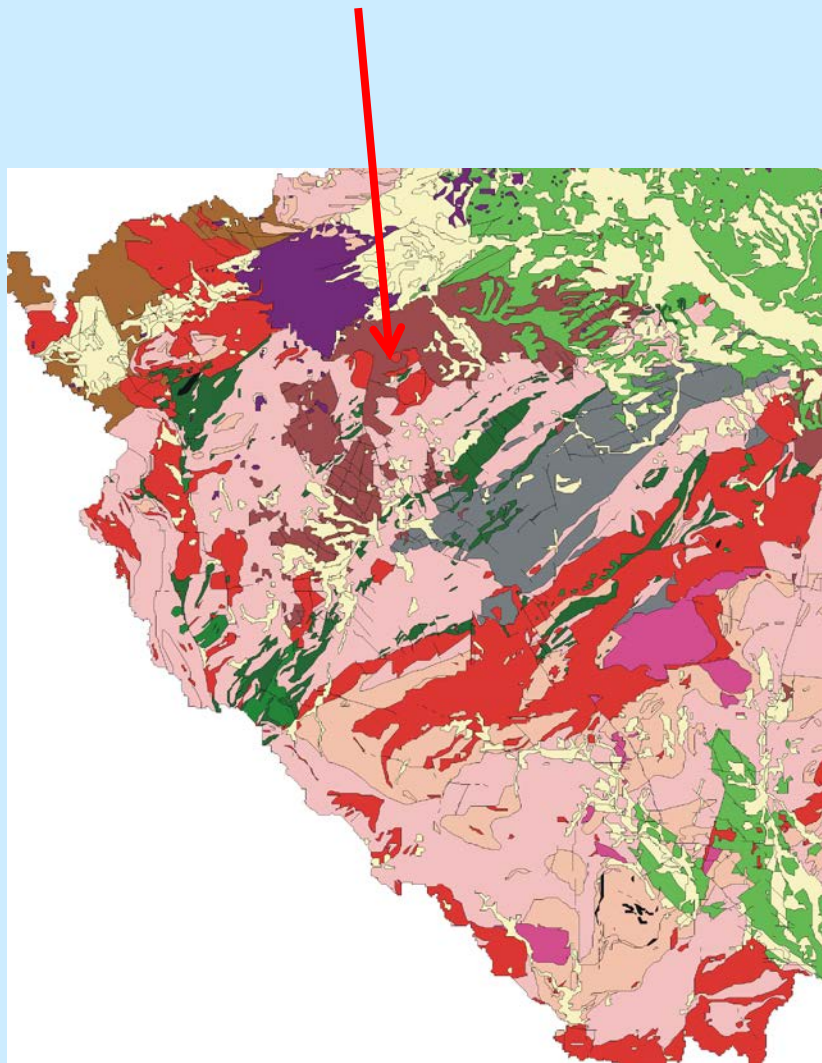
Tracing Metasomatic Changes

Interpretation of Magnetometric Anomalies

Application to Volcanology

Susceptibility in Economic Geology

Čistá - Jesenice Pluton



Granite Classifications

20 Classification and occurrence

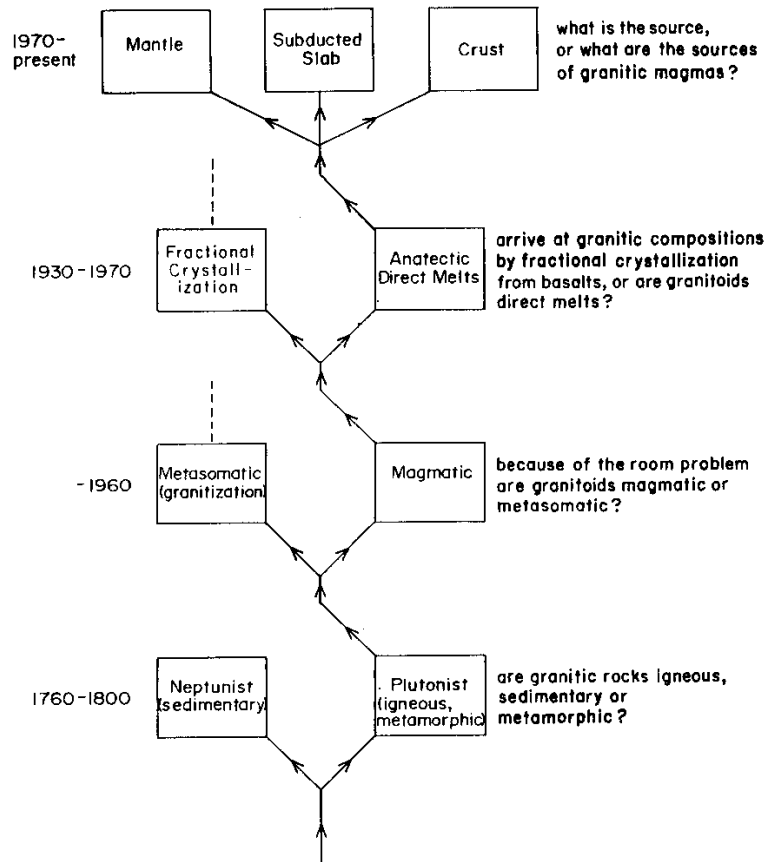
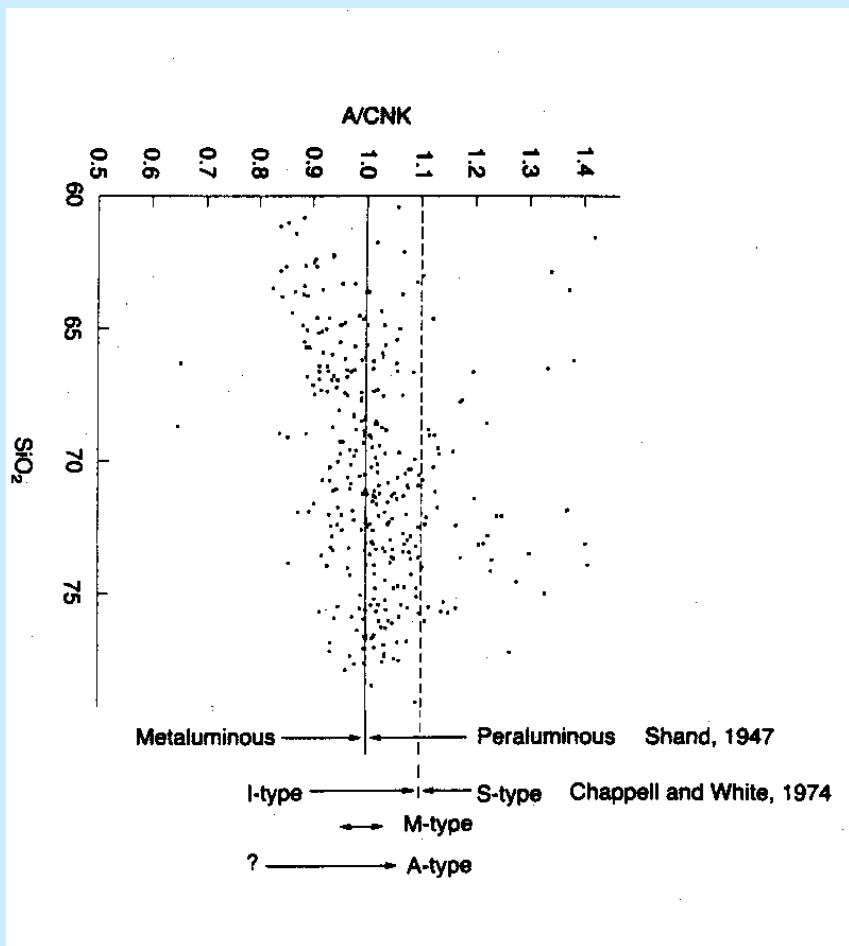


Fig. 1.6 Schematic flow chart to show the evolution of the granite problem over the past 200 years. Philosophical dead-ends have no exits; ideas that are largely discredited as general explanations, but which may still apply in specific cases, have dashed exit lines.

(after Clarke, 1992)

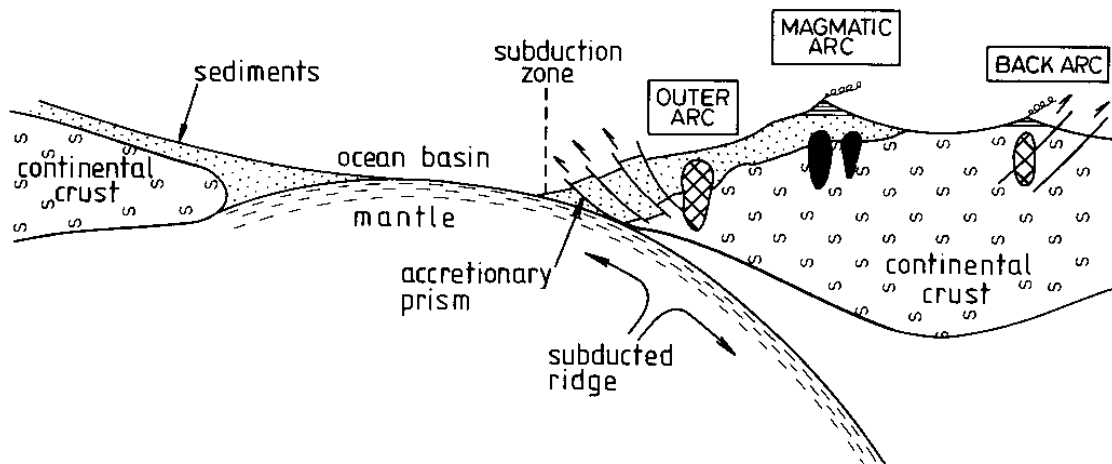


Granite Tectonic Setting (*I* and *S* Types)

(after Beckinsale & Mitchell, 1981)

Chapter 7

a) Pre-collision



b) Post-collision

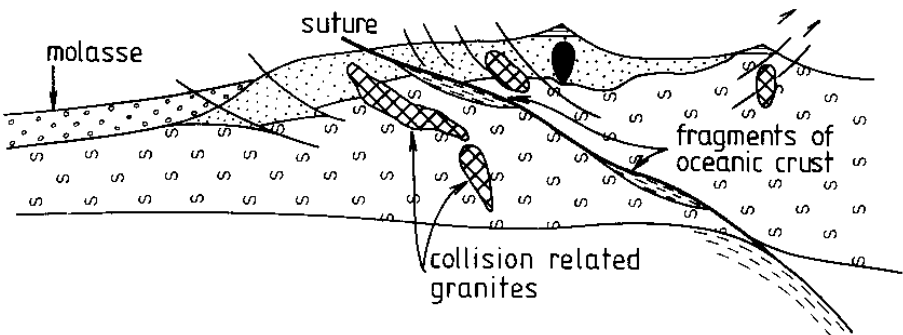


Fig. 7.1. Plate tectonic settings for magmatism and mineralisation. I-type granites black; S-type granite cross-hatched.

Magnetite and Ilmenite Series Granites

26

W.S. Pitcher

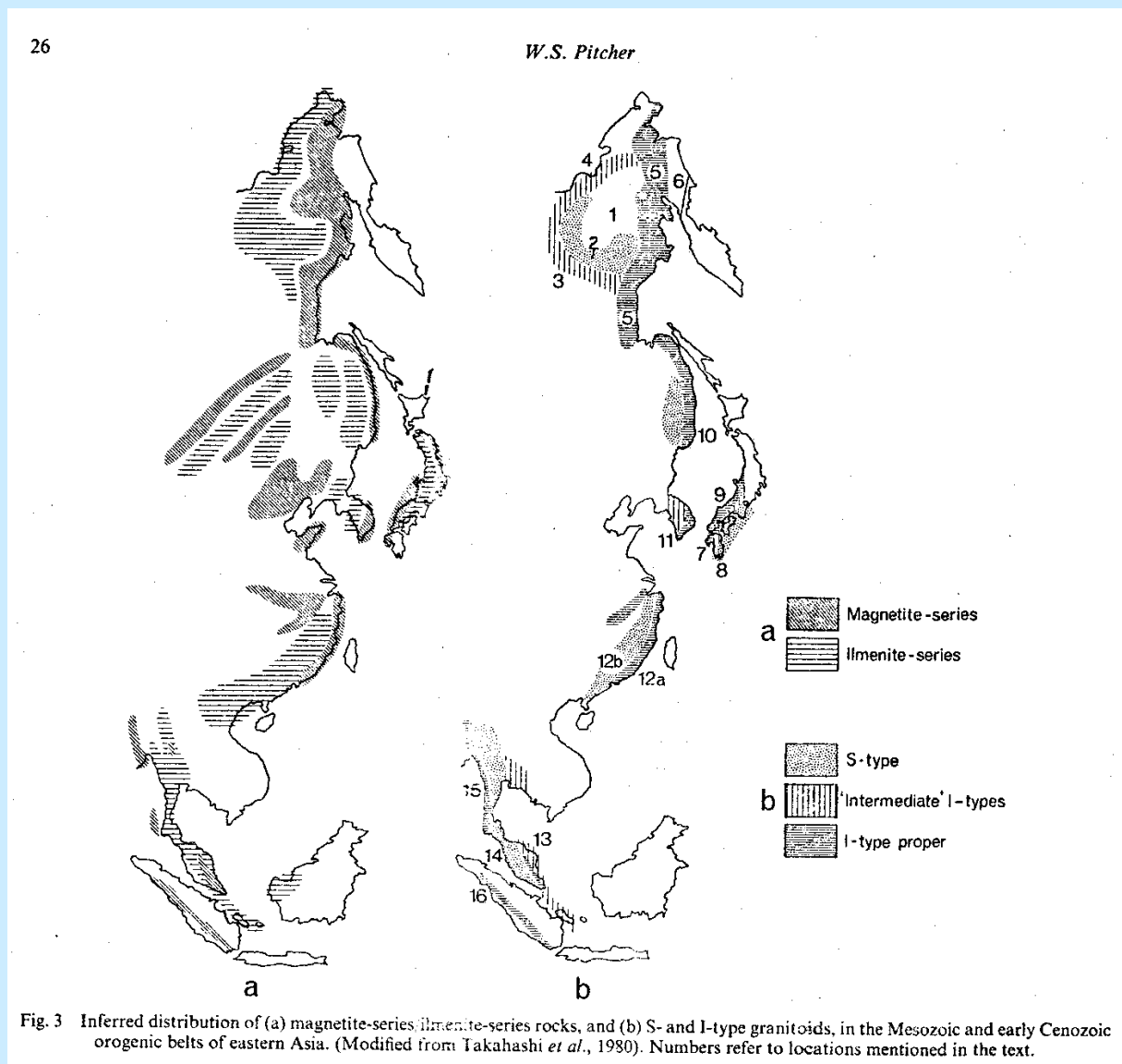
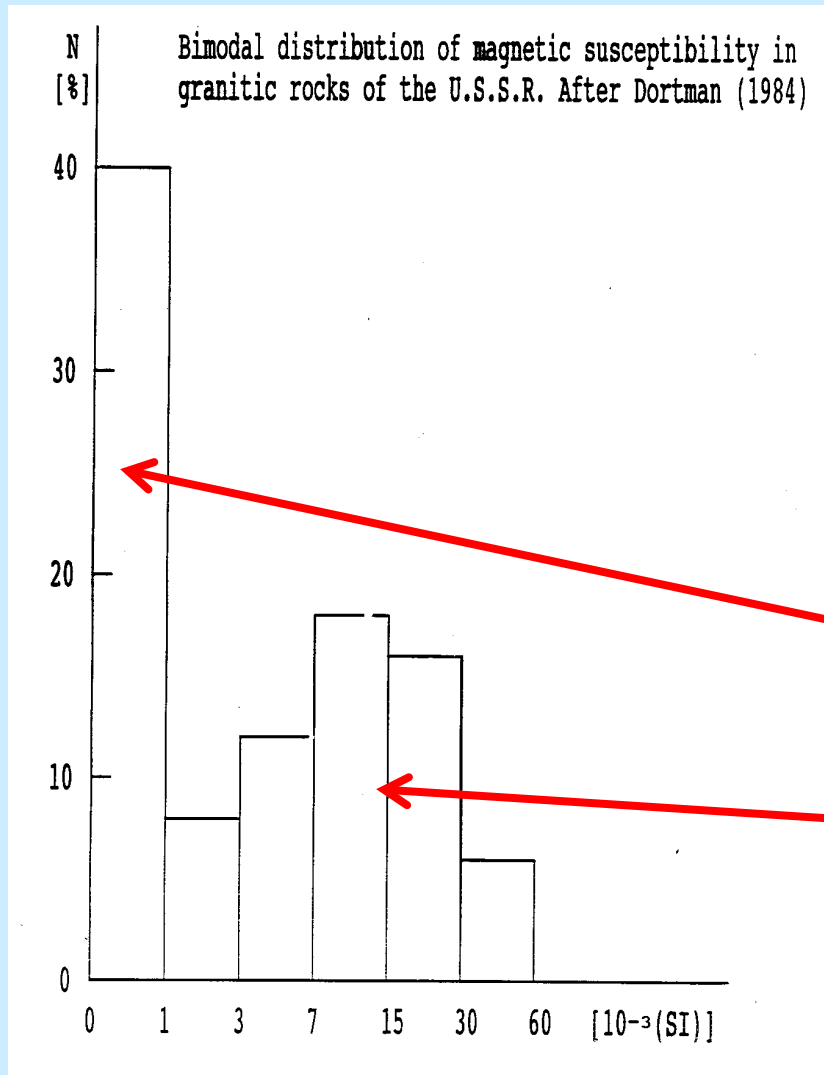


Fig. 3 Inferred distribution of (a) magnetite-series ilmenite-series rocks, and (b) S- and I-type granitoids, in the Mesozoic and early Cenozoic orogenic belts of eastern Asia. (Modified from Takahashi *et al.*, 1980). Numbers refer to locations mentioned in the text.

Magnetic Susceptibility in Granites



Magnetic susceptibility of granites is extremely variable, ranging from 10^{-6} [SI] to 10^{-1} and displaying a bimodal distribution.

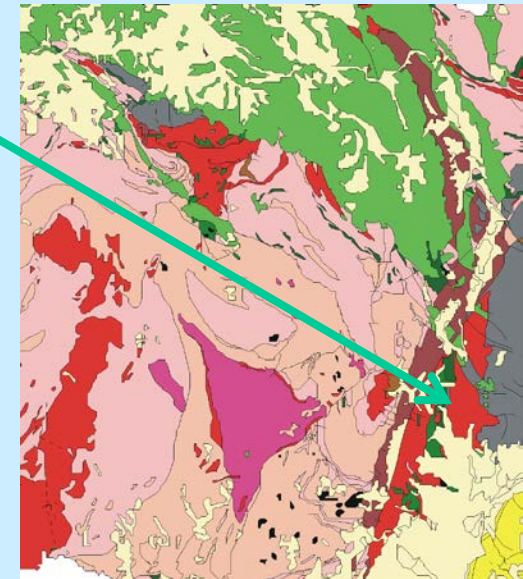
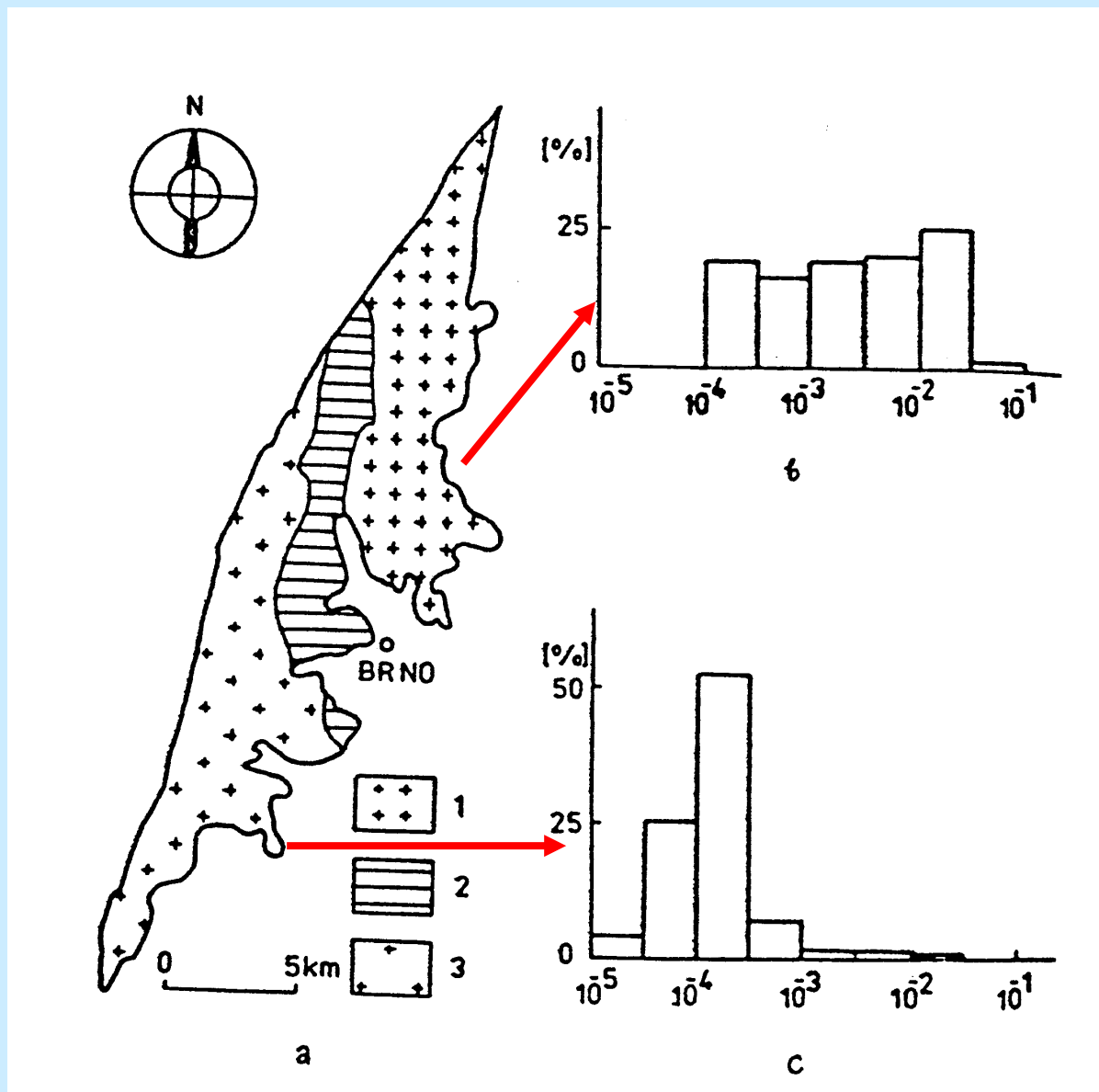
Weakly Magnetic Granites (Dortman)

Paramagnetic Granites (Bouchez)

Magnetic Granites (Dortman)

Ferromagnetic Granites (Bouchez)

Brno Massif

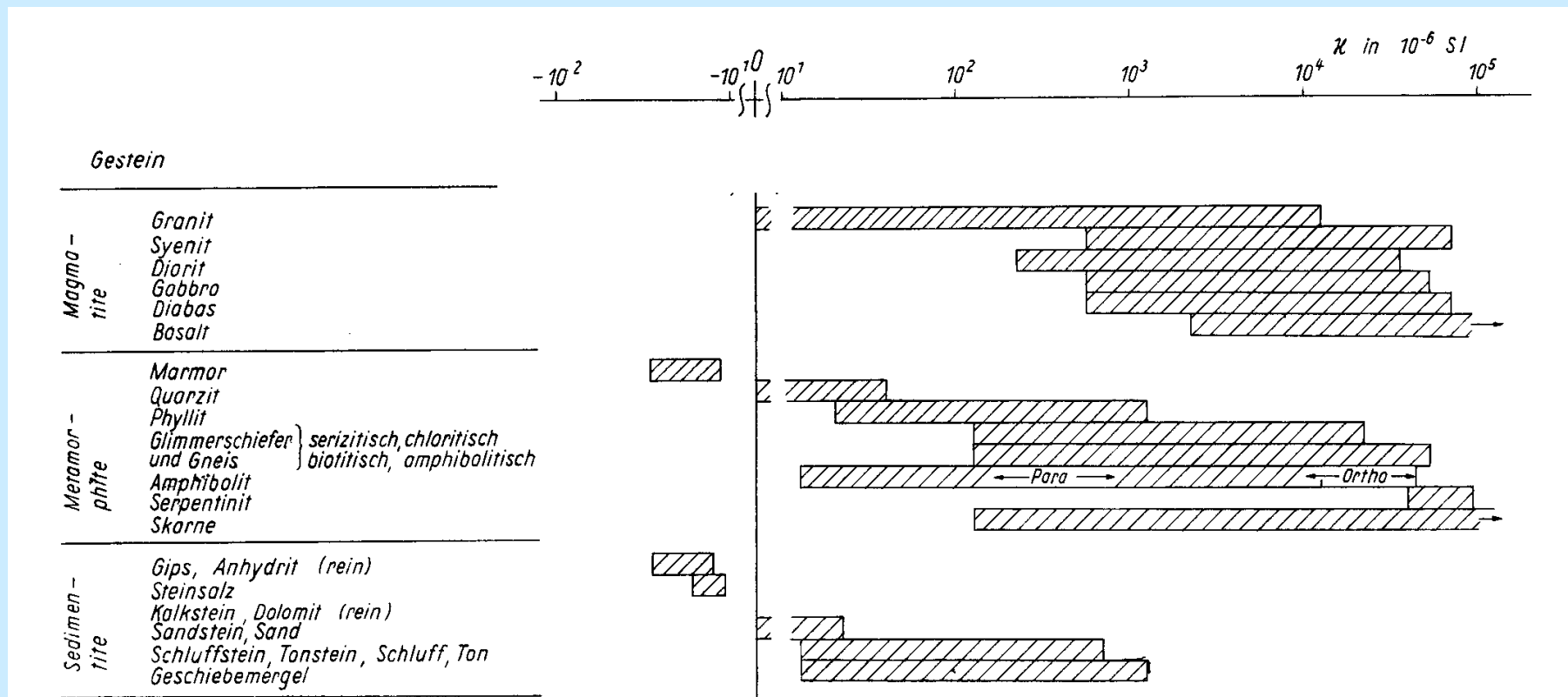


1 - Eastern Zone
2 - Metabasite Z.
3 - Western Zone

Eastern Zone
magnetic

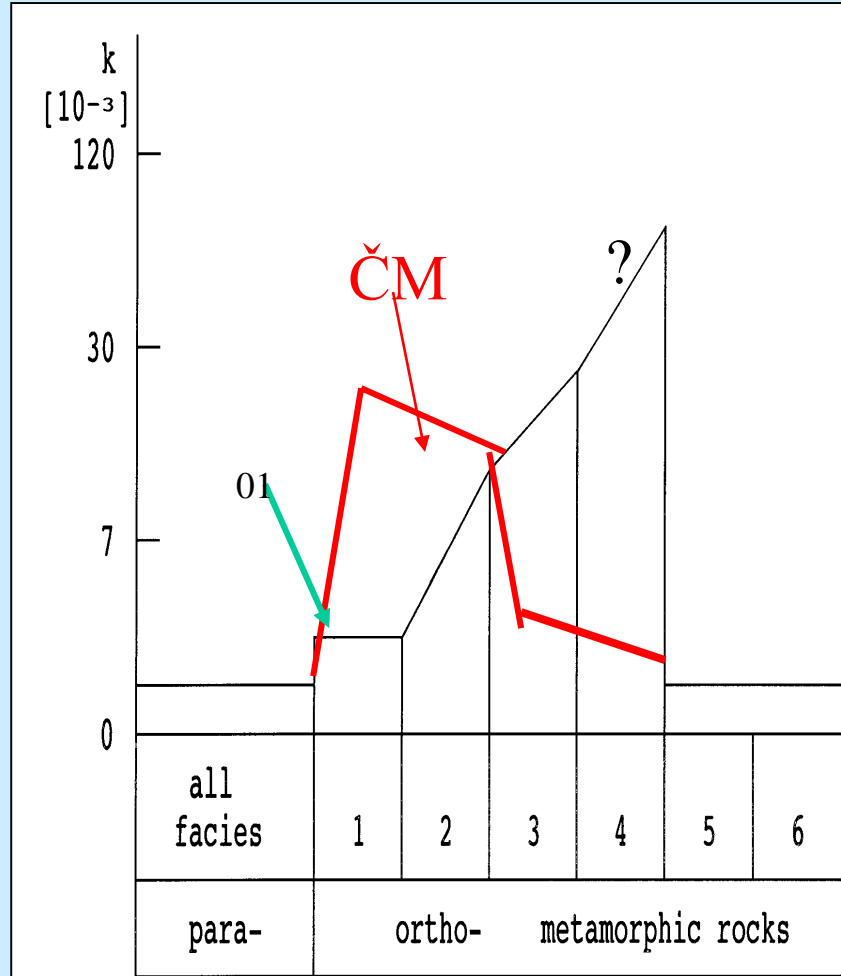
Western Zone
weakly magnetic

Magnetic Susceptibility in Various Rocks



Magnetic Susceptibility in Metamorphic Rocks

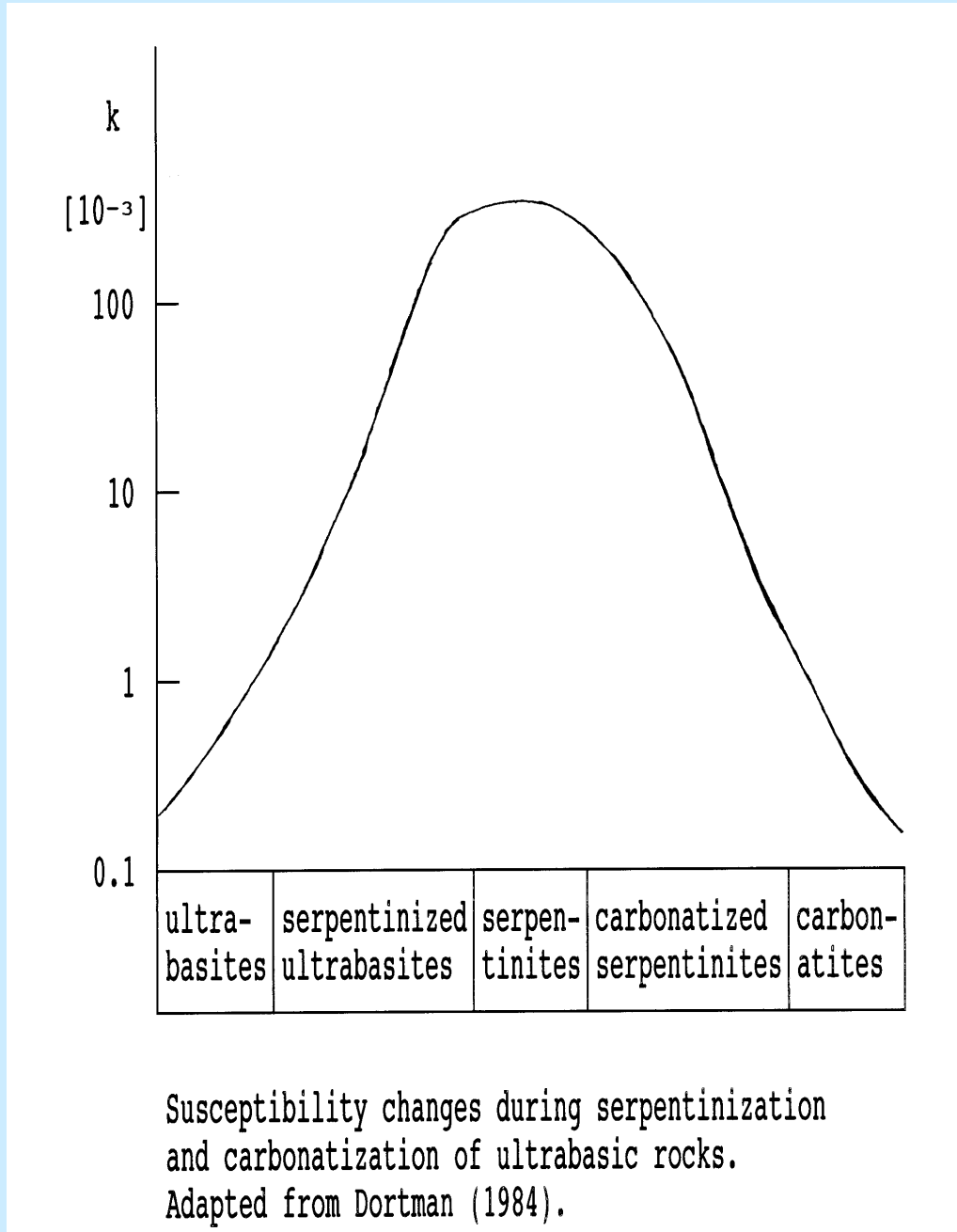
Susceptibilita anomálních ortometamorfitů stoupá zpravidla až do amfibolitové facie. V ČM mají granulty, i ty tmavé, jen zvýšenou susceptibilitu.



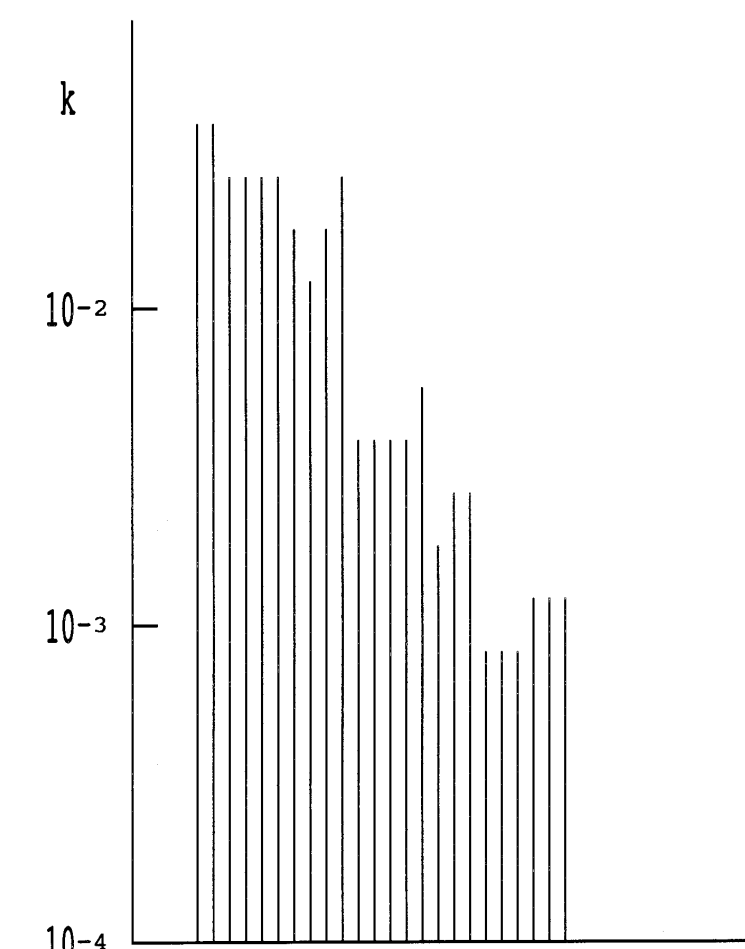
Magnetic susceptibility variation in metamorphic rocks.
Adapted from Dortman (1984).

Legend: 1 - green schist facies, 2 - epidote amphibolite facies,
3 - amphibolite facies, 4 - granulite facies,
5 - granulite-eclogite facies, 6 - eclogite facies
01 - bazika od extruze k prehnit-pumpellyitové facii

Magnetic Susceptibility in Serpentinized and Carbonatized Ultrabasic Rocks

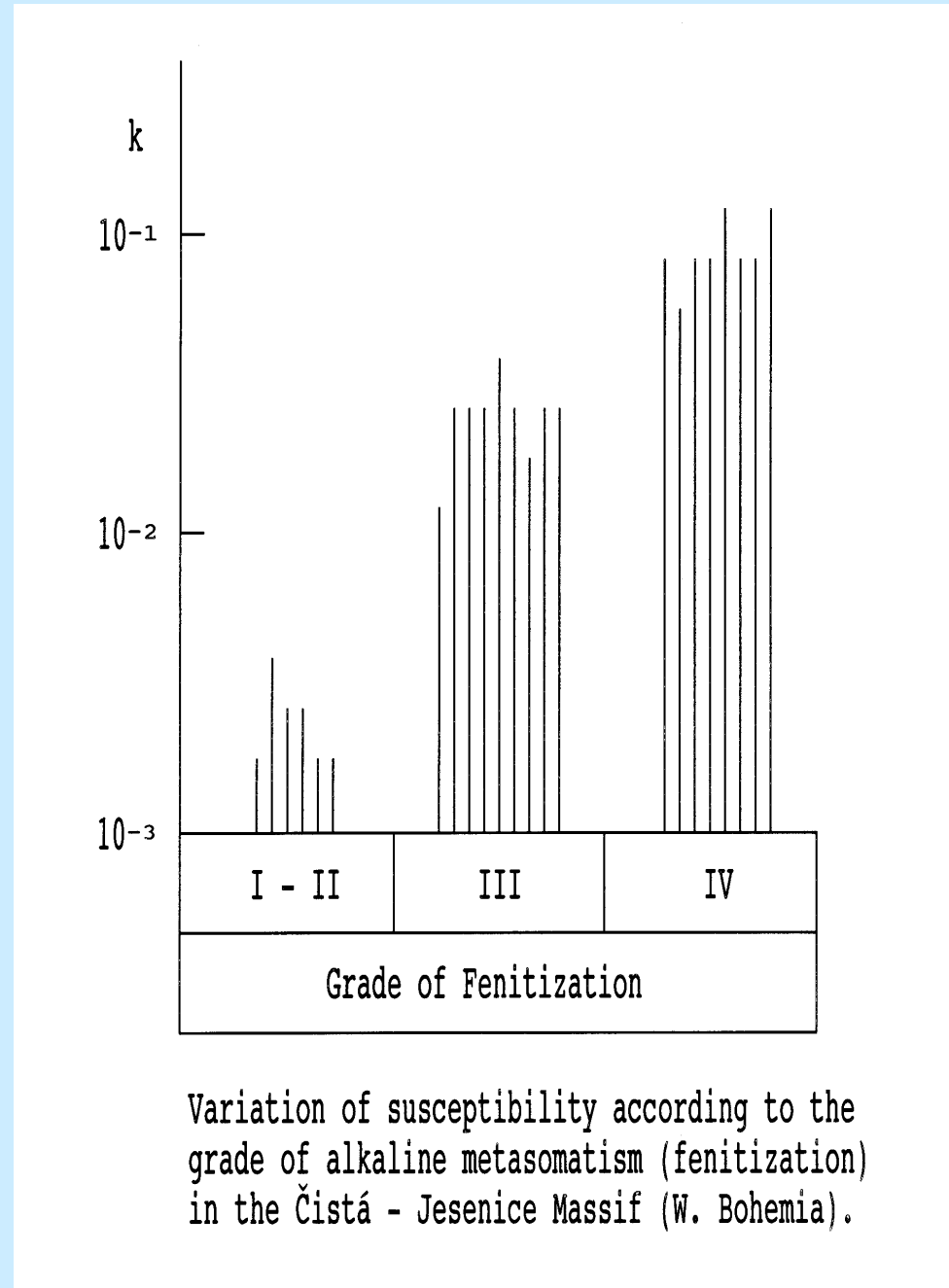
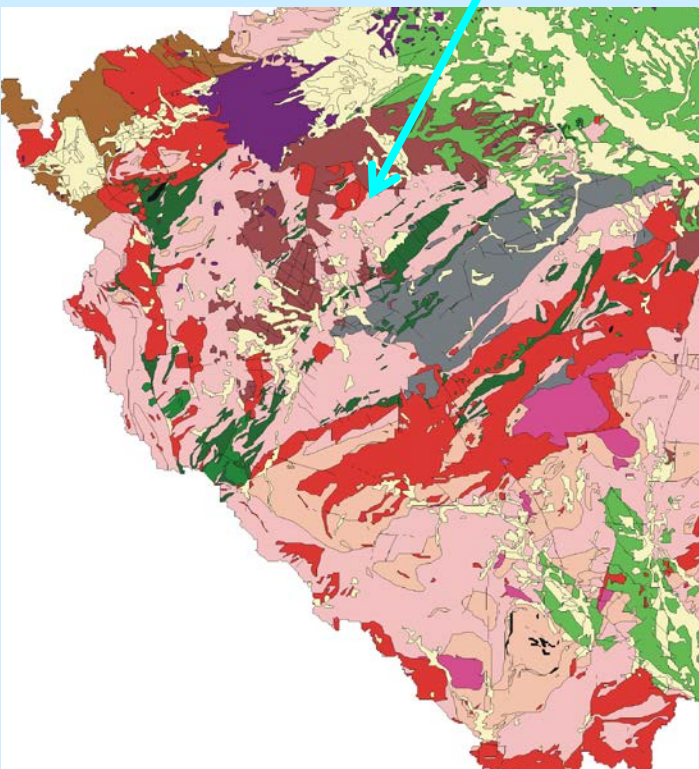


Magnetic Susceptibility in Altered (propylitized) Andesites

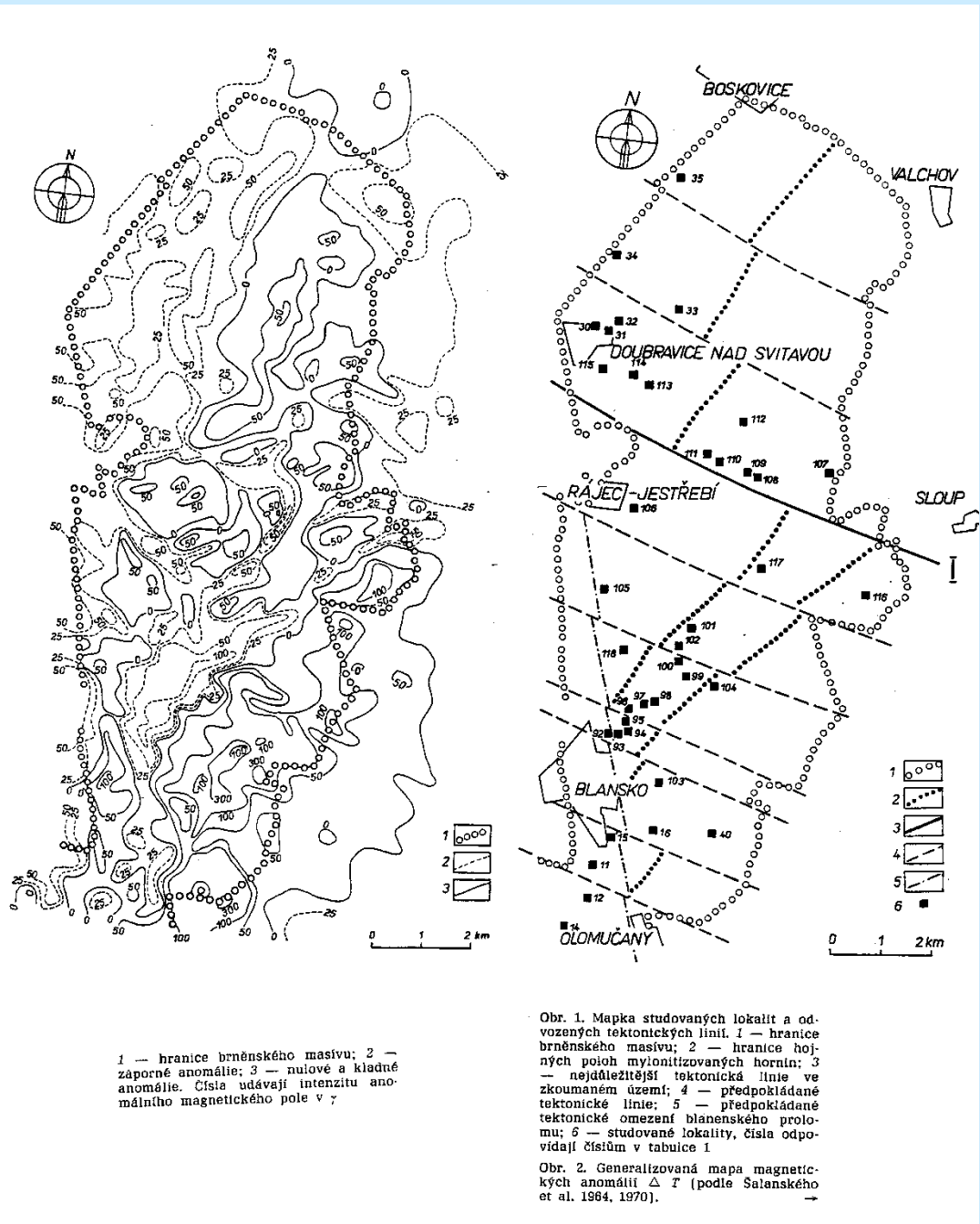
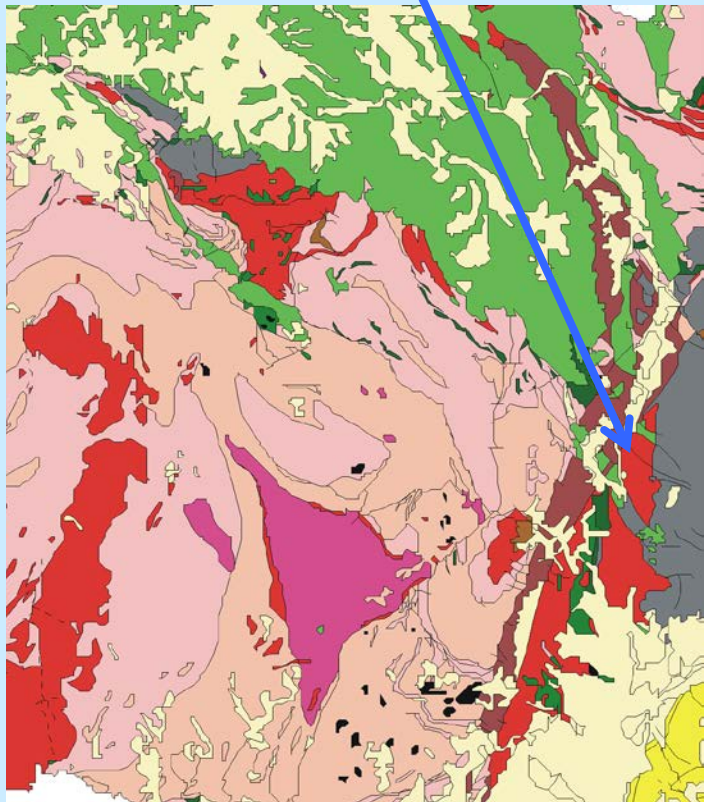


Magnetic susceptibility in non-altered
and altered andesites of the West Carpathians.
Compiled from data of Drs. Ondra and Hanák.

Magnetic Susceptibility in Rocks that Underwent Alkaline Metasomatism



Magnetic Susceptibility and Magnetometry

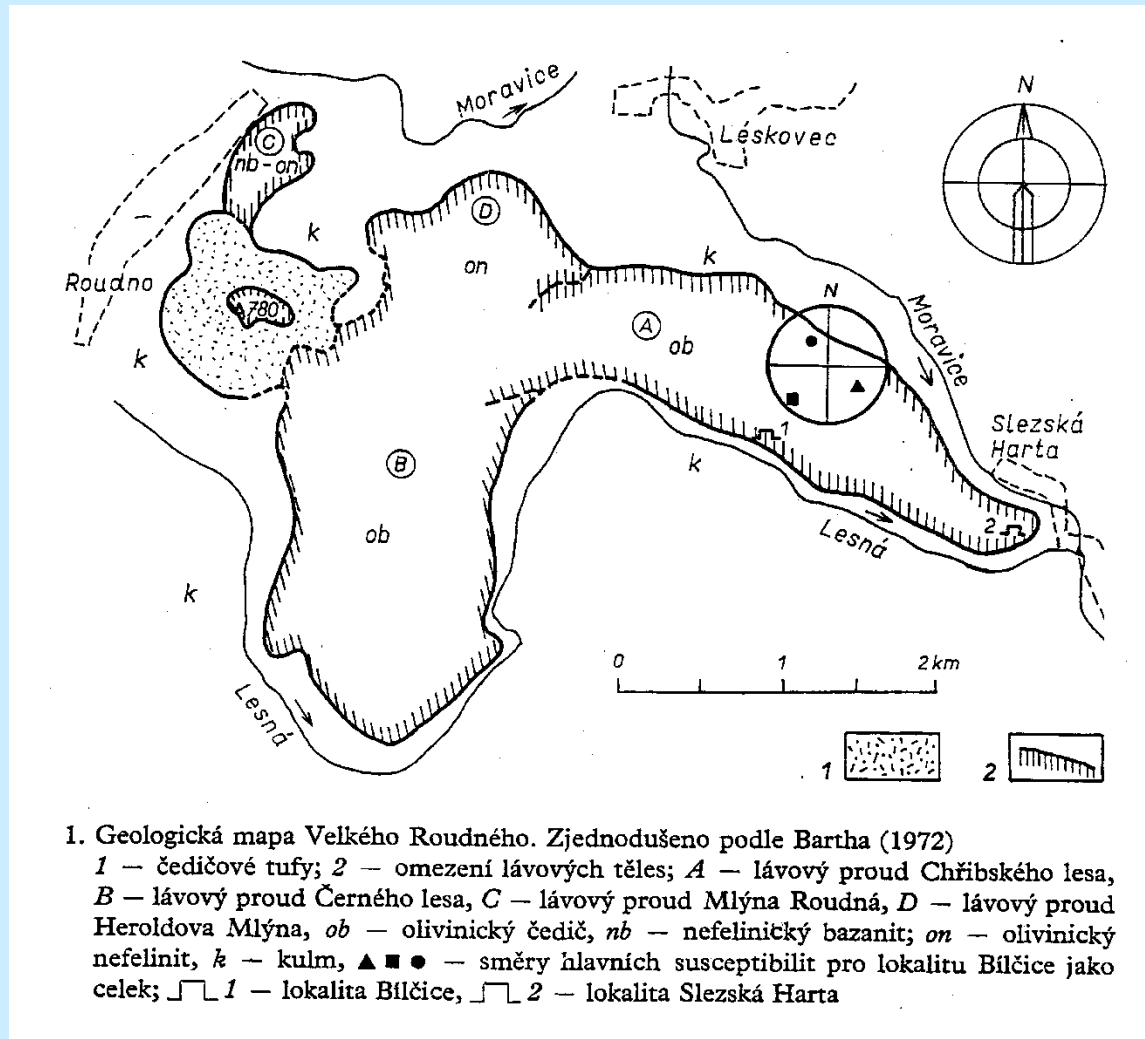


1 — hranice brněnského masívu; 2 — záporné anomálie; 3 — nulové a kladné anomálie. Císla udávají intenzitu anomálního magnetického pole v γ .

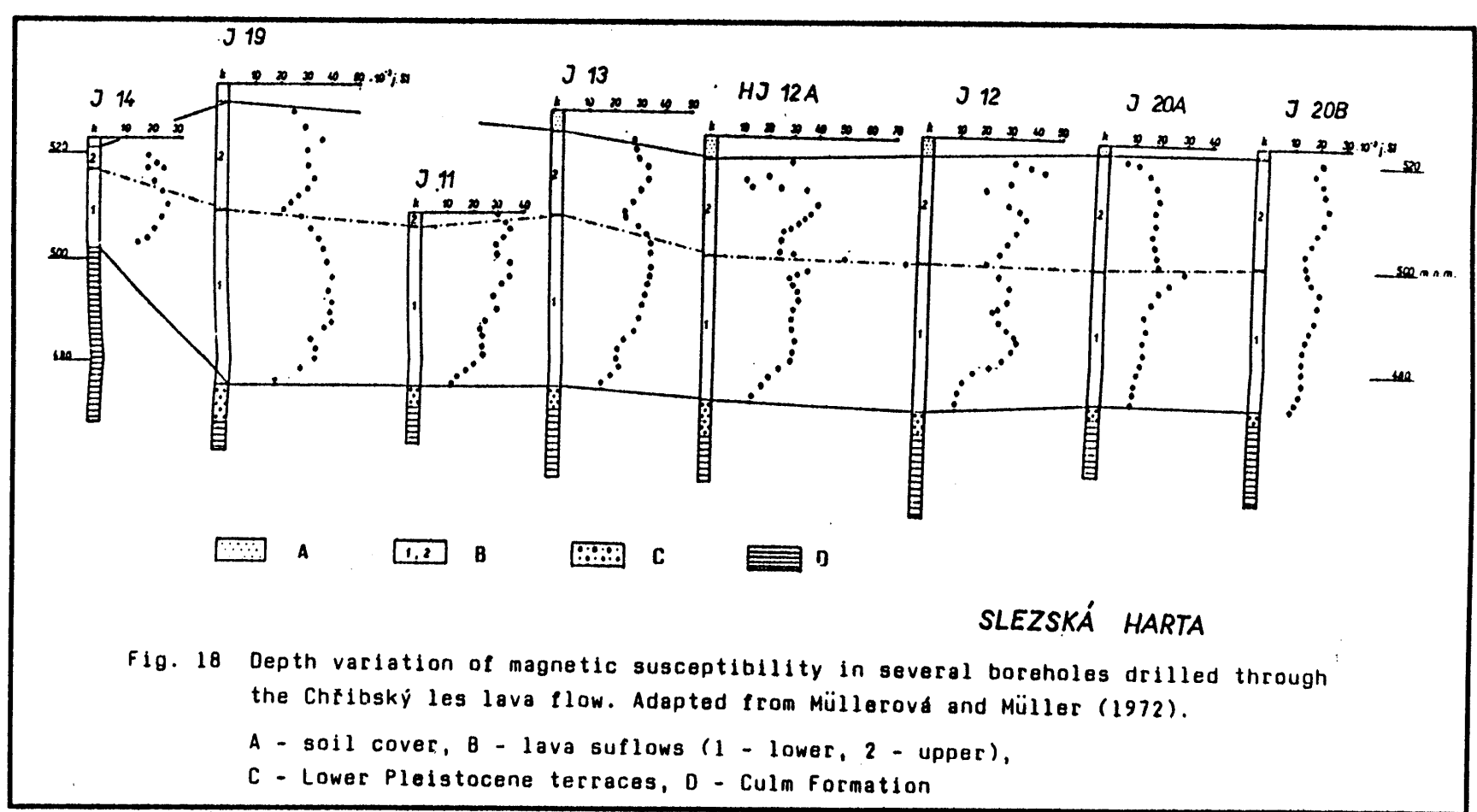
Obr. 1. Mapka studovaných lokalit a odvozených tektonických liní. 1 — hranice brněnského masívu; 2 — hranice bojňových pojoh mylonitizovaných hornin; 3 — nejdůležitější tektonická linie ve zkoumaném území; 4 — předpokládané tektonické linie; 5 — předpokládané tektonické omezení blanenského proluwu; 6 — studované lokality, čísla odpovídají čísům v tabulce 1

Obr. 2. Generalizovaná mapa magnetických anomalií ΔT (podle Salanského et al. 1964, 1970).

Magnetic Susceptibility in Lava Flows 1



Magnetic Susceptibility in Lava Flows 2



Sulphide Deposits

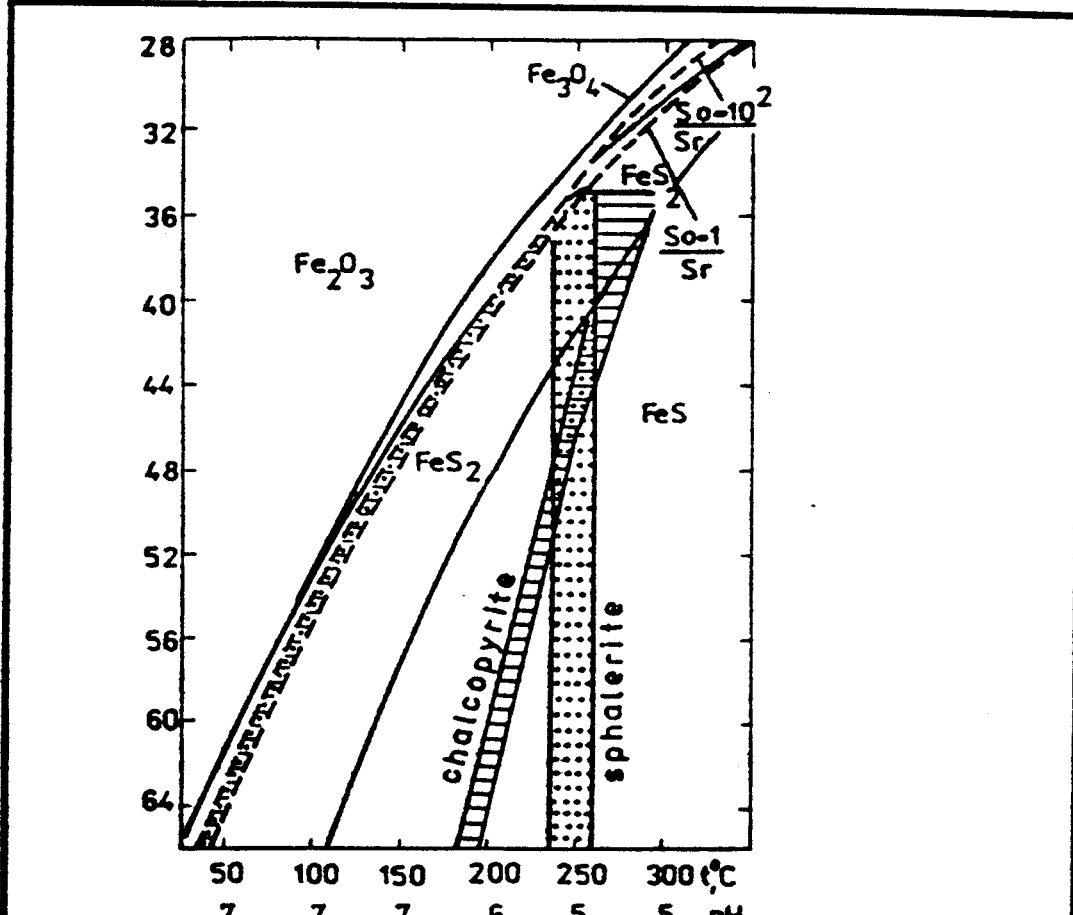


Fig. 19 Creation of volcanic-metasomatic, volcanic-sedimentary sulphide deposits during variable PH factor and temperature and constant concentrations of $\xi S = 10^{-2}$ mol and $\text{NaCl} = 1$ mol.
Adapted from Smirnov (1982)

Magnetic Susceptibility in Environs of Sulphide Deposits

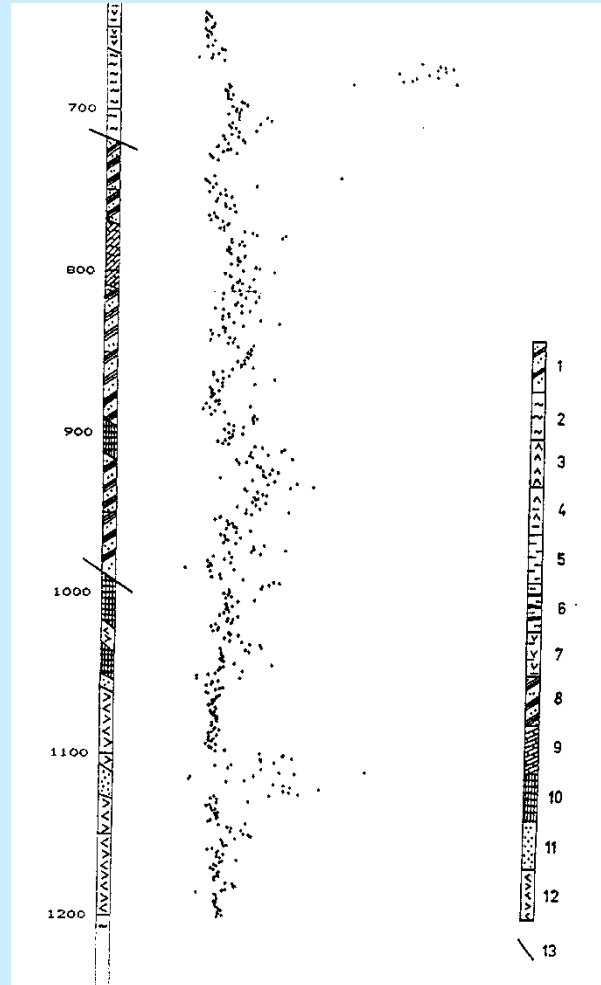
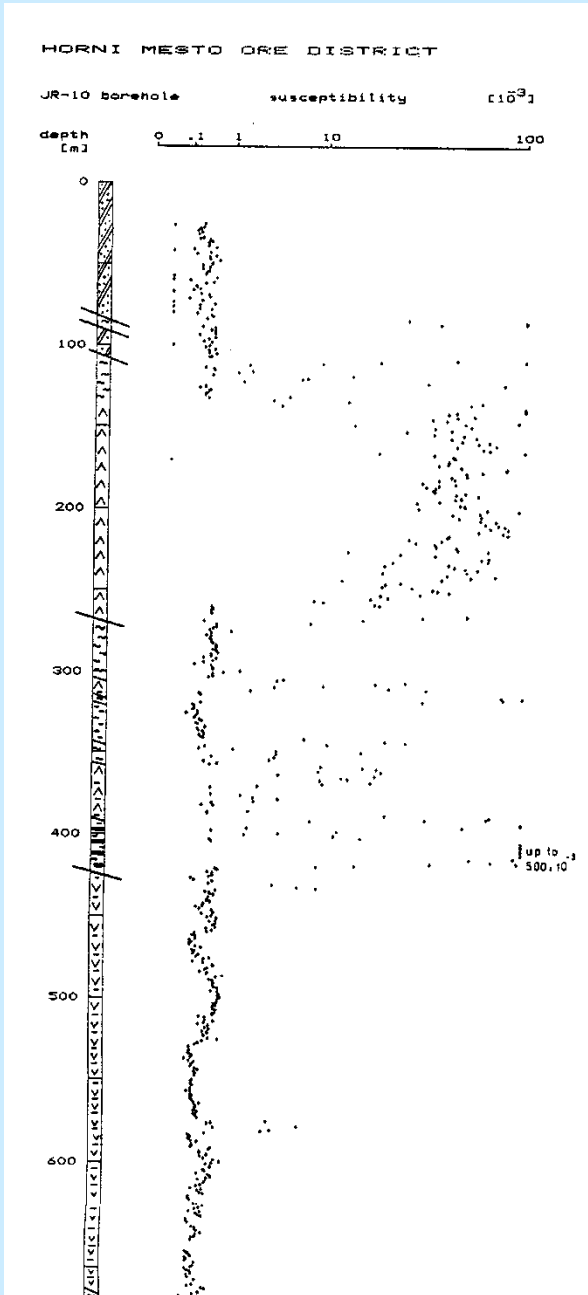


Fig. 20 Depth variation in magnetic susceptibility in the JR-10 borehole
Doln Formation

1 - psammitic to pelitic metasedimentary rocks (phyllites and metacrenwackes)

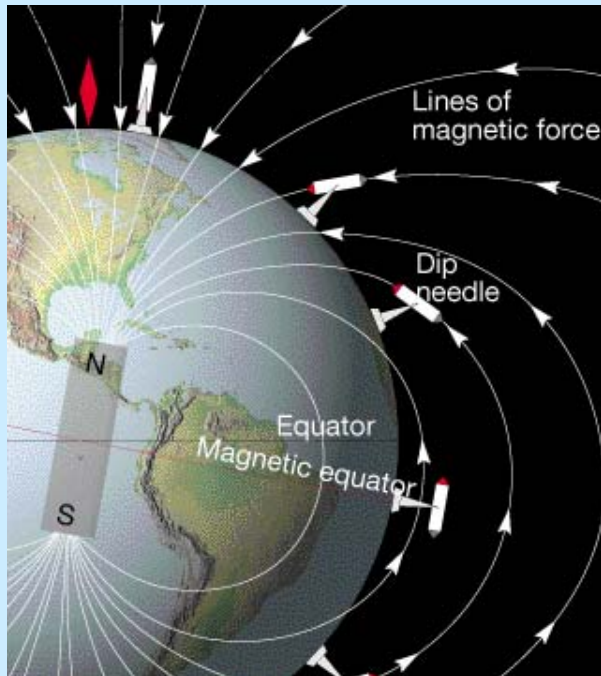
2 - chlorite slates and phyllites, 3 - metakeratophyres s.l.

(trachyanedesites and their tuffs) with magnetite and hematite,

4 - keratophyre metatuffs, mostly with magnetite + hematite,

5 - sericite slates to phyllites (metatuffites and/or strongly altered volcanic rocks), 6 - sericite slates with intercalations of metafelolites s.l. (trachyrhyolites and their tuffs) with hematite, in places albitized and silicified, 8 - metadolomites.

PALEOMAGNETISM



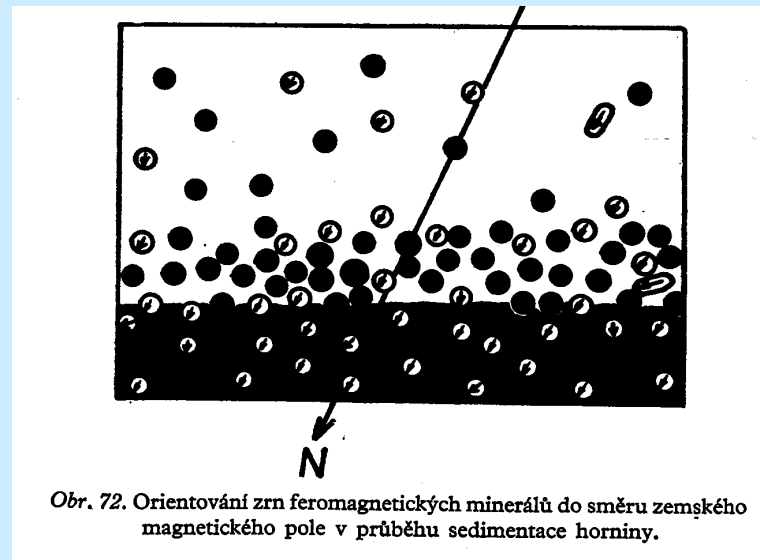
Magnetic field of the Earth - coaxial dipôle

Record in remanent magnetization (RM).

Volcanics – cooling under Curie temperature
(rock becomes ferromagnetic).

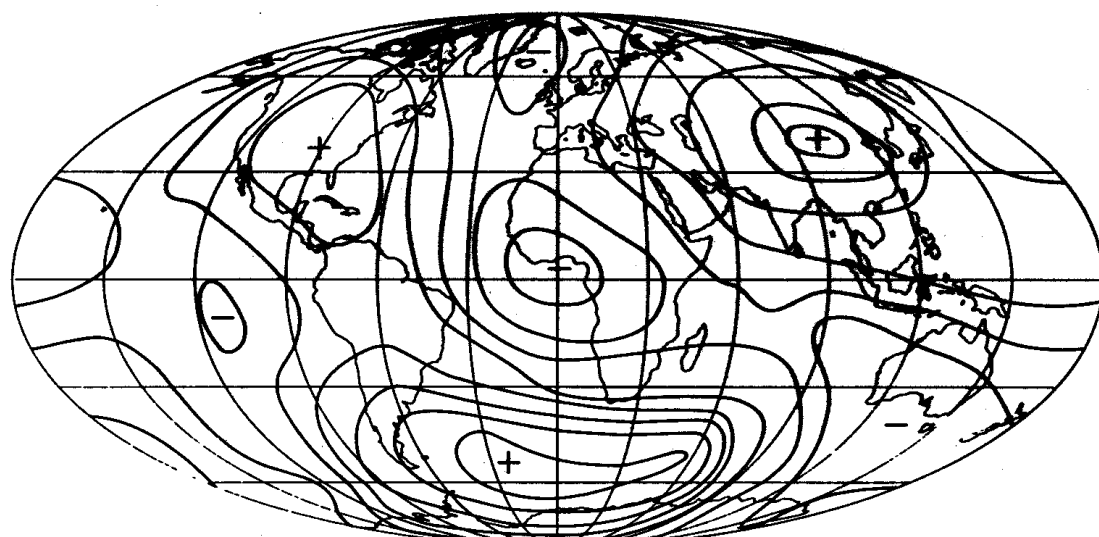
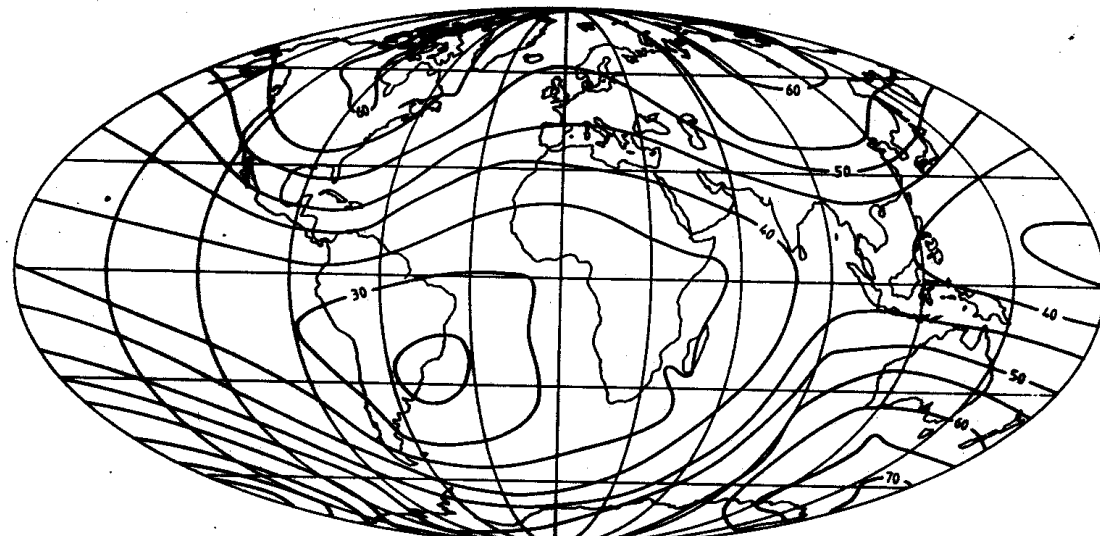
Sediments – during deposition

RM may preserve since its origin to present. Methods exist how to find whether the RM is fossil and stable.

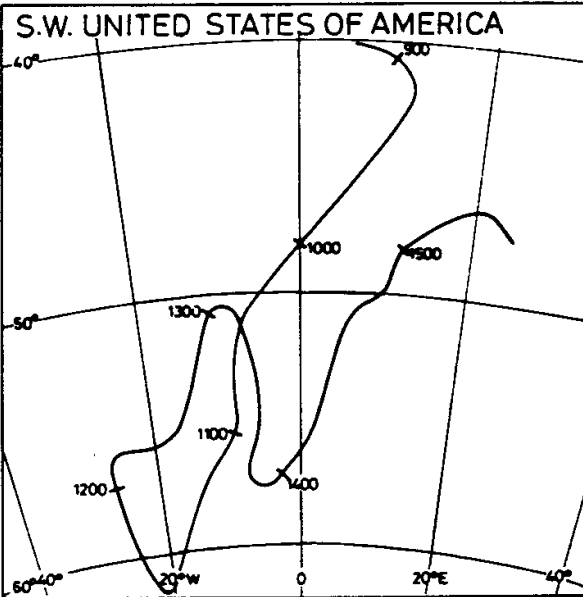
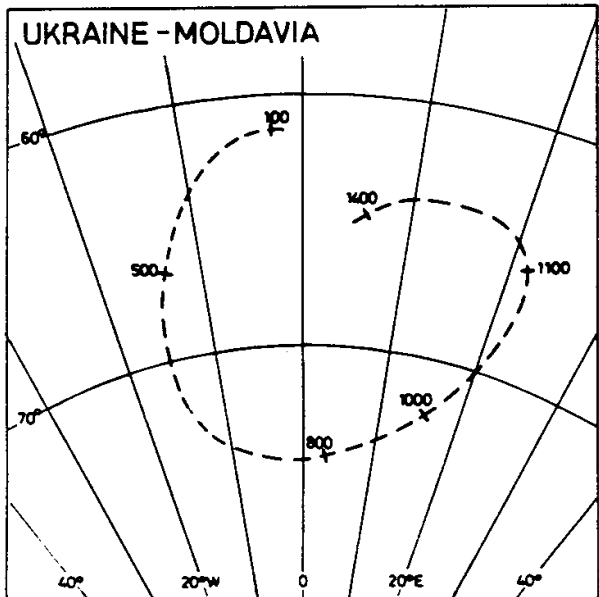
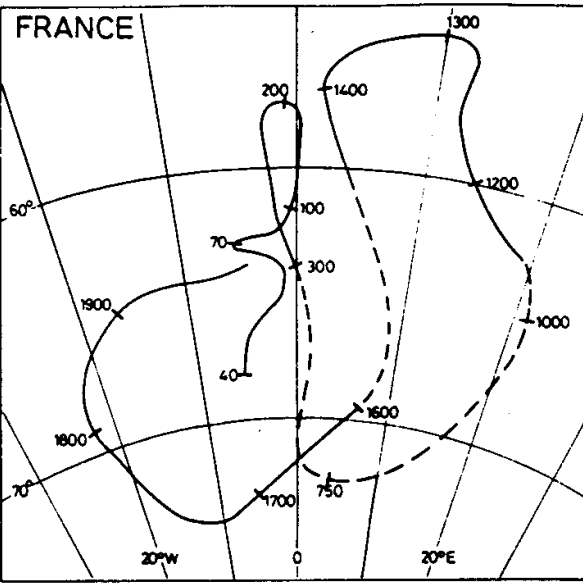
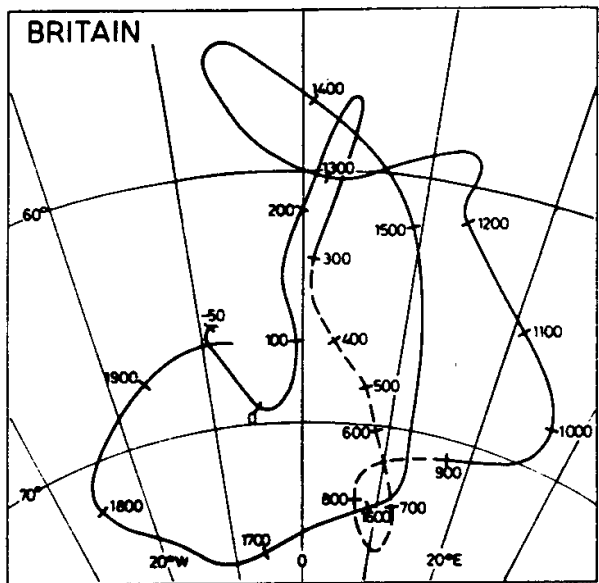


Obr. 72. Orientování zrn ferromagnetických minerálů do směru zemského magnetického pole v průběhu sedimentace horniny.

Magnetic Field of the Earth



Variations of Magnetic Field



Secular variations of directions on an archaeological time-scale.

Presentation of Palaeomagnetic Data

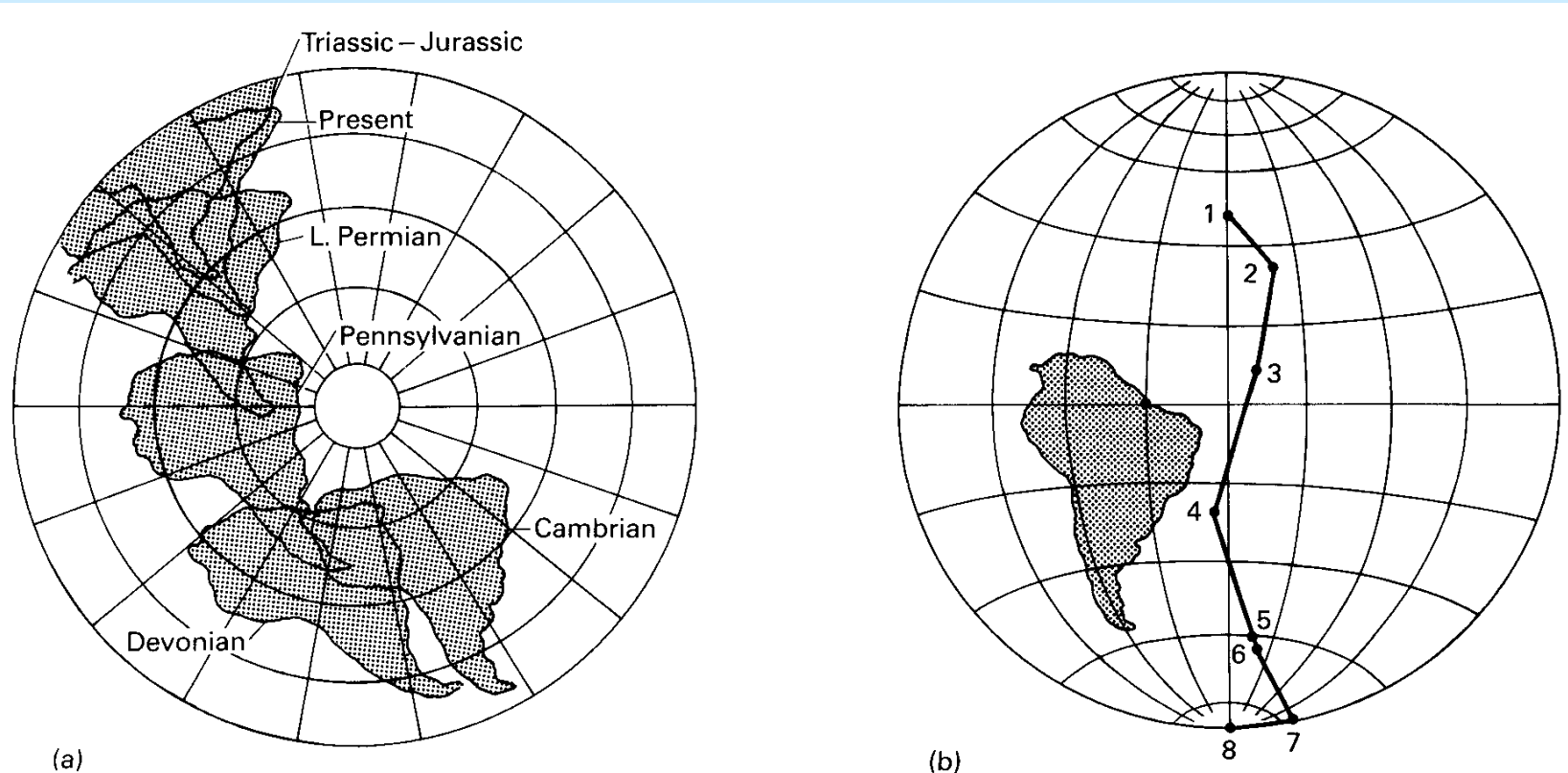
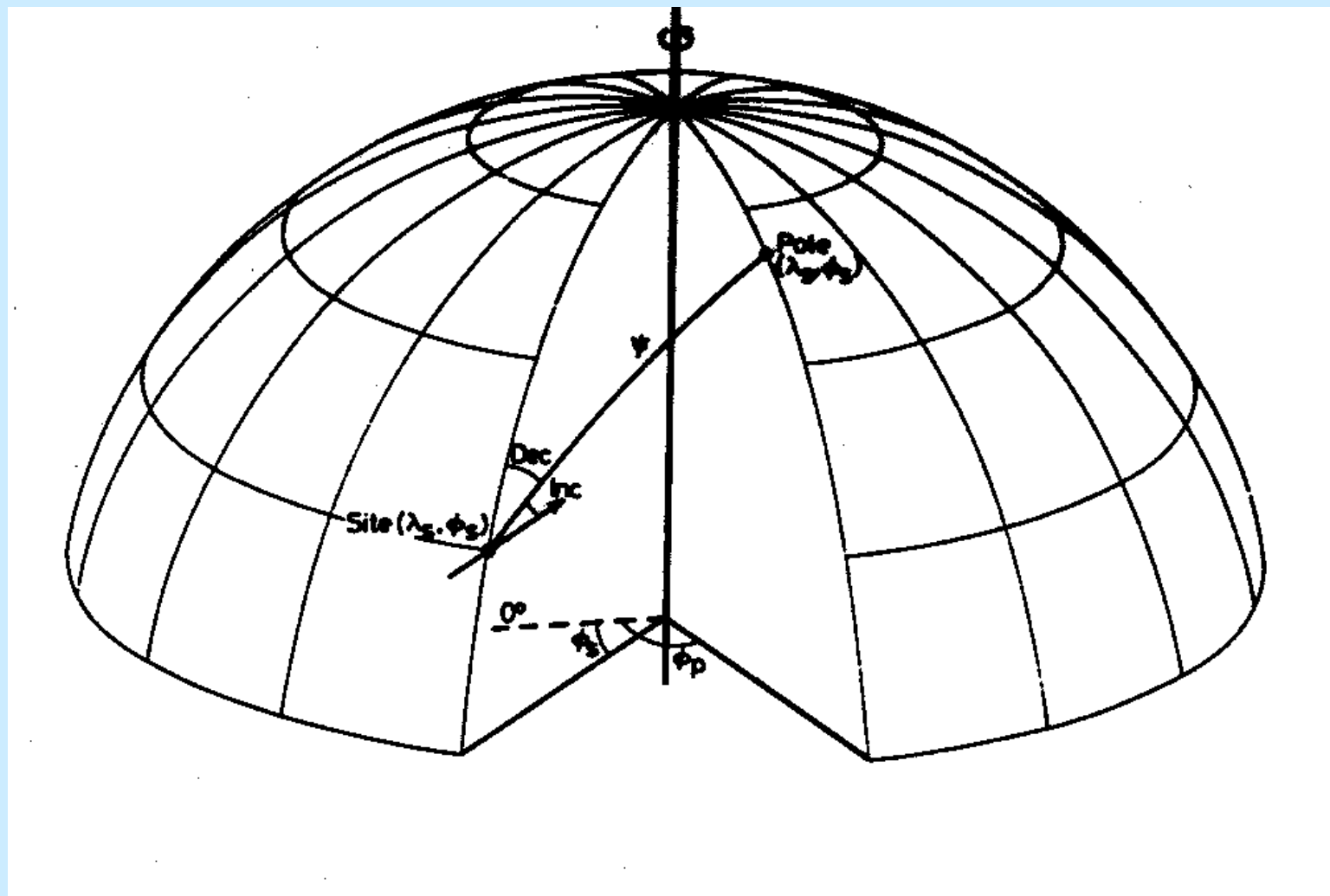


Fig. 3.13 Two methods of displaying palaeomagnetic data. (a) assuming fixed magnetic poles and applying latitudinal shifts to the continent. (b) assuming a fixed continent and plotting a polar wandering path. Subsequent work has modified the detail of the movements shown. Note that the *south* pole has been plotted (redrawn from Creer, 1965, with permission from the Royal Society).

fix pole, plate movement

fix plate, apparent pole path

Construction of Palaeopole



Apparent Polar Wandering Paths for Individual Continents

Key evidence of the continental drift.

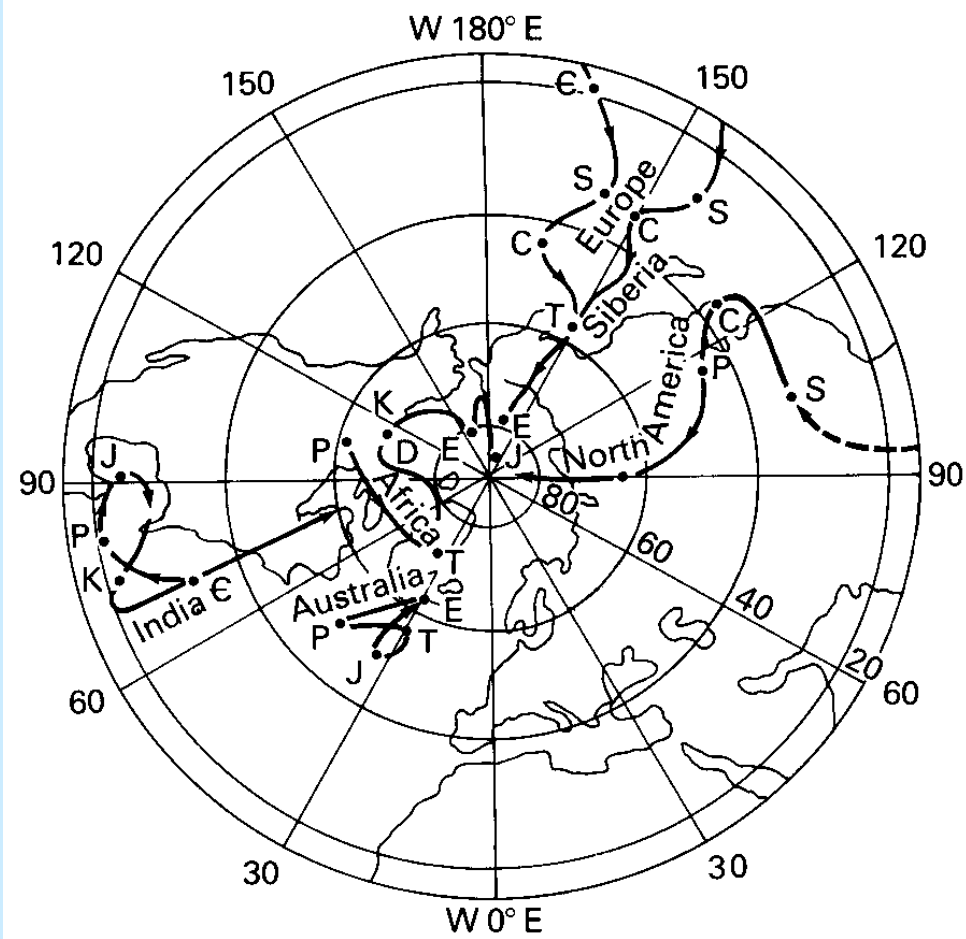
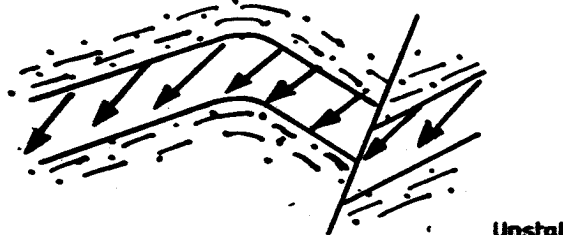
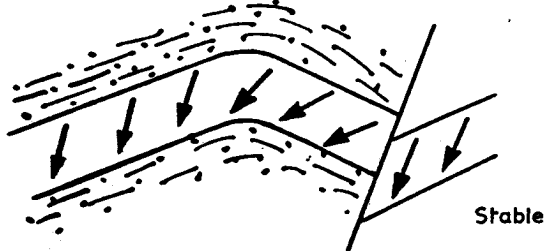
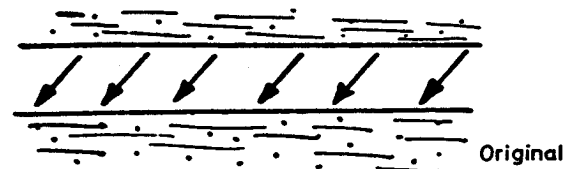
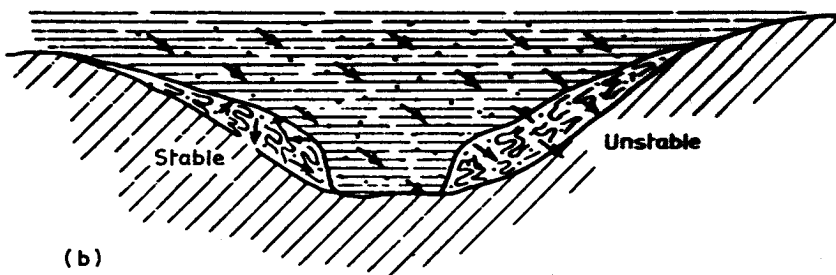


Fig. 3.14 Apparent polar wandering paths for North America, Europe, Siberia, Africa, Australia and India. ε, Cambrian; S, Silurian; C, Carboniferous; P, Permian; T, Triassic; J, Jurassic; K, Cretaceous; E, Eocene (redrawn from Condie, 1982, *Plate Tectonics and Crustal Evolution*, with permission from Pergamon Press Ltd).

Fold Tests of Palaeomagnetic Stability

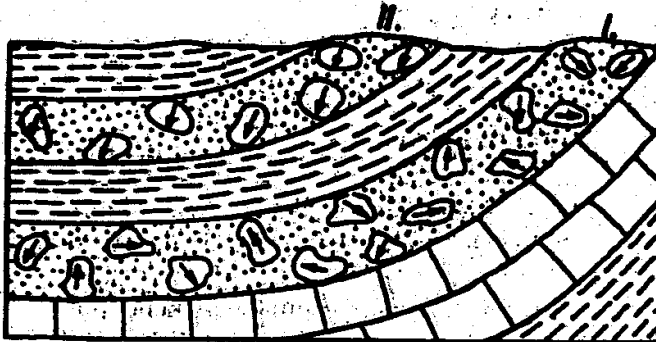


(a)



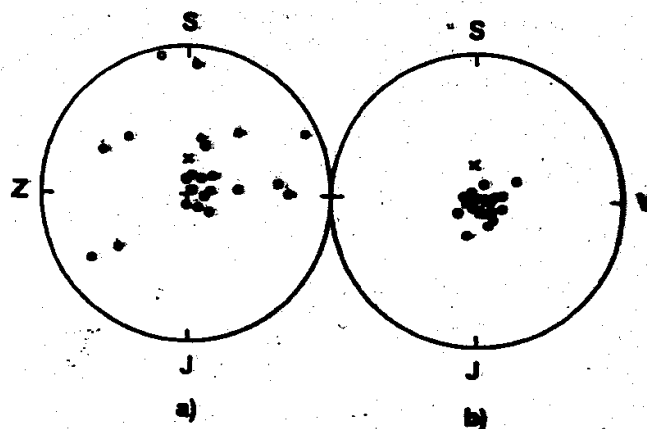
(b)

Fold tests. Where the rock strata, or other structures, have been simply tilted, then standard fold tests can be applied to determine the age of the magnetization relative to the age of the folding by testing the scatter of directions before and after correction for the folding (a, b). Magnetization which was acquired before folding, tilting or slumping, will have retained its original direction and will thus have the same angle to the immediately adjacent bedding plane.



Obr. 3.22 K slepencové zkoušce.

Předpokladem aplikace zkoušky je výskyt slepence s valouny testované horniny. Hornina vytvářející valouny ve slepencovém horizontu I má NRM paleomagneticky stabilní; v horizontu II nestabilní. Šipky vyznačují směr NRM.



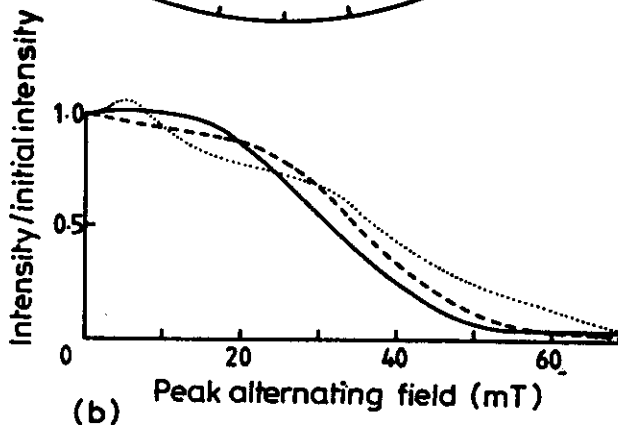
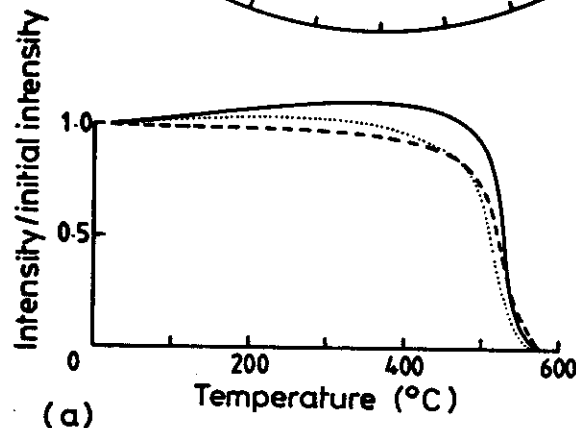
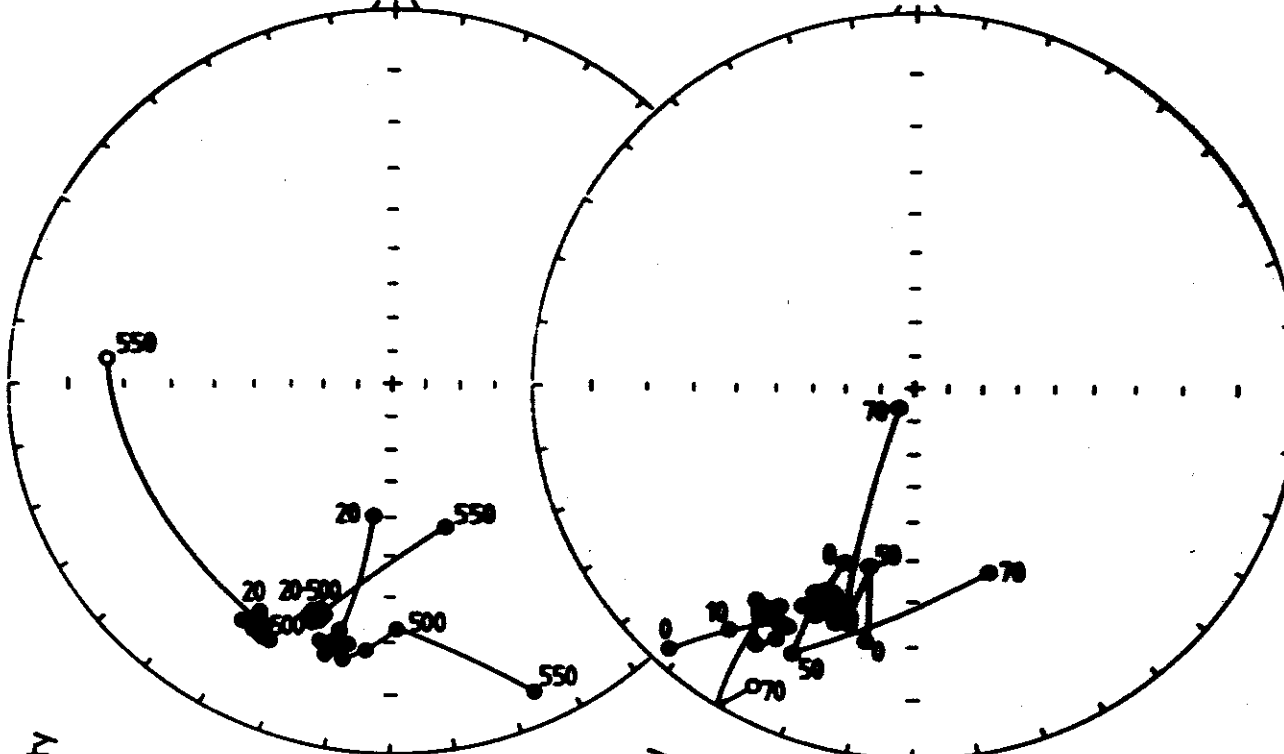
Obr. 3.23 Magnetické číslení vzorků olivinického čediče z lokality Zlatá Lípa, lávový proud sopky Červená hora (podle F. Marka 1969b, 1973).

a) směry přirozené remanentní magnetizace M_r ; b) směry primární remanentní magnetizace M_r (po číslení optimálním střídavým magnetickým polem 17 mT). Vysvětlivky viz obr. 3.13.

Conglomerate Test of Palaeomagnetic Stability

Thermal and AF Demagnetization

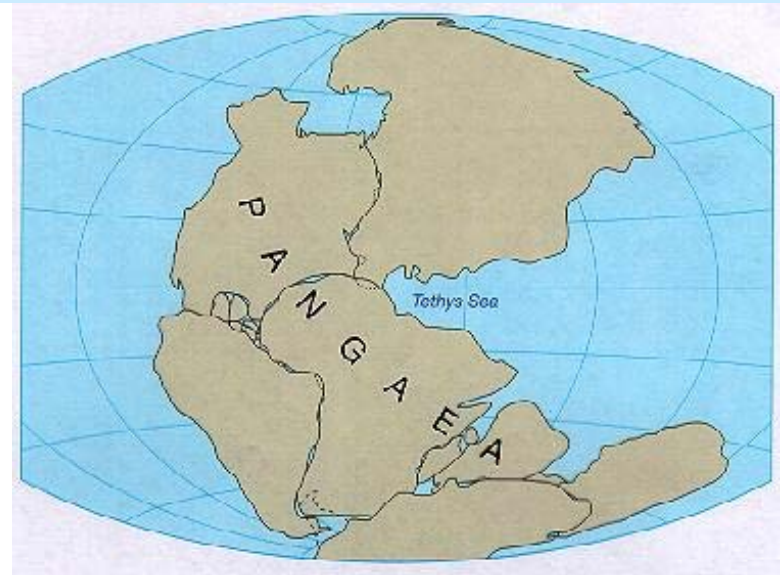
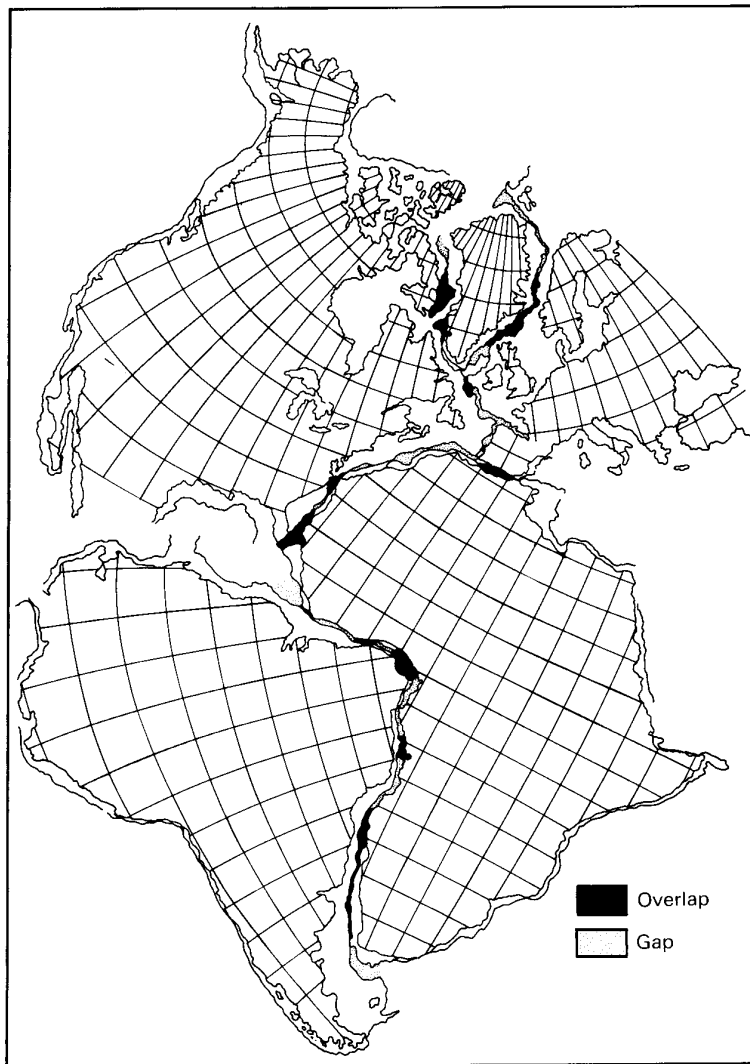
The relationship between temperature, volume and relaxation time.



Examples of demagnetization behavior for various minerals.

CONTINENTAL DRIFT

Reconstruction of continents about Atlantics



Bullard (1965)

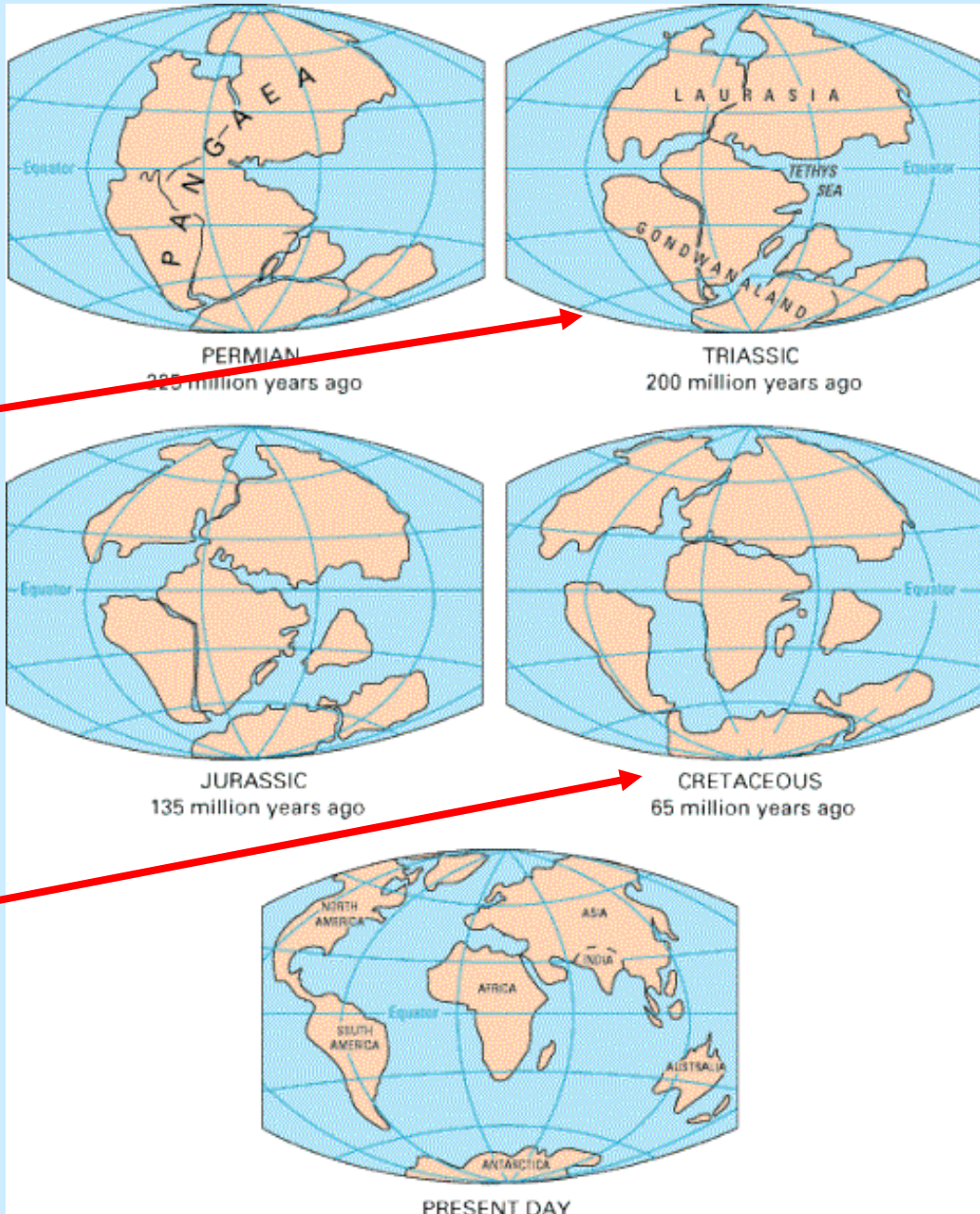
Fit of continental
margins in depth of
500 fathoms
(927 m)

Fig. 3.2 Fit of the continents around the Atlantic Ocean, obtained by matching the 500 fathom (927 m) isobath (redrawn from Bullard *et al.*, 1965, with permission from the Royal Society).

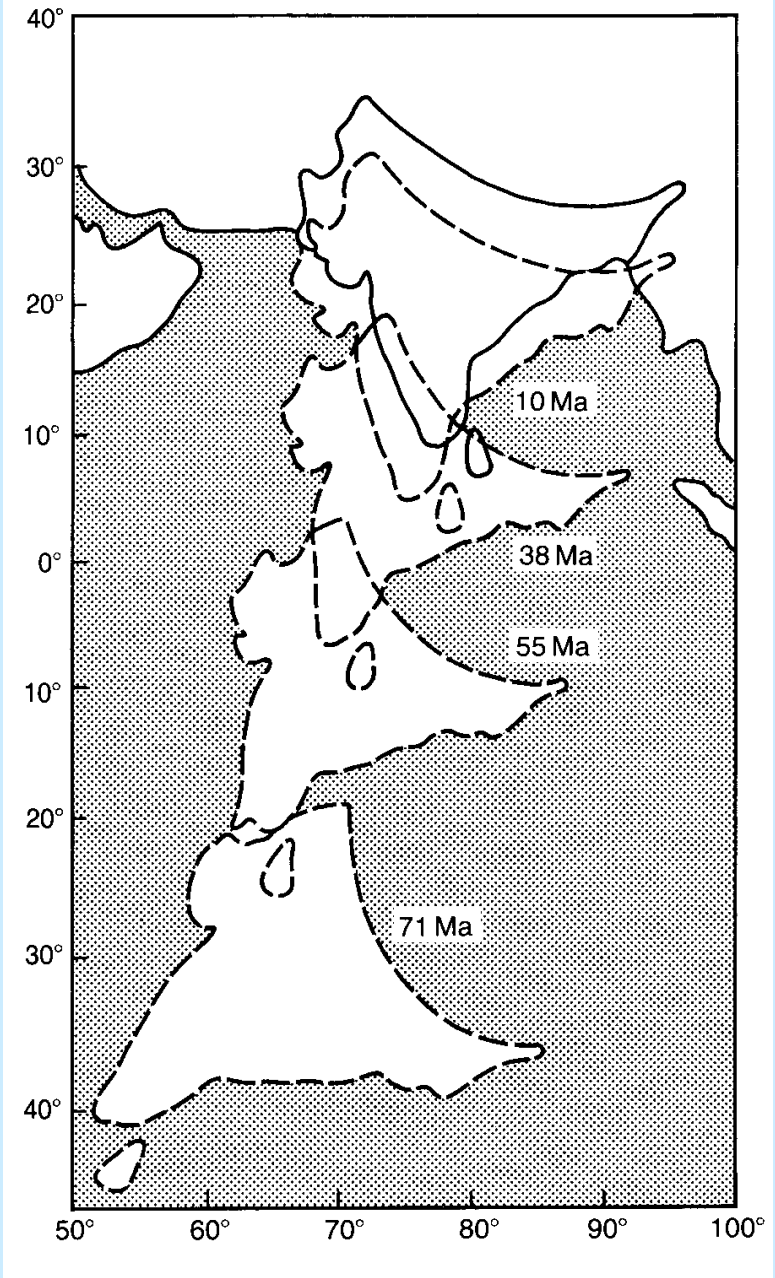
Plate Movements after Breakdown of Gondwana

Laurasia and Gondwana.

Atlantic Opening.

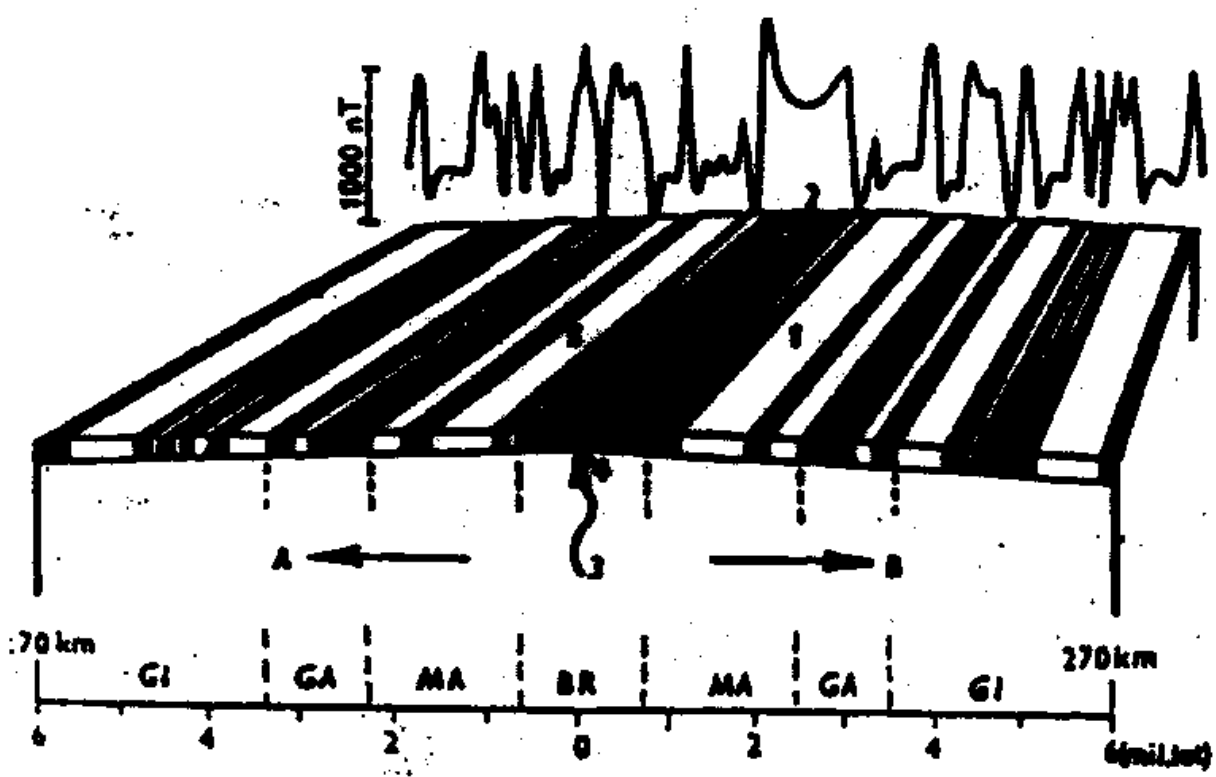


Drifting of India



The figure is a geological cross-section diagram. The vertical axis on the left lists geological periods: Krátkodobý zvrat polarity, Polarita, and K-Ar stáří (mil. let). The horizontal axis at the bottom is marked with numbers 1, 2, 3, and 4.
 - The first column (Epocha polarity) shows 'Krátkodobý zvrat polarity' with a pattern of alternating light and dark grey boxes, corresponding to the first two periods on the vertical axis.
 - The second column (SR) shows 'Sach' with a pattern of alternating light and dark grey boxes, corresponding to the first two periods on the vertical axis.
 - The third column (MA) shows 'Granit' with a pattern of alternating light and dark grey boxes, corresponding to the first two periods on the vertical axis.
 - The fourth column (G) shows 'Konec' with a pattern of alternating light and dark grey boxes, corresponding to the first two periods on the vertical axis.
 - The fifth column (G) shows 'Cestisti' with a pattern of alternating light and dark grey boxes, corresponding to the first two periods on the vertical axis.
 - The sixth column (N) shows 'Nenívka' with a pattern of alternating light and dark grey boxes, corresponding to the last two periods on the vertical axis.
 - The seventh column (K-Ar) shows numerical values: 1, 2, 3, and 4, corresponding to the periods 1, 2, 3, and 4 on the horizontal axis.

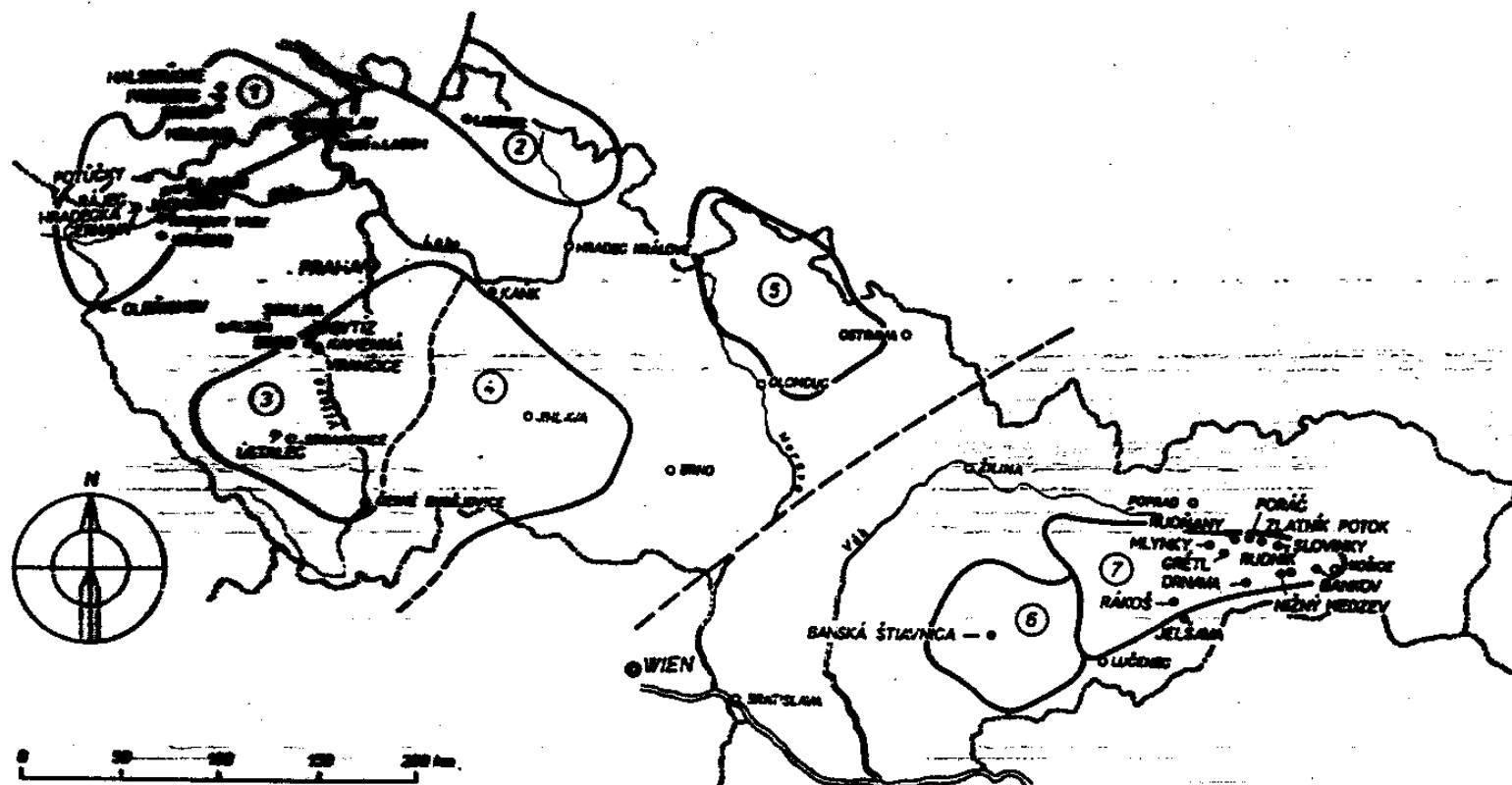
1



b)

Magnetic Stratigraphy

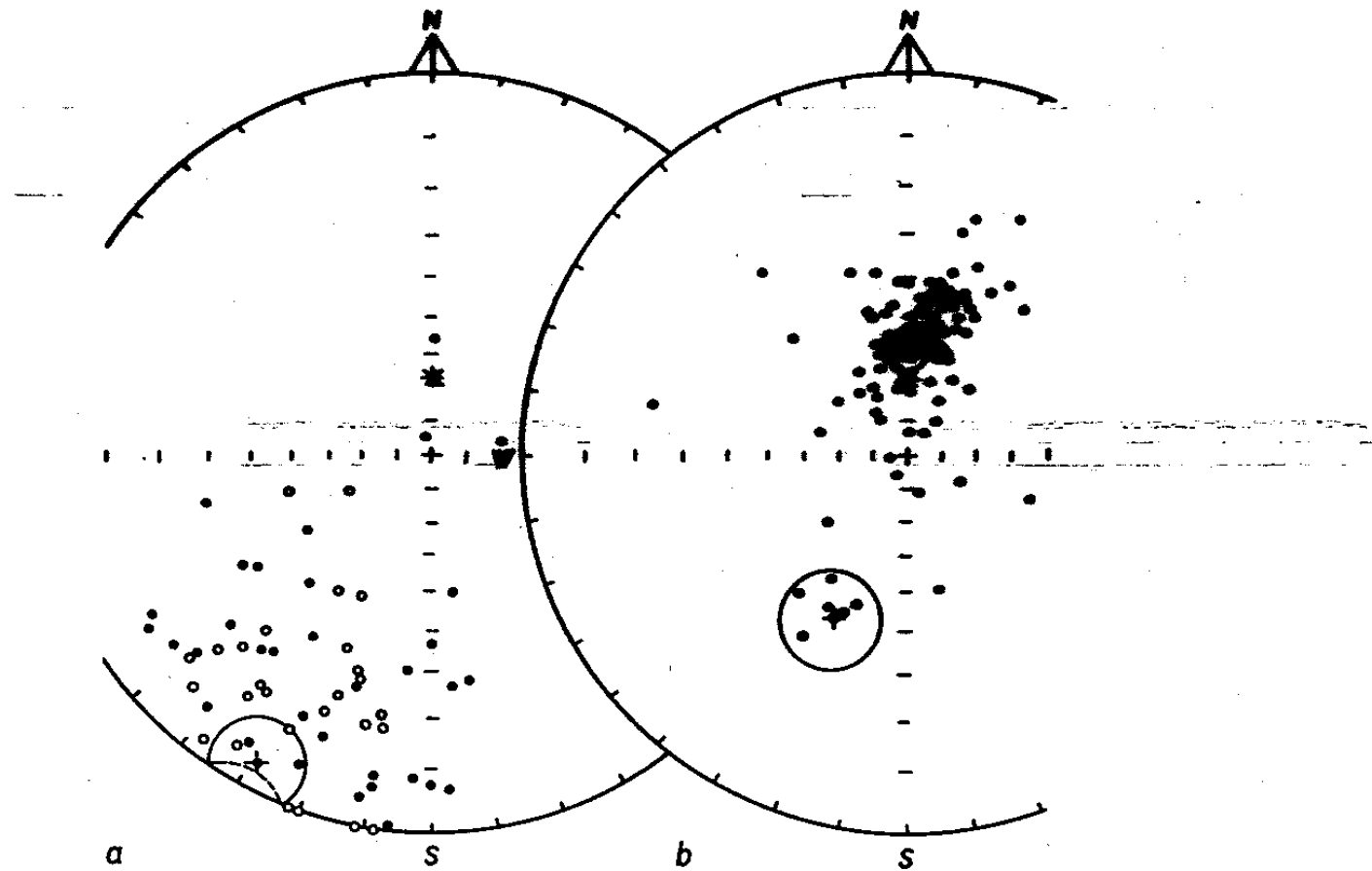
Palaeomagnetism of Ore Deposits



70. Přehled lokalit (přev. J. Švecové) nerostných ložisek zkoumaných paleomagneticky

Menzisové oblasti: 1 — Krkonošsko-jizerská oblast, 2 — západosudetská oblast, 3 — slezsko-sudetský plán, 4 — centrální moravsko-slezský masív, 5 — východosudetská oblast, 6 — Štiavnické pohoří, 7 — Spišsko-gemerské rudohorí a Nižné Tatry. Čárkování je součástí hornin Českého masivu a nizozemské konglomerátové.

Krusne hory Ore Deposits



78. Směry j_n hydrotermální mineralizace z širšího okolí Freibergu

a) Halßbrücke, Freiberg, Freiberg-Brand: I. mineralizační cyklus, převládají sulfidy kb-formace pigmentované hematitem; b) Halßbrücke, Freiberg, Brand: II. mineralizační cyklus, vzorky barytu a hematito-křemenného agregátu převážně z fba-formace